

FEB 18 1947

RM No. A7A30

~~LANGLEY SUB-LIBRARY~~

NACA

RESEARCH MEMORANDUM

for the

Bureau of Aeronautics, Navy Department
HIGH-SPEED LOAD DISTRIBUTION ON THE WING OF A
3/16-SCALE MODEL OF THE DOUGLAS XSB2D-1
AIRPLANE WITH FLAPS DEFLECTED

By Robert H. Barnes

Ames Aeronautical Laboratory
Moffett Field, Calif.

FOR []
NOT TO BE KEPT FROM THIS ROOM

TECHNICAL
EDITING
WAIVED

**NATIONAL ADVISORY COMMITTEE
FOR AERONAUTICS**

WASHINGTON

FEB 5 1947

NACA LIBRARY
LANGLEY MEMORIAL AERONAUTICAL
LABORATORY
Langley Field, Va.



NATIONAL ADVISORY COMMITTEE FOR AERONAUTICS

RESEARCH MEMORANDUM

for the

Bureau of Aeronautics, Navy Department

HIGH-SPEED LOAD DISTRIBUTION ON THE WING OF A

3/16-SCALE MODEL OF THE DOUGLAS XSB2D-1

AIRPLANE WITH FLAPS DEFLECTED

By Robert H. Barnes

SUMMARY

The tests reported herein were made for the purpose of determining the high-speed load distribution on the wing of a 3/16-scale model of the Douglas XSB2D-1 airplane. Comparisons are made between the root bending-moment and section torsional-moment coefficients as obtained experimentally and derived analytically. The results show good correlation for the bending-moment coefficients but considerable disagreement for the torsional-moment coefficients, the measured moments being greater than the analytical moments. The effects of Mach number on both the bending-moment and torsional-moment coefficients were small.

INTRODUCTION

In order to determine the spanwise loading at high speeds with landing flaps deflected, a series of tests of a 3/16-scale model of the Douglas XSB2D-1 airplane was made in the Ames 16-foot high-speed wind tunnel at the request of the Bureau of Aeronautics, Navy Department.

In order to compare the experimental results with those that would be calculated according to current design specifications, the spanwise load distribution was calculated by the method of reference 1.

MODEL AND APPARATUS

A three-view drawing of the airplane is given in figure 1. The wing of the model was equipped with plain flaps having a chord of 0.21 times the wing chord. The geometry of the flaps is given in figure 2. Pressure orifices were provided at seven spanwise stations as shown in figure 3. At each of these stations there were 45 orifices spaced at intervals of 5 percent of the chord except on the forward 10 percent where the spacing was closer.

The model was mounted on the three-strut support system shown in figure 4. The front struts were 5 percent thick; the rear strut was 7 percent thick.

Forces were measured by automatic balancing scales. The pressures were measured on multiple-tube manometers, the data being recorded photographically. Tests were made with the flaps deflected 0° , 10° , and 40° . The Mach number range of the tests was 0.296 to 0.778.

COEFFICIENTS AND SYMBOLS

The following standard NACA coefficients and symbols are used in this report:

C_L	lift coefficient (L/qS)
C_N	normal-force coefficient (N/qS)
c_l	section lift coefficient (l/qc)
c_n	section normal-force coefficient (n/qc)
c_m	section pitching-moment coefficient (m/qc^2)
L	lift, pounds
N	normal force, pounds
l	section lift, pounds per foot
n	section normal force, pounds per foot
m	section pitching moment, foot-pounds per foot
S	wing area, square feet
q	dynamic pressure, pounds per square foot

c	section chord, feet
α_u	uncorrected angle of attack, degrees
α	angle of attack, degrees
x	distance along chord from leading edge, feet
y	spanwise distance from center of model, feet
b	span, feet
M	Mach number
P	pressure coefficient $\left(\frac{p_t - p}{q}\right)$
p_t	local static pressure, pounds per square foot
p	free-stream static pressure, pounds per square foot

In addition to the standard NACA coefficients and symbols the following are used:

C_{BM}	root bending-moment coefficient (BM/qb^2C_S)
BM	root bending moment $(q \int_0^{b/2} c_n cy dy)$, foot-pounds
C_S	root chord, feet
C_{TM}	root torsional-moment coefficient (TM/qc^2b)
TM	root torsional moment $(q \int_0^{b/2} c^2 c_m dy)$, foot-pounds
\bar{c}	mean aerodynamic chord, feet

The lift coefficients used in this report are those for the standard model less tail as shown in figure 4.

REDUCTION AND PRESENTATION OF DATA

The data were corrected for tunnel-wall effects by the method of reference 2. Corrections were also made to account for the constriction and the upflow of the air stream.

Typical chordwise pressure distributions which show the effects of angle of attack, Mach number, and landing-flap deflection are shown in figures 5, 6, and 7, respectively.

The section normal-force and pitching-moment coefficients

were obtained by integration of the pressure distributions. The axis for the pitching-moment coefficient at each station is a line normal to the center line of the model and passing through the quarter-chord point of the M.A.C. It should be noted that no consideration was taken of the chordwise component of the pressure coefficient in obtaining the pitching-moment coefficient. These coefficients were then plotted against the model lift coefficient existing when the data were taken as found in figure 8. Figures 9 to 15 show the variations at each pressure station of the section normal-force coefficient with model lift coefficient, and figures 16 to 22 show the variations of section pitching-moment coefficient with model lift coefficient.

The product of the section normal-force coefficient times the section chord is an index of the section normal-force loading and so in order to present the spanwise variations of this loading the product c_n was plotted against span. Figures 23, 24, and 25 show these variations for the three flap deflections tested. Integration of these plots yielded the total normal-force coefficients and the corresponding root bending-moment coefficients which are plotted against lift coefficient in figures 26 and 27, respectively.

In a similar manner the product of the section pitching-moment coefficient times the square of the section chord (c^2c_m) is an index of the torsional-moment loading. From integration of spanwise plots of this quantity the root torsional-moment coefficients were obtained. They are plotted against lift coefficient in figure 28.

Figures 29, 30, and 31 present comparisons of the experimental and analytical values of root bending-moment coefficient for flap deflections of 0° , 10° , and 40° , respectively.

Figures 32, 33, and 34 show a similar comparison for the section pitching-moment coefficient.

Figures 35, 36, and 37 present some typical spanwise normal-force distributions showing effects of Mach number and flap deflection, and a comparison of experimental and analytical results.

ANALYTICAL CALCULATIONS

Calculations were made by the method of reference 3 of the chordwise pressure distribution at station 140 for the three flap deflections tested. Station 140 was chosen since it was on the outboard panel of the wing where the sections are

standard NACA sections for which necessary basic characteristics are known. Also this position was felt to be the best compromise to avoid flow effects due to dihedral reversal, support struts, and wing tips.

Calculations were also made of the spanwise normal-force distribution for the three flap deflections by the method of reference 1. In order to use this method it is necessary to know, among other things, the profile-drag coefficient and the angle of zero lift of the wing. The profile-drag coefficients with flaps deflected were obtained by adding increments of coefficients taken from figure 66 of reference 4 to the value of the profile-drag coefficient of the wing with flaps neutral. The angle of attack for zero lift was obtained from the force data for Mach number of 0.296 by extrapolating the curves of figure 8 to zero lift coefficient.

The spanwise load distributions so obtained were integrated to obtain the wing normal-force coefficient and the corresponding root bending-moment coefficient.

No calculation was made of the analytical root torsional-moment coefficient since it would involve calculating the chordwise pressure distribution at each station, and it was felt that the comparison of the analytical and experimental characteristics at one station indicates what can be expected for the entire wing.

DISCUSSION

Wind-Tunnel Data

There are no unusual effects of angle of attack upon the pressure distribution. (See fig. 5.) However, it should be noted that, contrary to what is considered normal, the local pressure coefficients over the forward 10 percent of the wing decrease as the Mach number increases. Data not presented herein for the other pressure stations show the same tendency in varying degrees.

Figure 23 shows that with the flaps neutral, separation and loss of lift at the point of dihedral reversal begins to occur at about 0.6 Mach number for a lift coefficient of 0.8, the largest for which data are presented. When the Mach number is increased to 0.73, this phenomenon is seen to occur throughout the range of lift coefficients tested. However, as the Mach number is further increased to 0.778 the local lift losses extend over the adjacent portions of the wing as evidenced by the flattening of the load distribution

curves for constant lift coefficients. (See figs. 23(f) and 23(g).) This effect is probably due to the shock occurring on the adjacent portions of the wing.

If the flaps are deflected 10° or 40° the pattern of events is similar to that previously described except that at the maximum Mach number of the tests there is no spreading of the local lift losses.

The following table summarizes the results:

Flap Deflection	Mach number at which separation is first noted at $C_L = 0.8$	Mach number at which separation is noted for all positive C_L 's tested
0°	0.591	0.73
10°	.591	.685
40°	.638	.778

Figure 28 indicates that the root torsional-moment coefficient remains practically constant for all positive lift coefficients up to 0.8. This is especially true at Mach numbers less than 0.685. It is to be noted also that the coefficients for each flap deflection remain approximately constant for all the test Mach numbers.

Comparison of Experimental and Analytical Results

The comparisons given in figures 29, 30, and 31 show that the calculated and experimental root bending-moment coefficients are in good agreement and in some cases in practically exact agreement.

Figures 32, 33, and 34 show that the experimental section pitching-moment coefficients are more negative than the analytical values. That is, the analytical method underestimates the loads. It will be seen that the amount of error is approximately constant at each Mach number and tends to increase with Mach number. Also, the percentage error based on the analytical value is greatest for the condition of flaps neutral or deflected 40° and least with flaps deflected 10° . For example, with neutral flaps the error varies from 30 percent at 0.296 Mach number to 100 percent at 0.778 Mach number. Also,

at 0.296 Mach number the error is 30 percent with neutral flaps, 19 percent with flaps deflected 10° , and 30 percent with flaps deflected 40° .

CONCLUDING REMARKS

It has been seen that the dihedral reversal of the wing affects the spanwise normal-force distribution. Therefore, the results of these tests should be considered applicable only to similar wings.

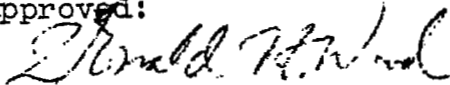
The correlation between experimental and analytical variation of root bending-moment coefficient with wing normal-force coefficient is good.

The root torsional-moment coefficient for each flap deflection remains approximately constant throughout the lift-coefficient and Mach number range of the tests.

The experimental value of the section pitching-moment coefficient was in all cases greater than the analytical value. The discrepancy varied from 20 to 100 percent of the analytical value.

Ames Aeronautical Laboratory,
National Advisory Committee for Aeronautics,
Moffett Field, Calif.

Approved:


Donald H. Wood,
Aeronautical Engineer,


Robert H. Barnes,
Aeronautical Engineer,

REFERENCES

1. Anon: Spanwise Air-Load Distribution, ANC-1(1). Army-Navy-Commerce Committee on Aircraft Requirements. April 1938.
2. Silverstein, Abe and White, James A.: Wind-Tunnel Interference with Particular Reference to Off-Center Positions of the Wing and to the Downwash at the Tail. NACA Rep. No. 547, 1935.
3. Anon: Chordwise Air-Load Distribution, ANC-1(2). Army-Navy-Commerce Committee on Aircraft Requirements. Oct. 28, 1942.
4. Diehl, Walter Stuart.: Engineering Aerodynamics. The Ronald Press Co., N.Y. 1936.

FIGURE LEGENDS

Figure 1.- Three-view drawing of the Douglas XSB2D-1 airplane.

Figure 2.- Geometry of the landing flaps on the XSB2D-1 model.

Figure 3.- Wing geometry and pressure orifice stations for the XSB2D-1 model.

Figure 4.- The XSB2D-1 model mounted in the 16-foot wind tunnel. For these tests the propeller was replaced by a dummy spinner.

Figure 5.- Effects of angle of attack on the chordwise pressure distribution at station 140.000 on the wing of the XSB2D-1 model. Flaps neutral, $M = 0.494$.

Figure 6.- Effects of Mach number on the chordwise pressure distribution at station 140.000 on the wing of the XSB2D-1 model. Flaps neutral; $\alpha = 0.2^\circ$.

Figure 7.- Effects of flap deflection on the chordwise pressure distribution at station 140.000 on the wing of the XSB2D-1 model. $M = 0.494$; $\alpha_u = 0^\circ$.

Figure 8.- Variation of the lift coefficient with angle of attack at several Mach numbers. XSB2D-1 model; tail off.
(a) $M = 0.296, 0.494, 0.591, \text{ and } 0.638$.

Figure 8.- Concluded. (b) $M = 0.685, 0.73, \text{ and } 0.778$.

Figure 9.- Variation of the section normal-force coefficient at station 40.102 with tail-off lift coefficient. XSB2D-1 model. (a) $M = 0.296, 0.494, \text{ and } 0.591$.

Figure 9.- Concluded. (b) $M = 0.638, 0.685, 0.730, \text{ and } 0.778$.

Figure 10.- Variation of the section normal-force coefficient at station 77.500 with tail-off lift coefficient. XSB2D-1 model. (a) $M = 0.296, 0.494, \text{ and } 0.591$.

Figure 10.- Concluded. (b) $M = 0.638, 0.685, 0.73, \text{ and } 0.778$.

Figure 11.- Variation of the section normal-force coefficient at station 110.000 with tail-off lift coefficient. XSB2D-1 model. (a) $M = 0.296, 0.494, \text{ and } 0.591$.

Figure 11.- Concluded. (b) $M = 0.638, 0.685, 0.73, \text{ and } 0.778$.

Figure 12.- Variation of the section normal-force coefficient at station 140.000 with tail-off lift coefficient. XSB2D-1 model. (a) $M = 0.296, 0.494, \text{ and } 0.591$.

Figure 12.- Concluded. (b) $M = 0.638, 0.685, 0.73 \text{ and } 0.778$.

Figure 13.- Variation of the section normal-force coefficient at station 170.334 with tail-off lift coefficient. XSB2D-1 model. (a) $M = 0.296, 0.494, \text{ and } 0.591$.

Figure 13.- Concluded. (b) $M = 0.638, 0.685, 0.73, \text{ and } 0.778$.

Figure 14.- Variation of the section normal-force coefficient at station 219.093 with tail-off lift coefficient. XSB2D-1 model. (a) $M = 0.296, 0.494, \text{ and } 0.591$.

Figure 14.- Continued. (b) $M = 0.638, 0.685, \text{ and } 0.73$.

Figure 14.- Concluded. (c) $M = 0.778$.

Figure 15.- Variation of the section normal-force coefficient at station 266.334 with tail-off lift coefficient. XSB2D-1 model. (a) $M = 0.296, 0.494, 0.591, \text{ and } 0.638$.

Figure 15.- Concluded. (b) $M = 0.685, 0.730, \text{ and } 0.778$.

Figure 16.- Variation of section pitching-moment coefficient at station 40.102 with tail-off lift coefficient. XSB2D-1 model; moment axis at 25.75 percent chord. (a) $M = 0.296, 0.494, 0.591, 0.638, \text{ and } 0.685$.

Figure 16.- Concluded. (b) $M = 0.73, \text{ and } 0.778$.

Figure 17.- Variation of the section pitching-moment coefficient at station 77.500 with tail-off lift coefficient. XSB2D-1 model; moment axis at 25.4 percent chord. (a) $M = 0.296, 0.494, 0.591, 0.638, \text{ and } 0.685$.

Figure 17.- Concluded. (b) $M = 0.73, \text{ and } 0.778$.

Figure 18.- Variation of the section pitching-moment coefficient at station 110.000 with tail-off lift coefficient. XSB2D-1 model; moment axis at 25.1 percent chord. (a) $M = 0.296, 0.494, 0.591, 0.638, \text{ and } 0.685$.

Figure 18.- Concluded. (b) $M = 0.73, \text{ and } 0.778$.

Figure 19.- Variation of the section pitching-moment coefficient at station 140.000 with tail-off lift coefficient. XSB2D-1 model; moment axis at 24.7 percent chord.
(a) $M = 0.296, 0.494, 0.591, 0.638, \text{ and } 0.685.$

Figure 19.- Concluded. (b) $M = 0.73 \text{ and } 0.778.$

Figure 20.- Variation of the section pitching-moment coefficient at station 170.334 with tail-off lift coefficient. XSB2D-1 model; moment axis at 24.3 percent chord.
(a) $M = 0.296, 0.494, 0.591, 0.638, \text{ and } 0.685.$

Figure 20.- Concluded. (b) $M = 0.73 \text{ and } 0.778.$

Figure 21.- Variation of the section pitching-moment coefficient at station 219.093 with tail-off lift coefficient. XSB2D-1 model; moment axis at 23.5 percent chord.

Figure 22.- Variation of the section pitching-moment coefficient at station 266.334 with tail-off lift coefficient. XSB2D-1 model; moment axis at 22.5 percent chord.

Figure 23.- Spanwise variation of the normal force on the wing of the XSB2D-1 model with landing flaps neutral.
(a) $M = 0.296.$

Figure 23.- Continued. (b) $M = 0.494.$

Figure 23.- Continued. (c) $M = 0.591.$

Figure 23.- Continued. (d) $M = 0.638.$

Figure 23.- Continued. (e) $M = 0.685.$

Figure 23.- Continued. (f) $M = 0.73.$

Figure 23.- Concluded. (g) $M = 0.778.$

Figure 24.- Spanwise variation of the normal force on the wing of the XSB2D-1 model with landing flaps deflected 10° .
(a) $M = 0.296.$

Figure 24.- Continued. (b) $M = 0.494.$

Figure 24.- Continued. (c) $M = 0.591.$

Figure 24.- Continued. (d) $M = 0.638.$

Figure 24.- Continued. (e) $M = 0.685.$

Figure 24.- Continued. (f) $M = 0.73.$

Figure 24.- Concluded. (g) $M = 0.778$.

Figure 25.- Spanwise variation of the normal force on the wing of the XSB2D-1 model with landing flaps deflected 40° .
(a) $M = 0.296$.

Figure 25.- Continued. (b) $M = 0.494$.

Figure 25.- Continued. (c) $M = 0.591$.

Figure 25.- Continued. (d) $M = 0.638$.

Figure 25.- Continued. (e) $M = 0.685$.

Figure 25.- Continued. (f) $M = 0.73$.

Figure 25.- Concluded. (g) $M = 0.778$.

Figure 26.- Variation of the wing normal-force coefficient with the tail-off lift coefficient for the XSB2D-1 model with three landing-flap deflections. (a) $M = 0.296, 0.494, 0.591, \text{ and } 0.638$.

Figure 26.- Concluded. (b) $M = 0.685, 0.73, \text{ and } 0.778$.

Figure 27.- Variation of the root bending-moment coefficient with the tail-off lift coefficient for the XSB2D-1 model with three landing-flap deflections. (a) $M = 0.296, 0.494, 0.591, \text{ and } 0.638$.

Figure 27.- Concluded. (b) $M = 0.685, 0.73, \text{ and } 0.778$.

Figure 28.- Variation of the root torsional-moment coefficient with the tail-off lift coefficient for the XSB2D-1 model with three landing flap deflections. (a) $M = 0.296, 0.494, 0.591, \text{ and } 0.638$.

Figure 28.- Concluded. (b) $M = 0.685, 0.73, \text{ and } 0.778$.

Figure 29.- Comparison of the variation of root bending-moment coefficient with normal-force coefficient as determined experimentally and by method of reference 1. XSB2D-1 model, landing flaps neutral. (a) $M = 0.296, 0.494, 0.591, \text{ and } 0.638$.

Figure 29.- Concluded. (b) $M = 0.685, 0.73, \text{ and } 0.778$.

Figure 30.- Comparison of the variation of root bending-moment coefficient with normal-force coefficient as determined experimentally and by method of reference 1. XSB2D-1 model; landing flaps deflected 10° . (a) $M = 0.296, 0.494, 0.591, \text{ and } 0.638$.

Figure 30.- Concluded. (b) $M = 0.685, 0.73, 0.778$.

Figure 31.- Comparison of the variation of root bending-moment coefficient with normal-force coefficient as determined experimentally and by method of reference 1. XSB2D-1 model; landing flaps deflected 40° .
(a) $M = 0.296, 0.494, 0.591, \text{ and } 0.638$.

Figure 31.- Concluded. (b) $M = 0.685, 0.73, \text{ and } 0.778$.

Figure 32.- Comparison of the variation of section pitching-moment coefficient with section normal-force coefficient with landing flaps neutral as determined experimentally and by the method of reference 3. XSB2D-1 model; station 140; moment axis 24.7 percent chord.

Figure 33.- Comparison of the variation of section pitching-moment coefficient with section normal-force coefficient for a landing flap deflection of 10° as determined experimentally and by the method of reference 3. XSB2D-1 model; station 140; moment axis 24.7 percent chord. (a) $M = 0.296, 0.494, 0.591, \text{ and } 0.638$.

Figure 33.- Concluded. (b) $M = 0.685, 0.73, \text{ and } 0.778$.

Figure 34.- Comparison of the variation of section pitching-moment coefficient with section normal-force coefficient for a landing flap deflection of 40° as determined experimentally and by the method of reference 3. XSB2D-1; station 140; moment axis 24.7 percent chord.
(a) $M = 0.296, 0.494, 0.591, \text{ and } 0.638$.

Figure 34.- Concluded. (b) $M = 0.685, 0.73, \text{ and } 0.778$.

Figure 35.- Effects of Mach number on the spanwise normal-force distribution on the XSB2D-1 model. Flaps neutral; $C_L = 0.4$.

Figure 36.- Comparison of spanwise normal-force distribution as determined experimentally and by method of reference 1 for the XSB2D-1 model. $M = 0.296$. (a) Landing flaps neutral.

Figure 36.- Continued. (b) Landing flaps deflected 10° .

Figure 36.- Concluded. (c) Landing flaps deflected 40° .

Figure 37.- Typical effects of landing-flap deflection on the spanwise normal-force distribution on the XSB2D-1 model. $M = 0.296$; $C_L = 0.4$.

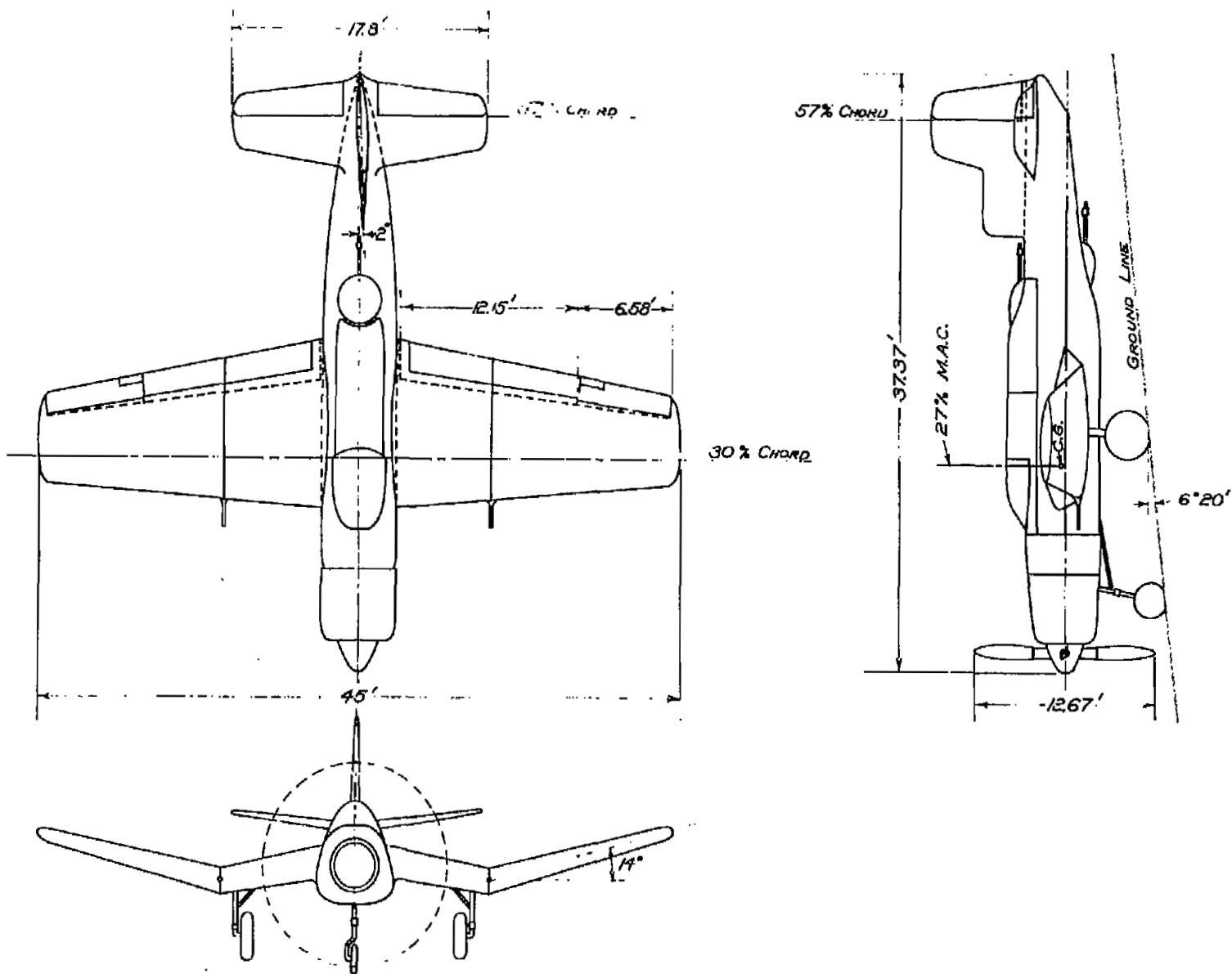


FIGURE 1. THREE VIEW DRAWING OF THE DOUGLAS XSB2D-1 AIRPLANE.

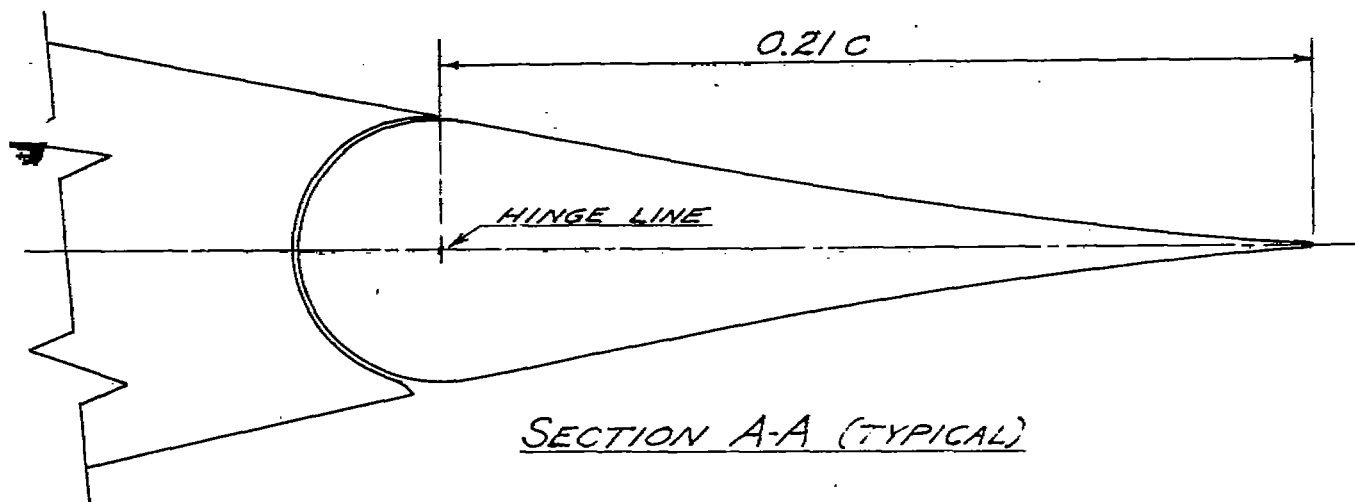
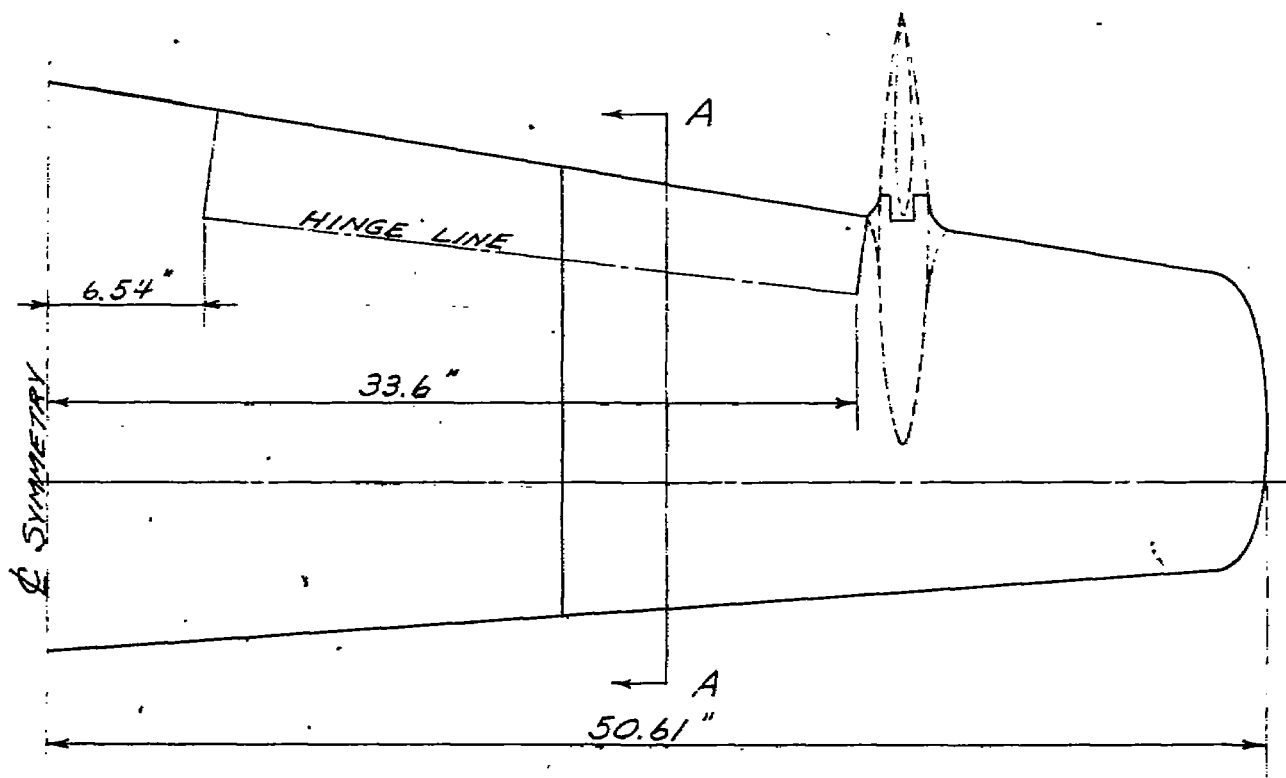


FIGURE 2.- GEOMETRY OF THE LANDING FLAPS ON THE XSB2D-1 MODEL.

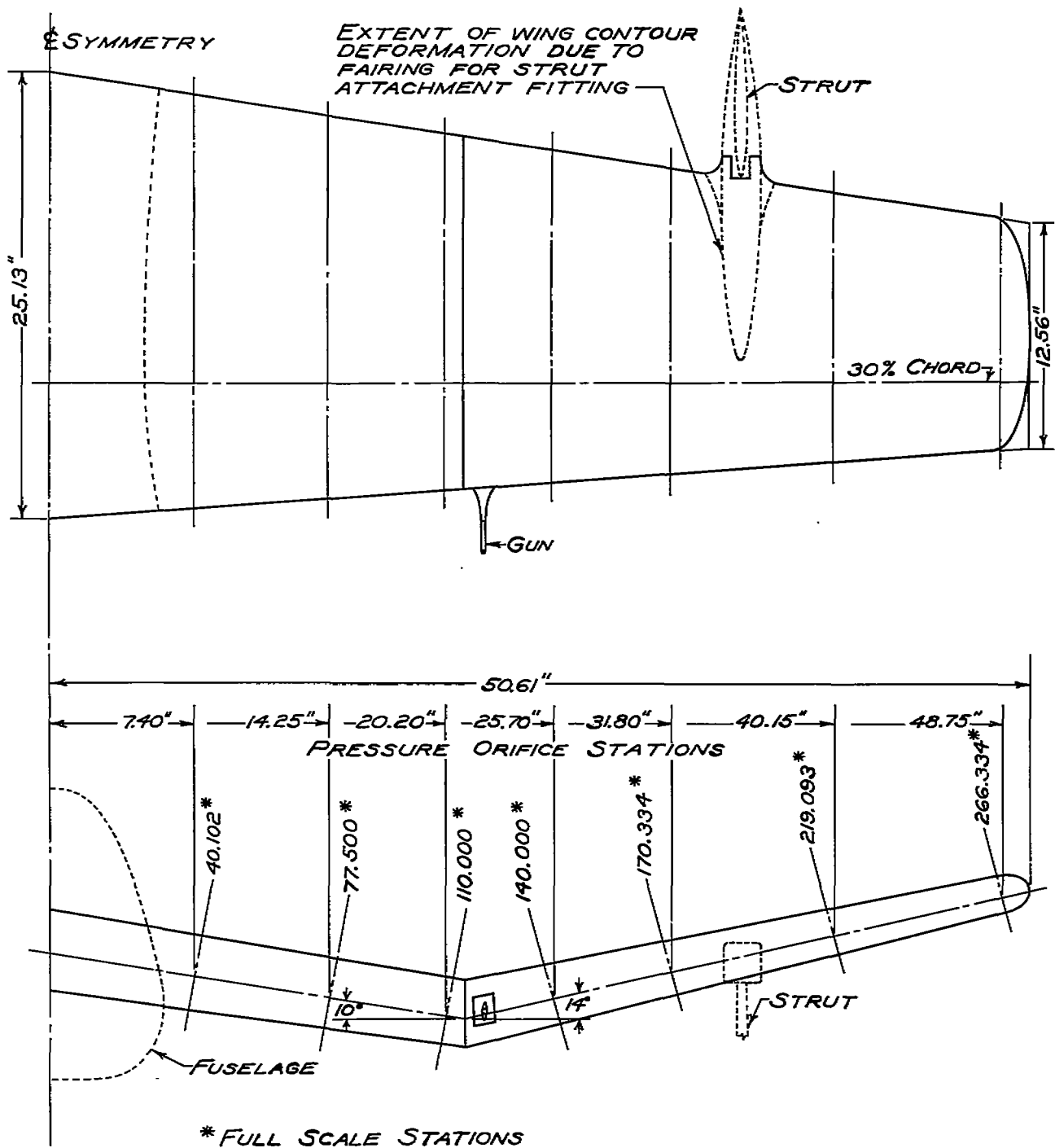


FIGURE 3. - WING GEOMETRY AND PRESSURE ORIFICE STATIONS FOR THE XSB2D-1 MODEL.



Figure 4.- The XSB2D-1 Model mounted in the 16-foot wind tunnel. For these tests the propeller was replaced by a dummy spinner.

**N. A. C. A. PHOTOGRAPH
NOT FOR PUBLICATION
UNLESS AUTHORIZED BY
NATIONAL ADVISORY COMMITTEE
FOR AERONAUTICS, WASHINGTON, D. C.**

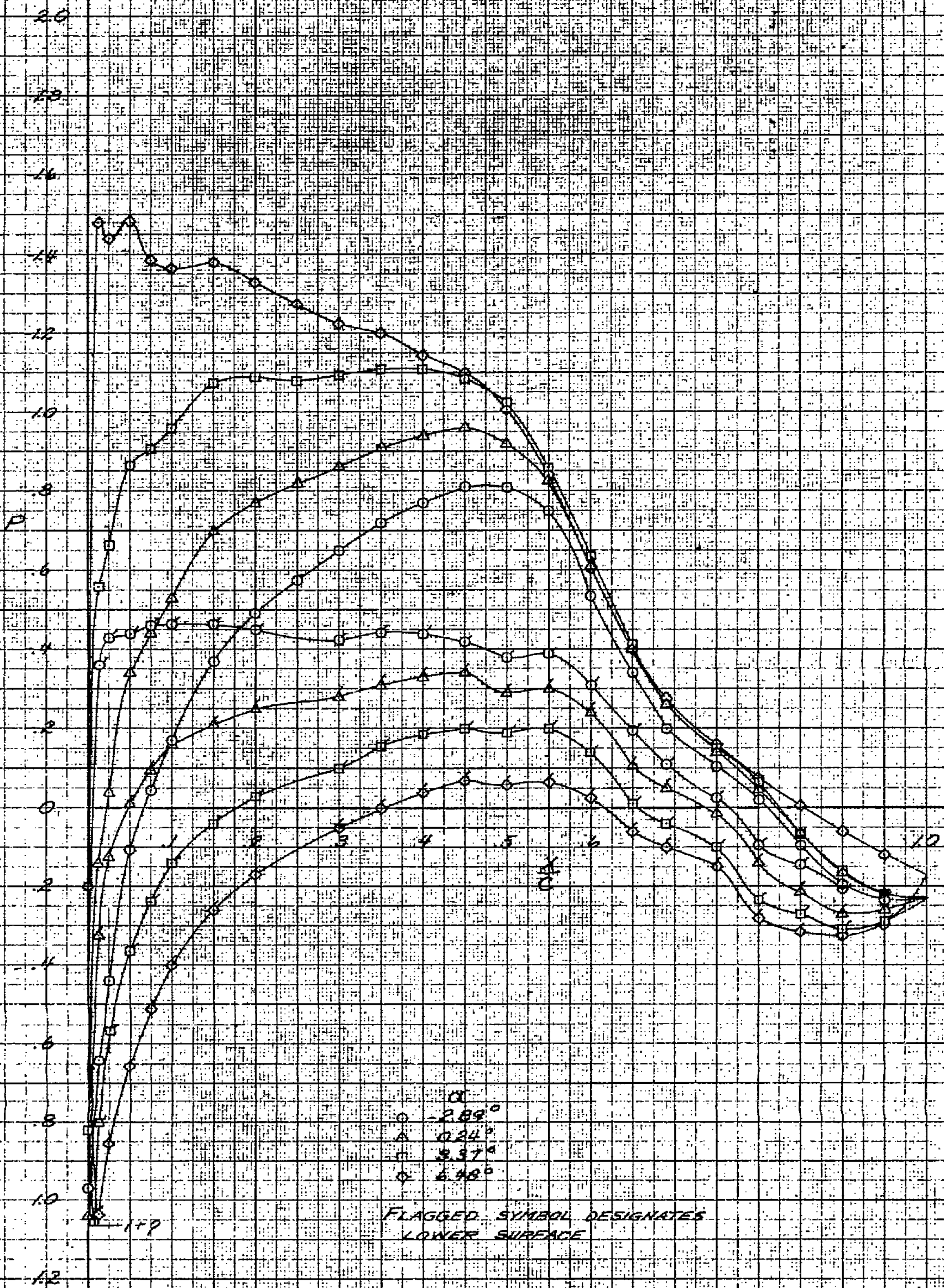


FIGURE 5. - EFFECTS OF ANGLE OF ATTACK ON THE CHORDWISE PRESSURE DISTRIBUTION
 AT STATION 140.000 ON THE WING OF THE X5B20-1 MODEL. FLAPS NEUTRAL;
 $M = 0.494$

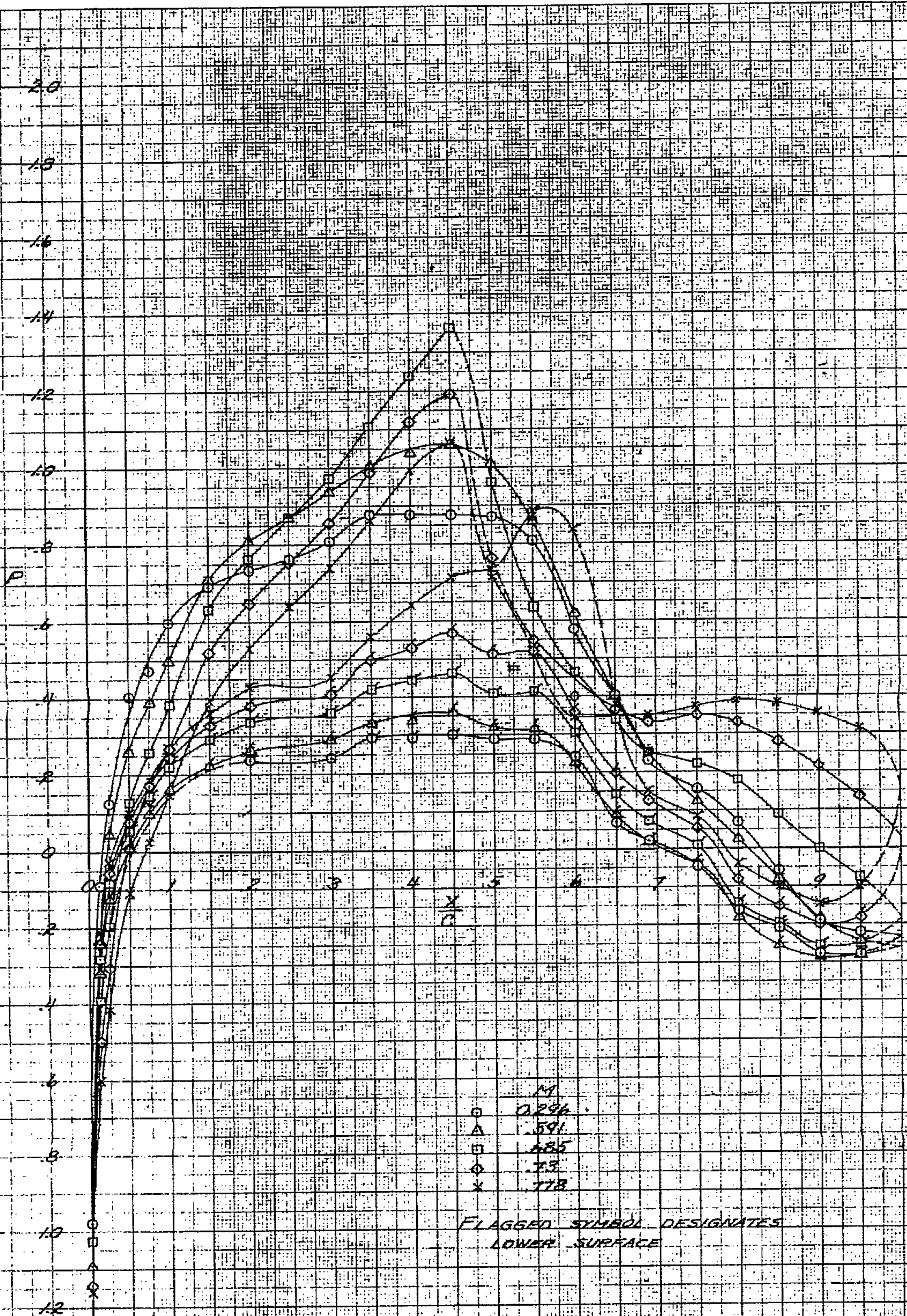


FIGURE 6. EFFECTS OF MACH NUMBER ON THE CHORDWISE PRESSURE DISTRIBUTION AT STATION 140,000 ON THE WING OF THE X-5 MODEL. FLAPS NEUTRAL. $\alpha = 0.2^\circ$

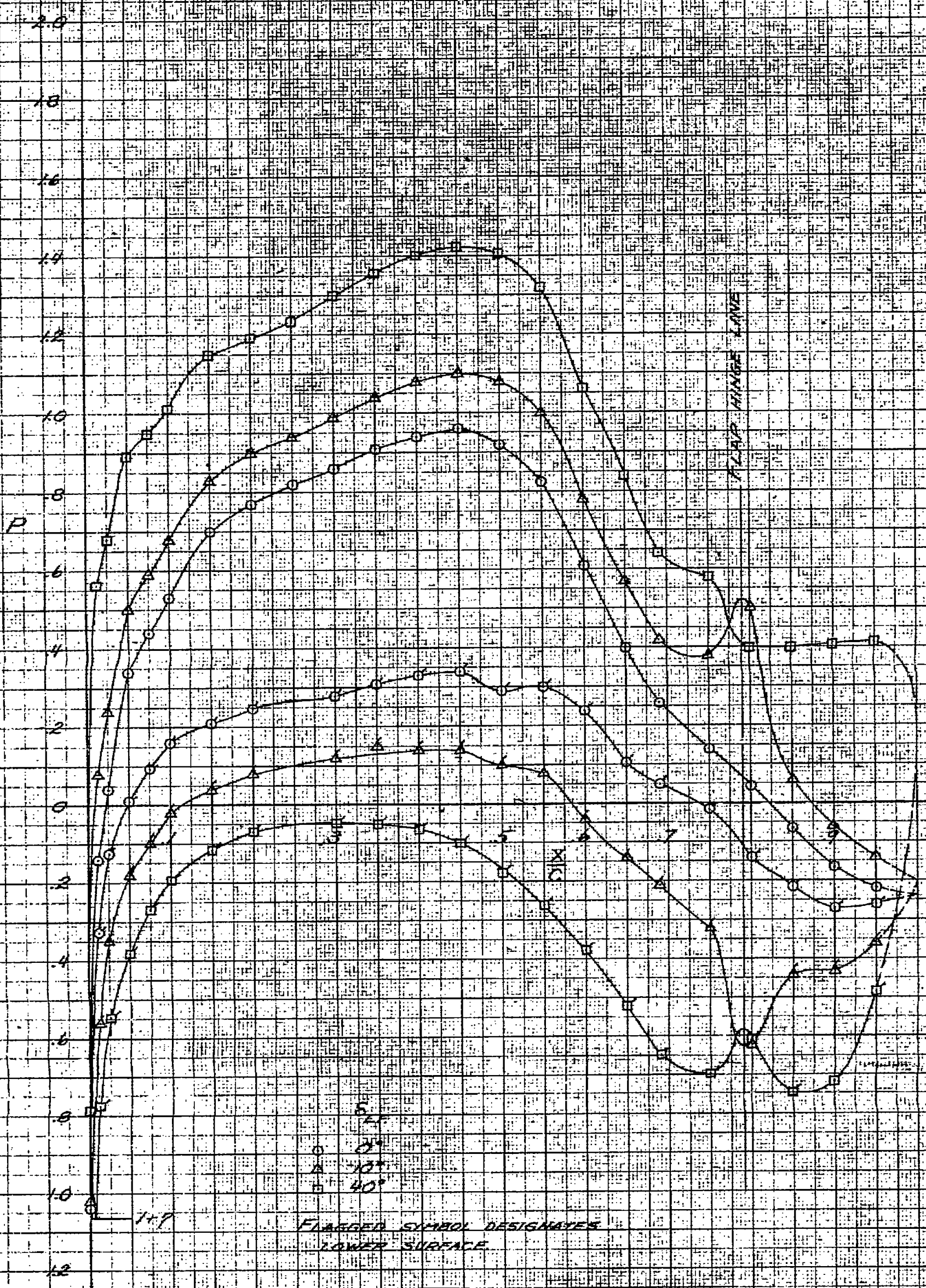
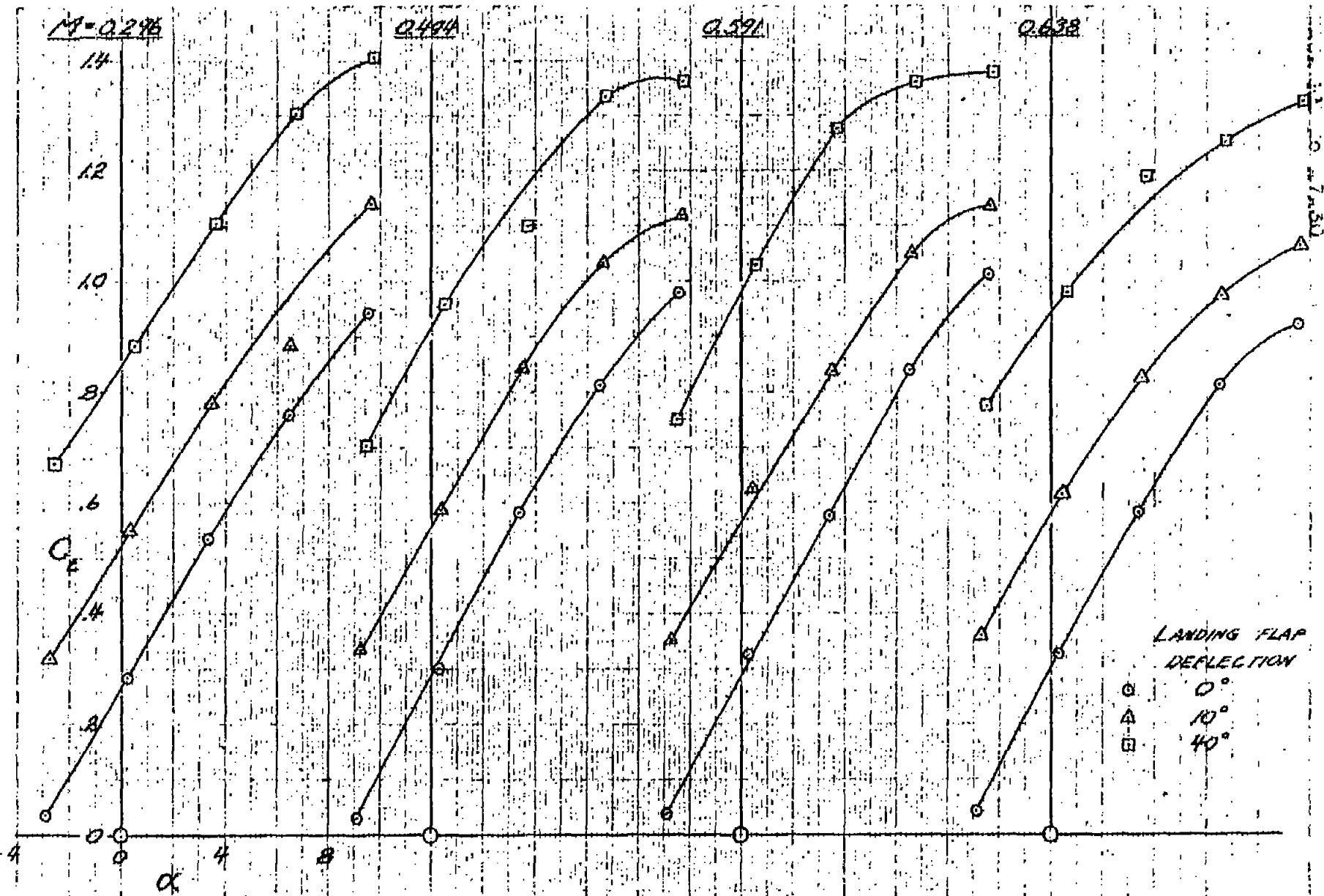


FIGURE 7. - EFFECTS OF FLAP DEFLECTION ON THE CHORDWISE PRESSURE DISTRIBUTION AT STATION 140,000 ON THE WING OF THE X582D-1 MODEL. $M=0.894$; $\alpha_1 = 0^\circ$



(2) $M = 0.296, 0.494, 0.591, \text{ AND } 0.638$
 FIGURE 8. - VARIATION OF THE LIFT COEFFICIENT WITH ANGLE OF ATTACK AT SEVERAL MACH NUMBERS, XSRD-1 MODEL, TAIL OFF.

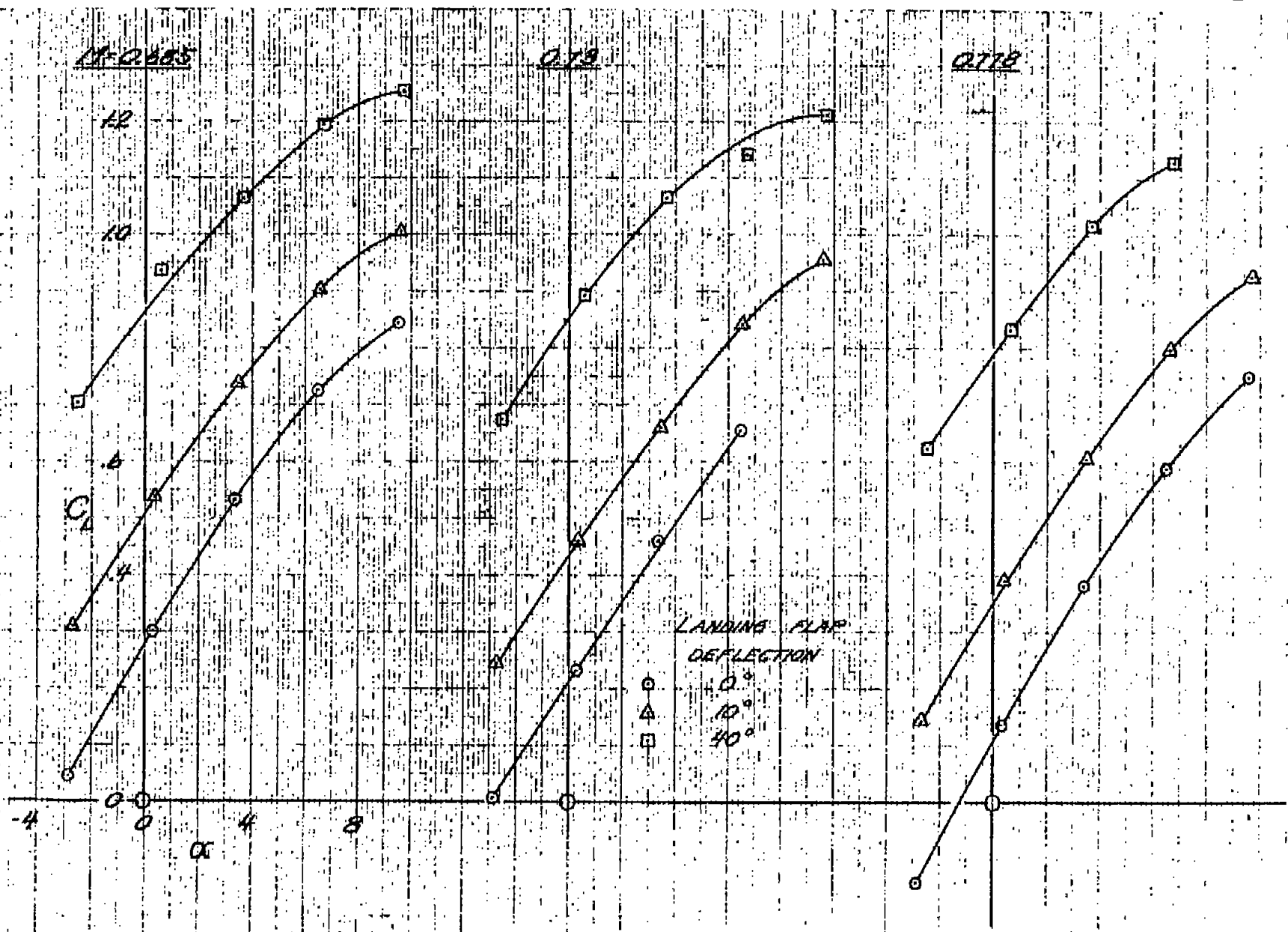
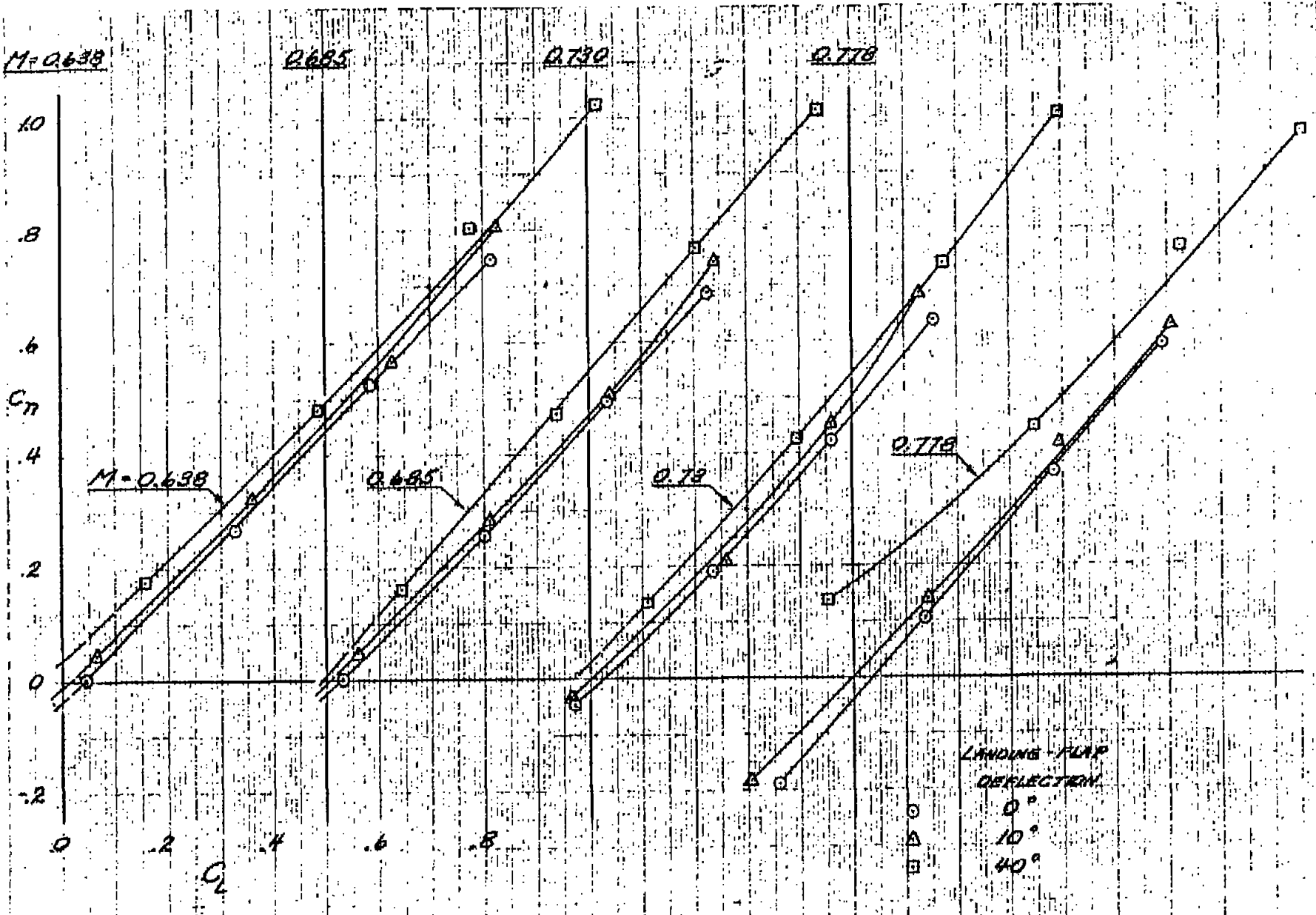


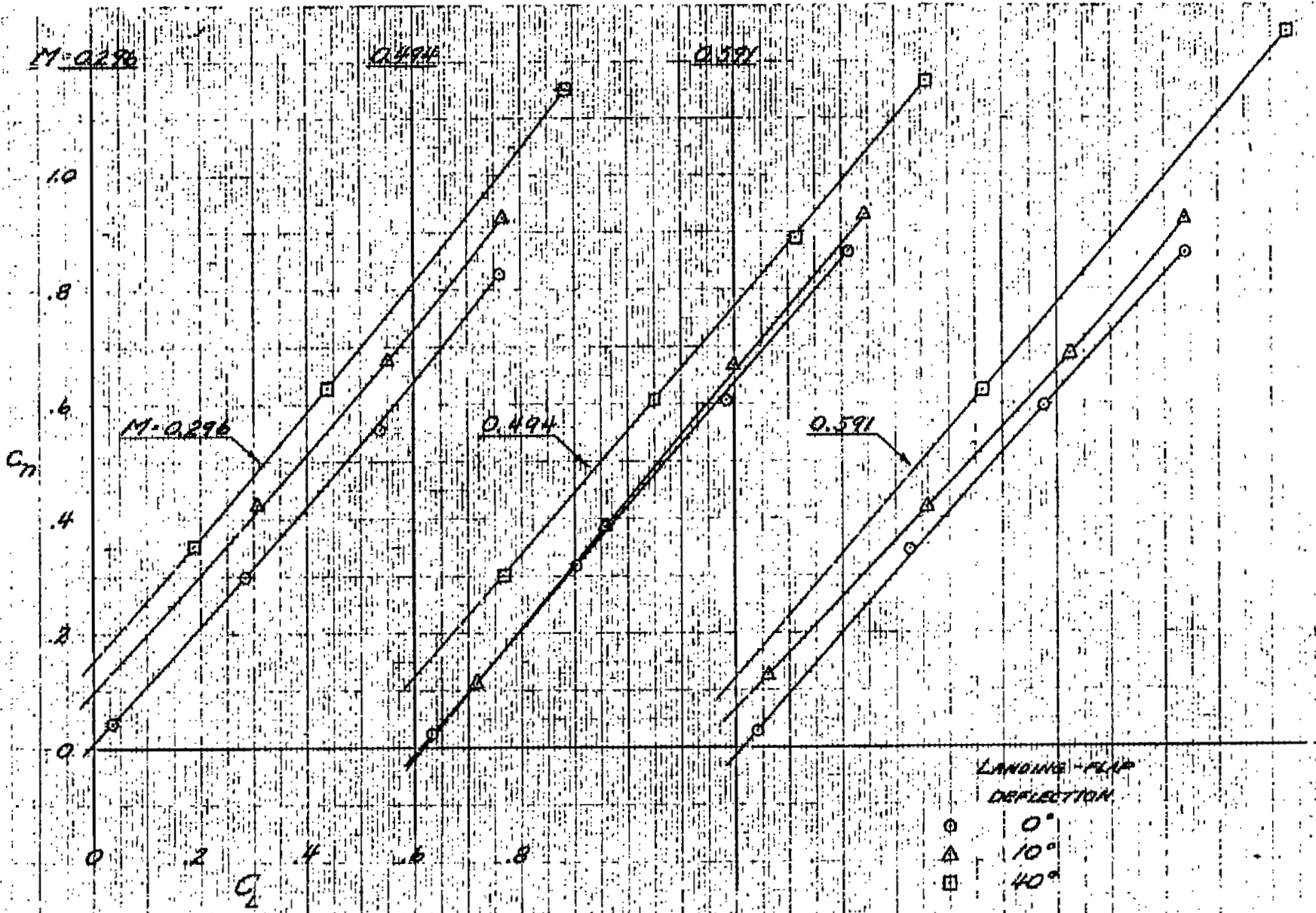
FIGURE 8. (b) $M=0.685, 0.73, \text{ AND } 0.778$
 CONCLUDED



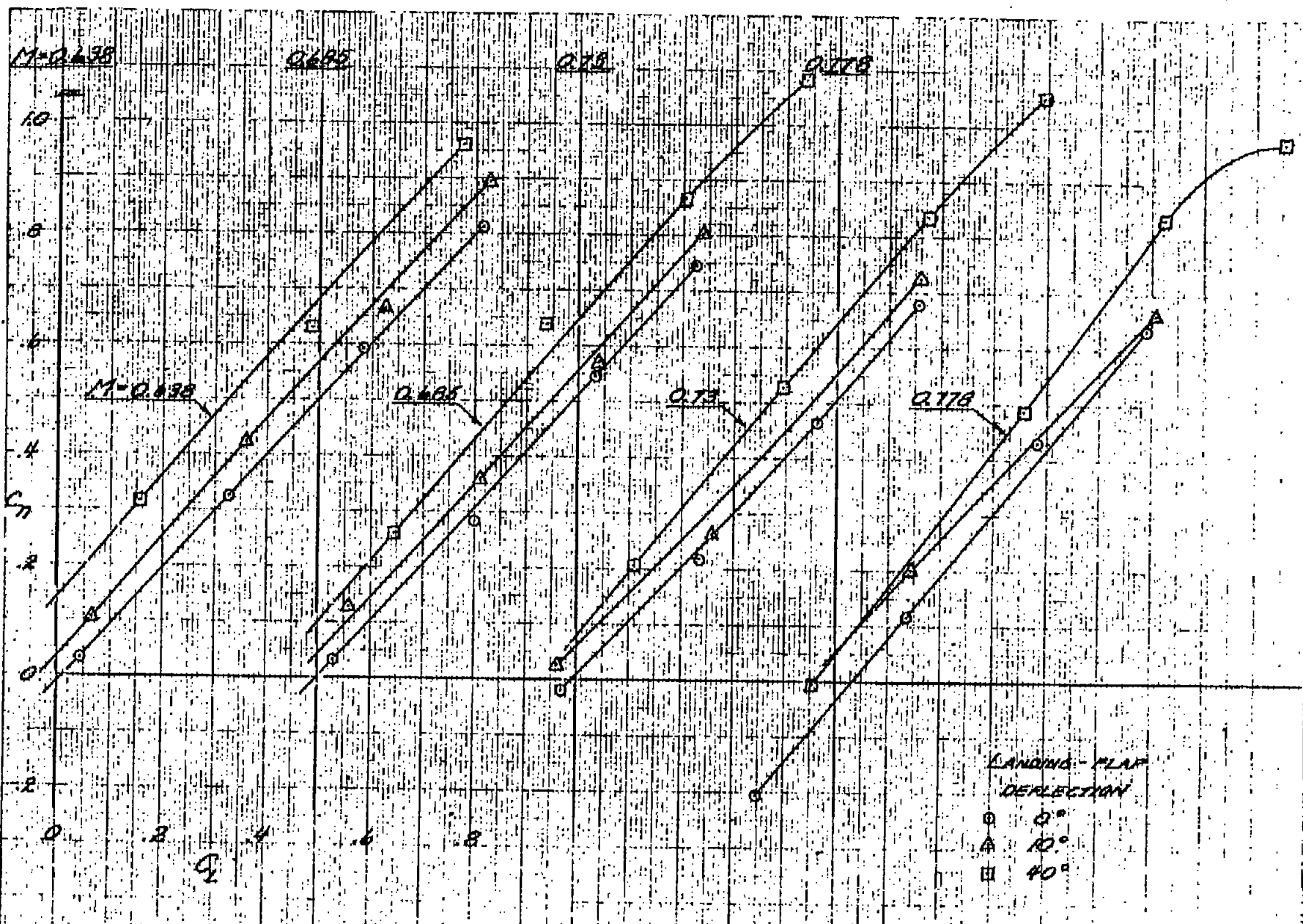
LANDING FLAP
DEFLECTION
 0°
 10°
 40°

National Advisory Committee for Aeronautics

(b) $M=0.638, 0.685, 0.730, \text{ AND } 0.778$
FIGURE 9. - CONCLUDED

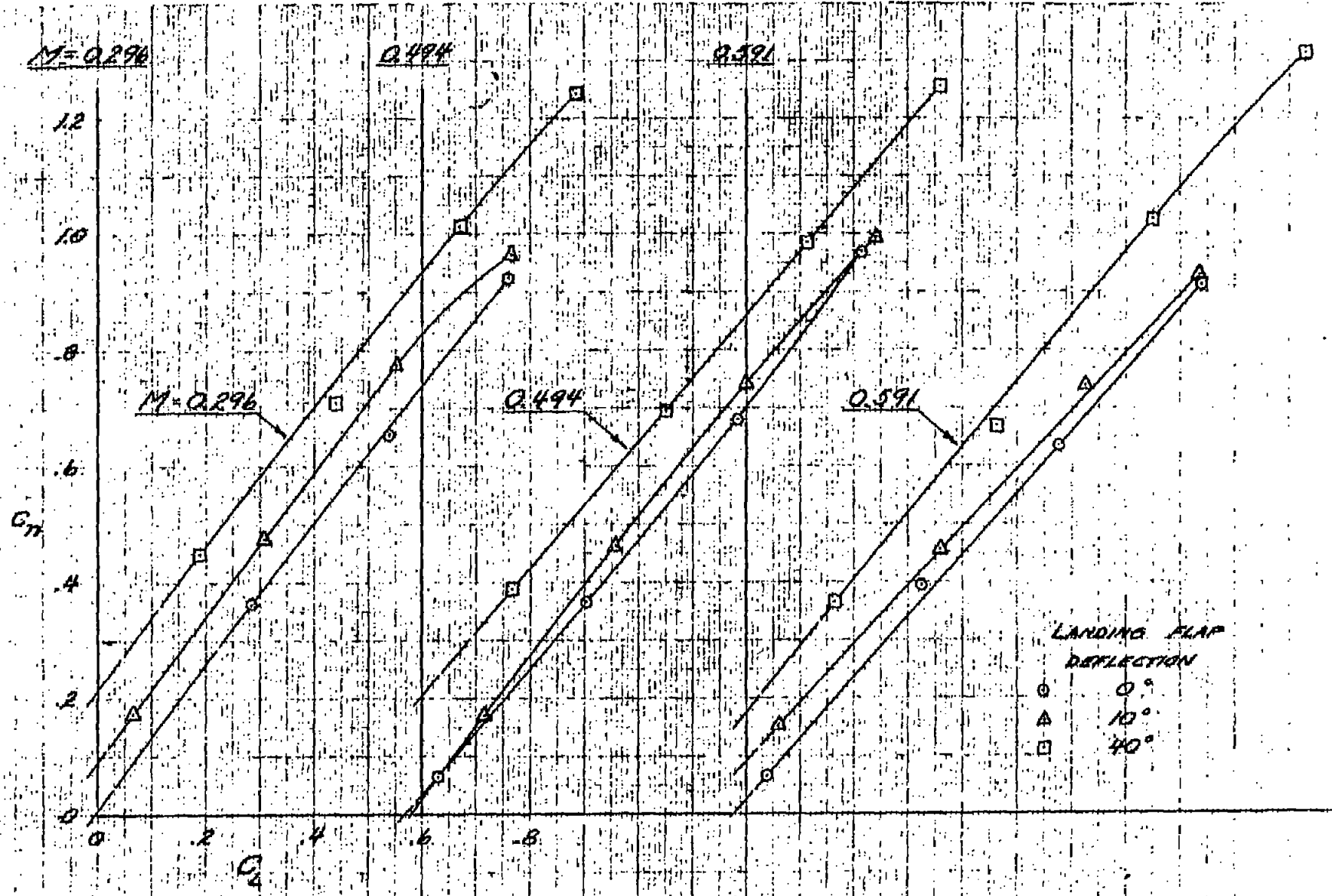


(2) $M = 0.296, 0.494, \text{ and } 0.591$
FIGURE 10.- VARIATION OF THE SECTION NORMAL-FORCE COEFFICIENT AT STATION 77.500 WITH TAIL-QUARTER LIFT COEFFICIENT, X5BRD-1 MODEL.
 National Advisory Committee for Aeronautics



LANDING-FLAP
DEFLECTION
 O 0°
 A 10°
 □ 40°

(b) $M=0.638, 0.695, 0.73, \text{ AND } 0.778$
 FIGURE 10.- CONCLUDED



(a) $M = 0.296, 0.494, \text{ and } 0.591$
 FIGURE 11. - VARIATION OF THE SECTION NORMAL-FORCE COEFFICIENT AT STATION 110.000 WITH TAIL-OFF LIFT COEFFICIENT. XSRD-1 MODEL.

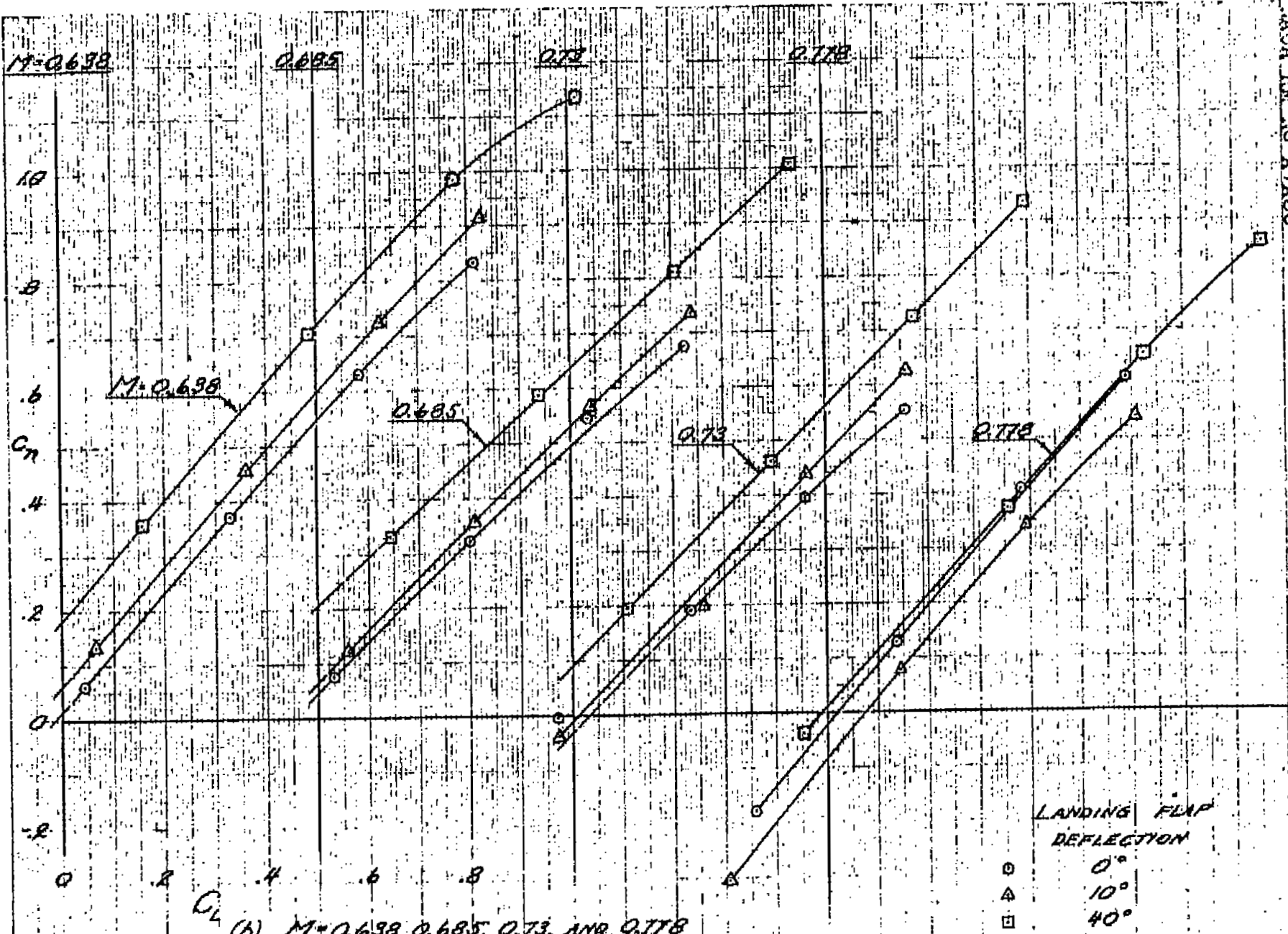
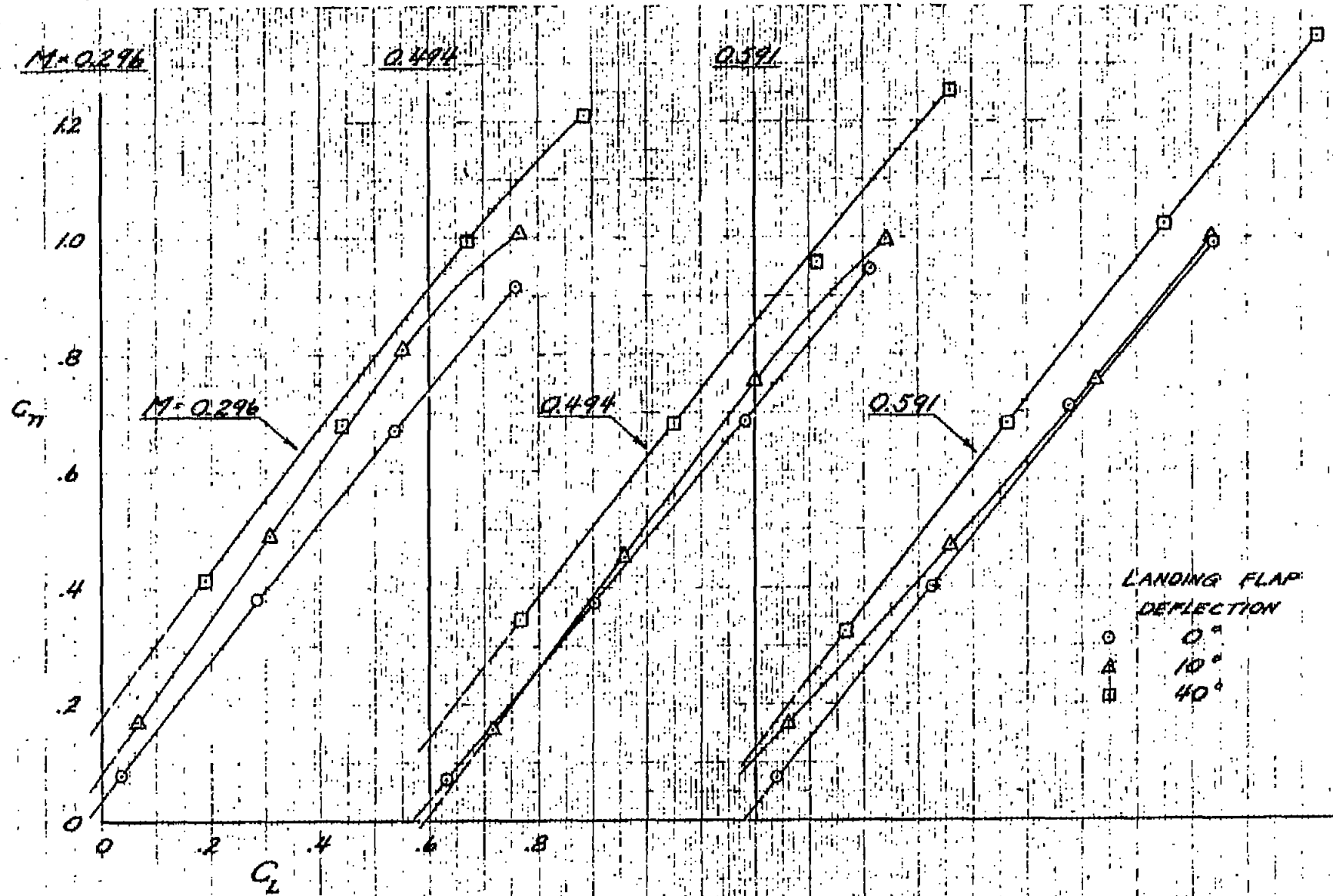


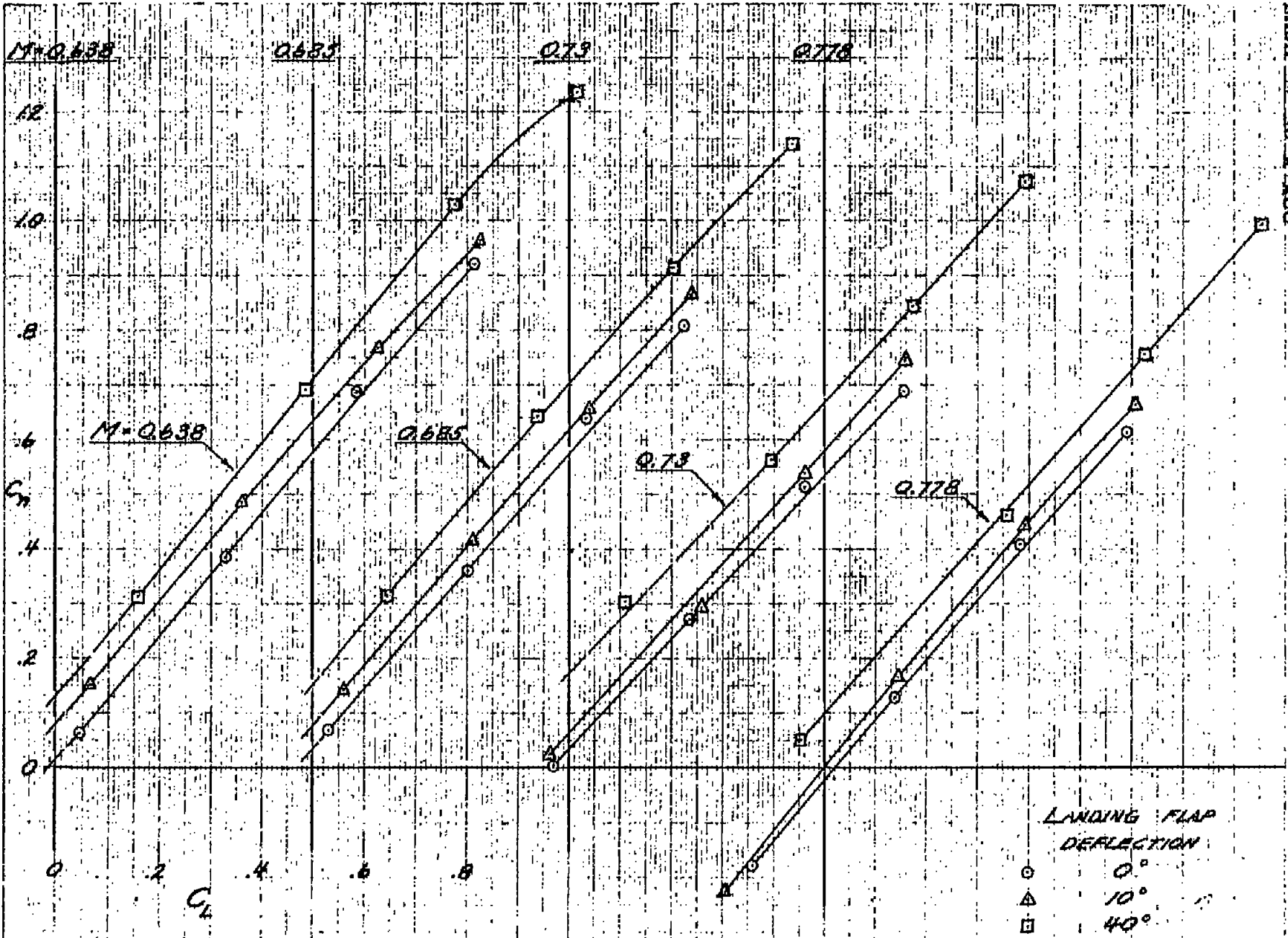
FIGURE 11. - CONCLUDED
 (b) $M=0.638, 0.685, 0.73, \text{ AND } 0.778$

LANDING FLAP DEFLECTION
 \circ 0°
 \triangle 10°
 \square 40°



LANDING FLAP DEFLECTION
 ○ 0°
 △ 10°
 □ 40°

(Q) $M=0.296, 0.494, \text{ AND } 0.591$
 FIGURE 12. - VARIATION OF THE SECTION NORMAL-FORCE COEFFICIENT AT STATION 140.000 WITH TAIL-OFF LIFT COEFFICIENT XSB2D-1 MODEL.
 National Advisory Committee for Aeronautics



(b) $M = 0.638, 0.685, 0.73, \text{ AND } 0.778$

FIGURE 12. - CONCLUDED

$M=0.296$

0.494

0.591

C_n

1.2

1.0

0.8

0.6

0.4

0.2

0

0

0.2

0.4

0.6

0.8

C_L

$M=0.296$

0.494

0.591

LANDING FLAP DEFLECTION

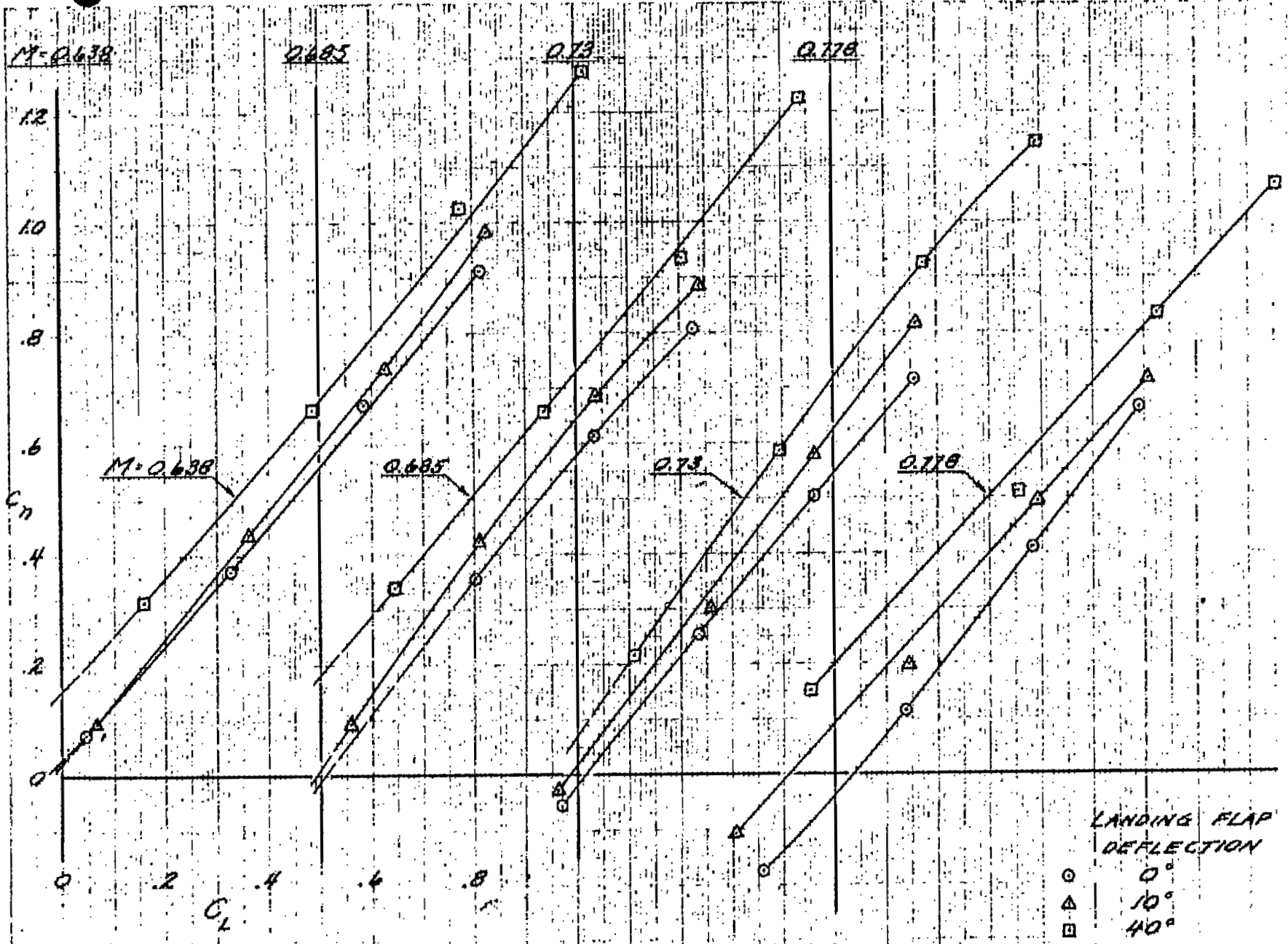
○ 0°

△ 10°

□ 40°

(2) $M=0.296, 0.494, \text{ AND } 0.591$

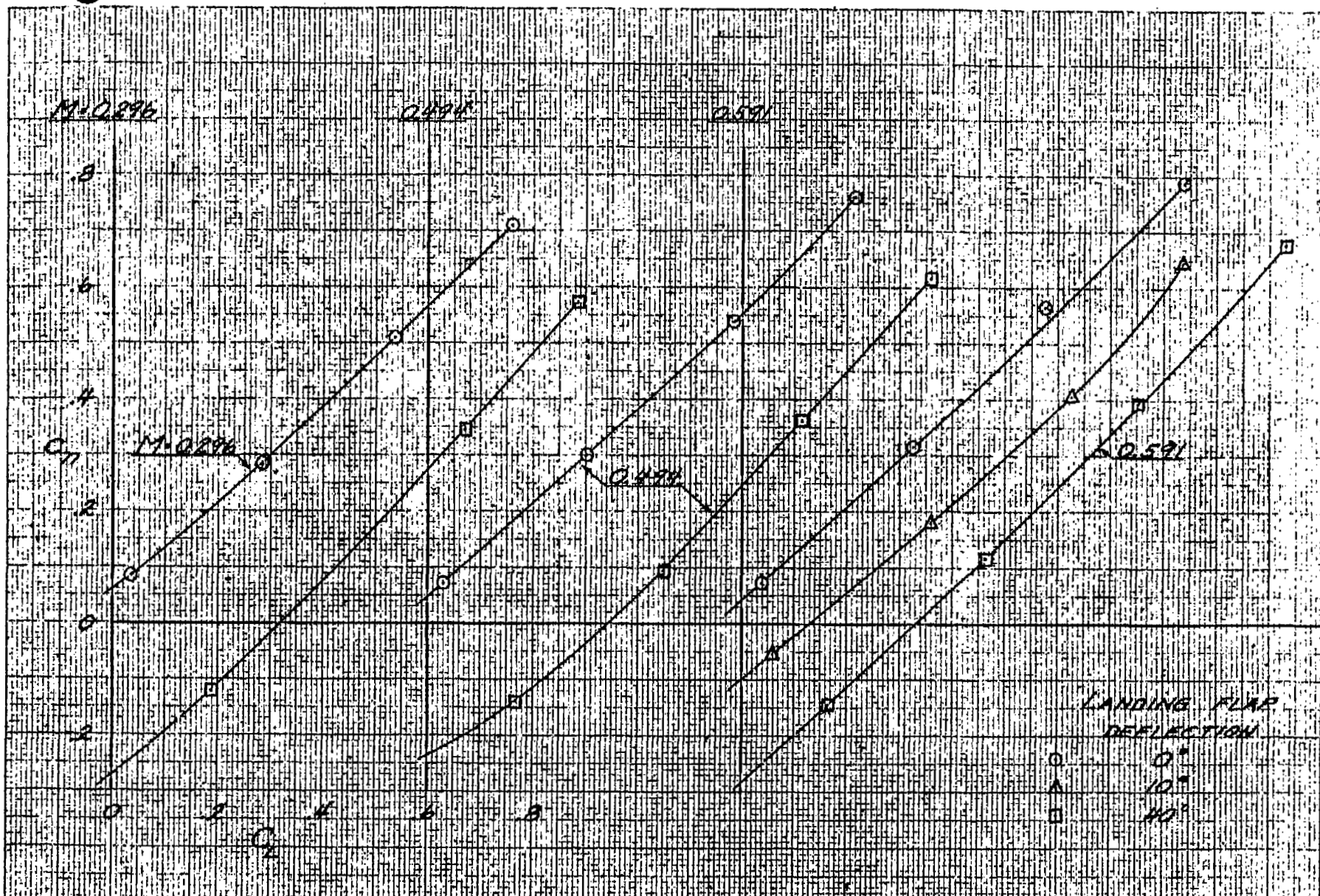
FIGURE 13. - VARIATION OF THE SECTION NORMAL-FORCE COEFFICIENT AT STATION 170.834 WITH TAIL-OFF LIFT COEFFICIENT. XSB30-1 MODEL.



(b) $M=0.638, 0.685, 0.73, \text{ AND } 0.778$

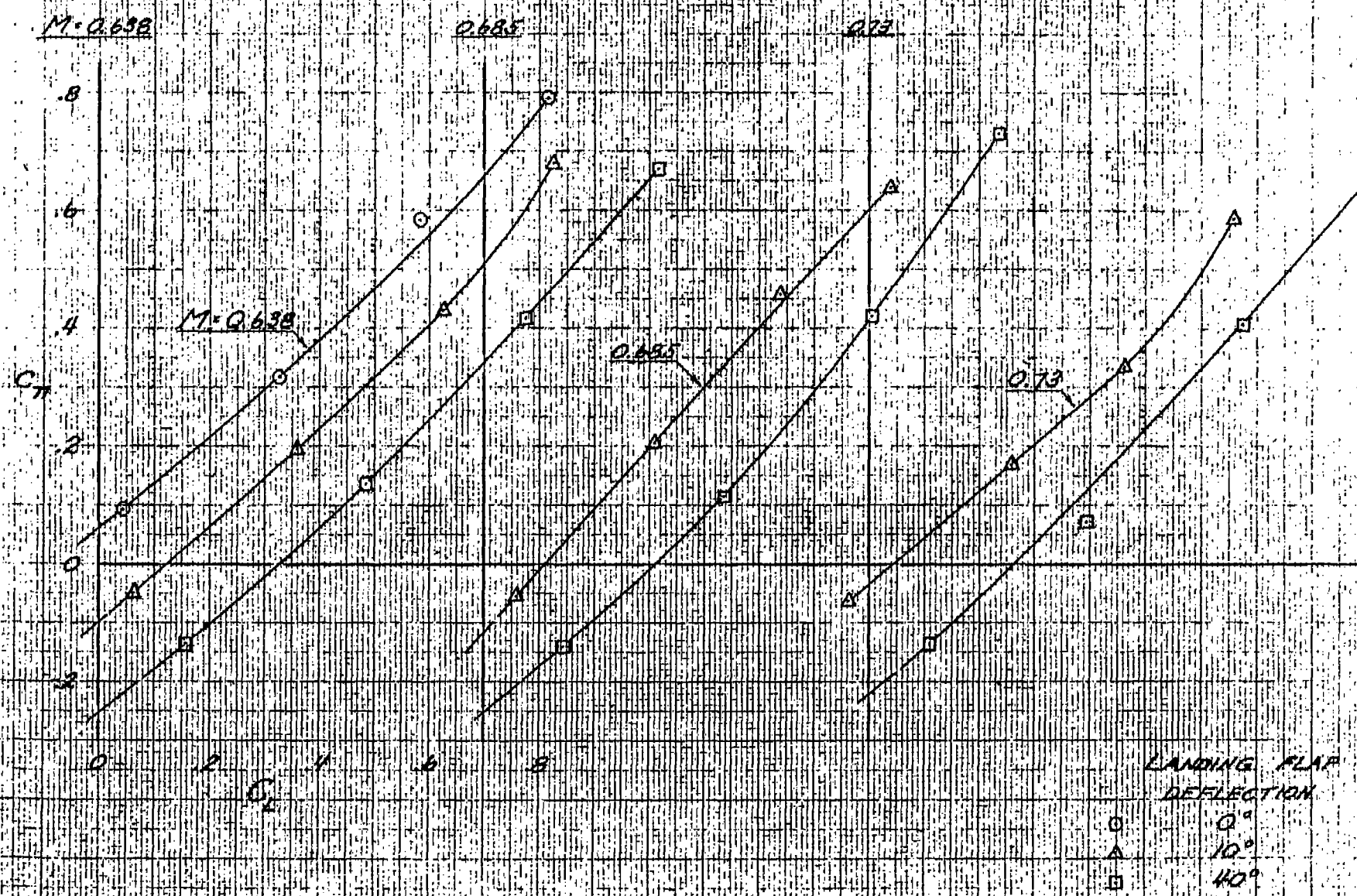
FIGURE 13: CONCLUDED

National Advisory Committee for Aeronautics



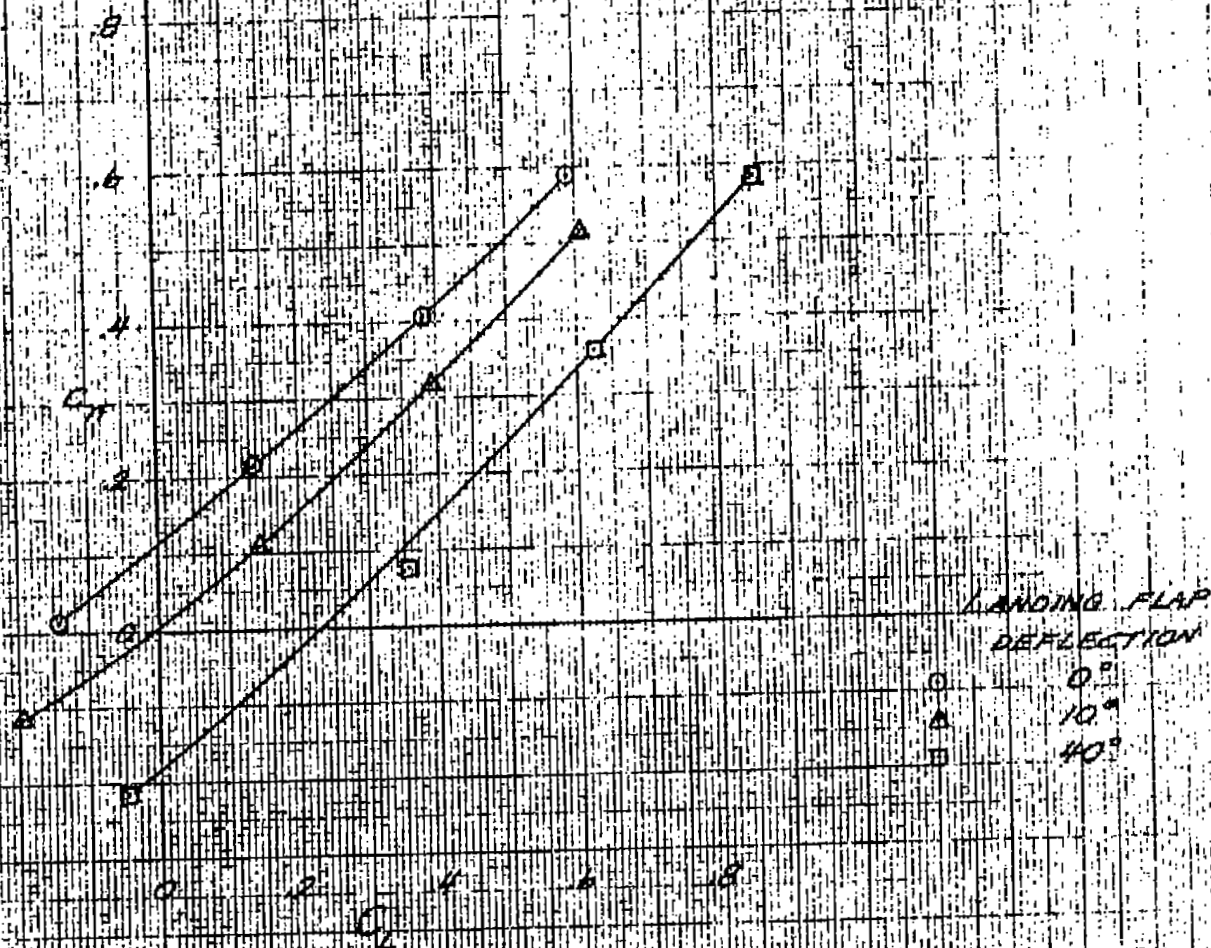
(C) $M=0.296$, 0.474 AND 0.591

FIGURE 14. - VARIATION OF THE SECTION NORMAL-FORCE COEFFICIENT AT SECTION 218.093 WITH TAIL-OFF LIFT COEFFICIENT, X5620-J MODEL

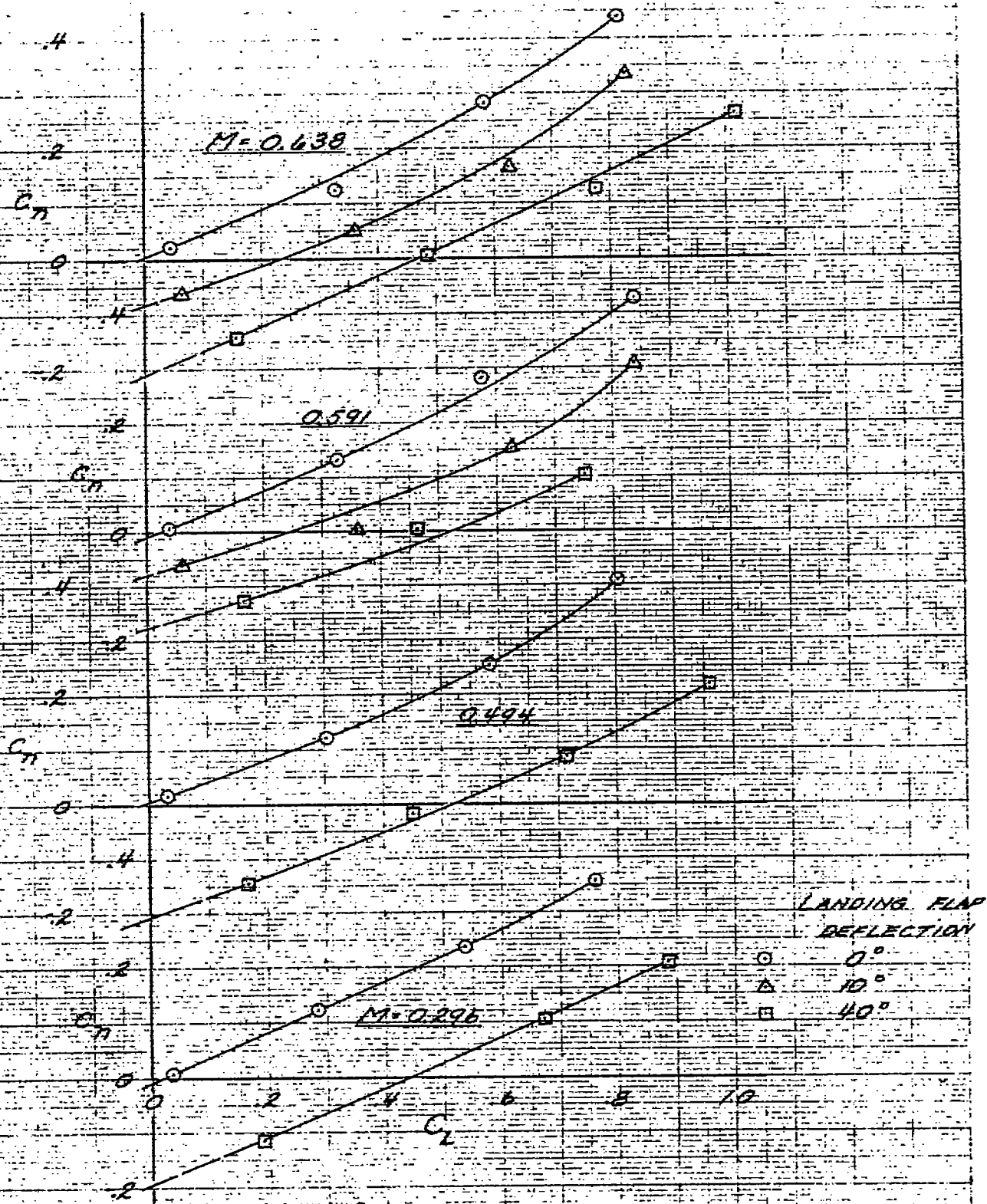


(b) $M=0.638, 0.685, \text{ AND } 0.73$

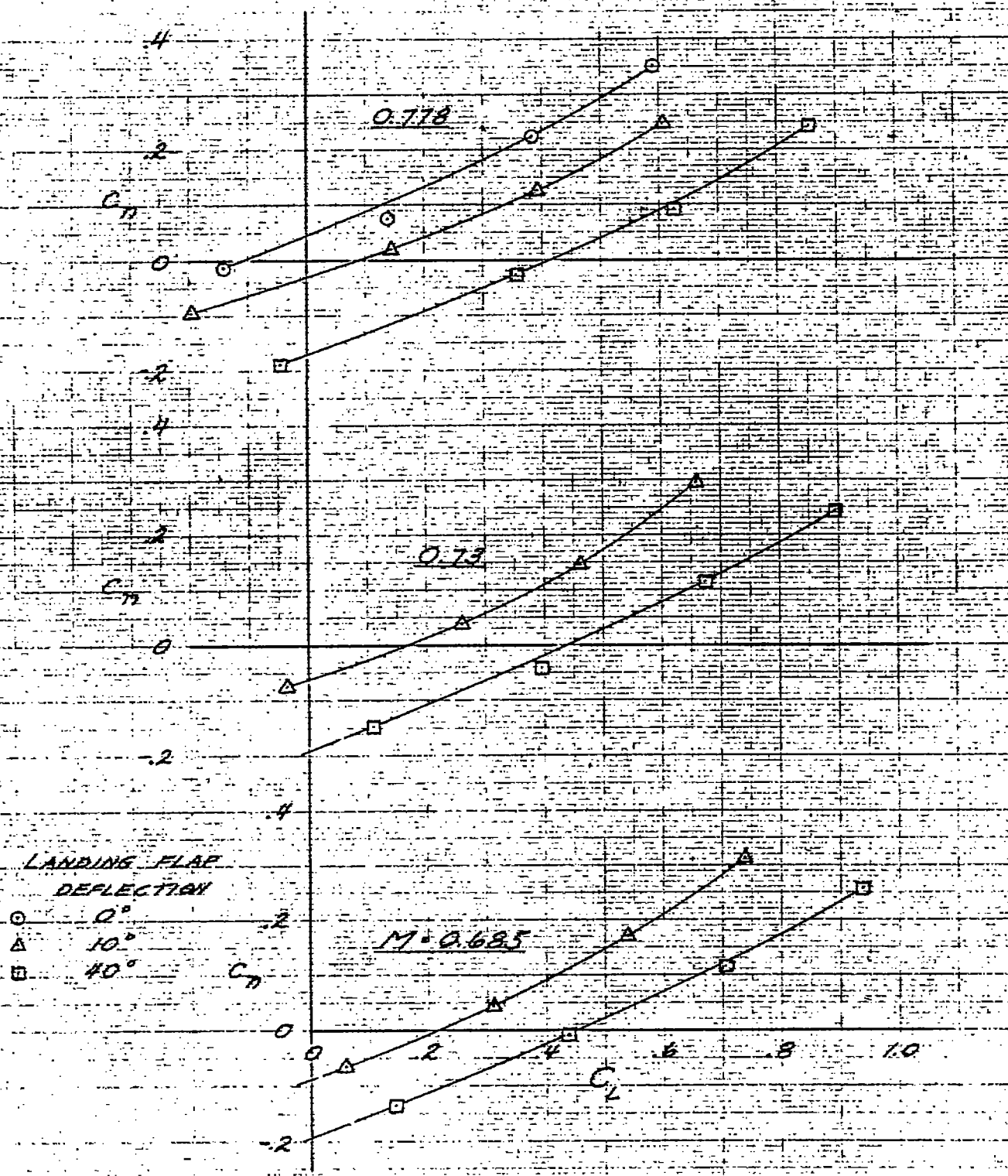
FIGURE 14 - CONTINUED



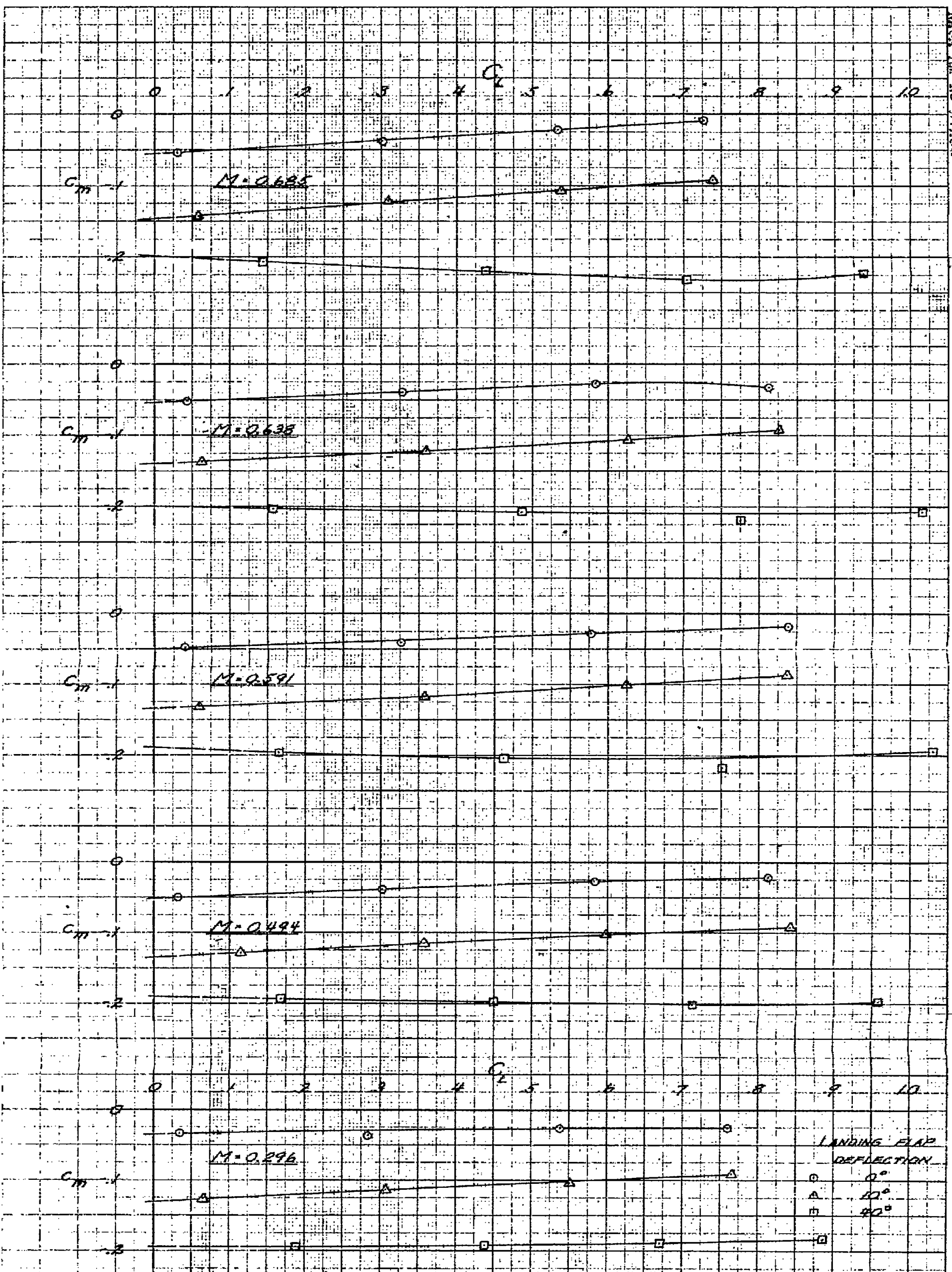
(C) $M = 0.118$
 FIGURE 1A - CONCLUDED



(*) $M=0.296, 0.494, 0.591, \text{ AND } 0.638$
 FIGURE 15. - VARIATION OF THE SECTION NORMAL FORCE COEFFICIENT AT STATION 266.394 WITH TAIL-ORD ORIGIN LIFT COEFFICIENT. XSB2D-1 MODEL.

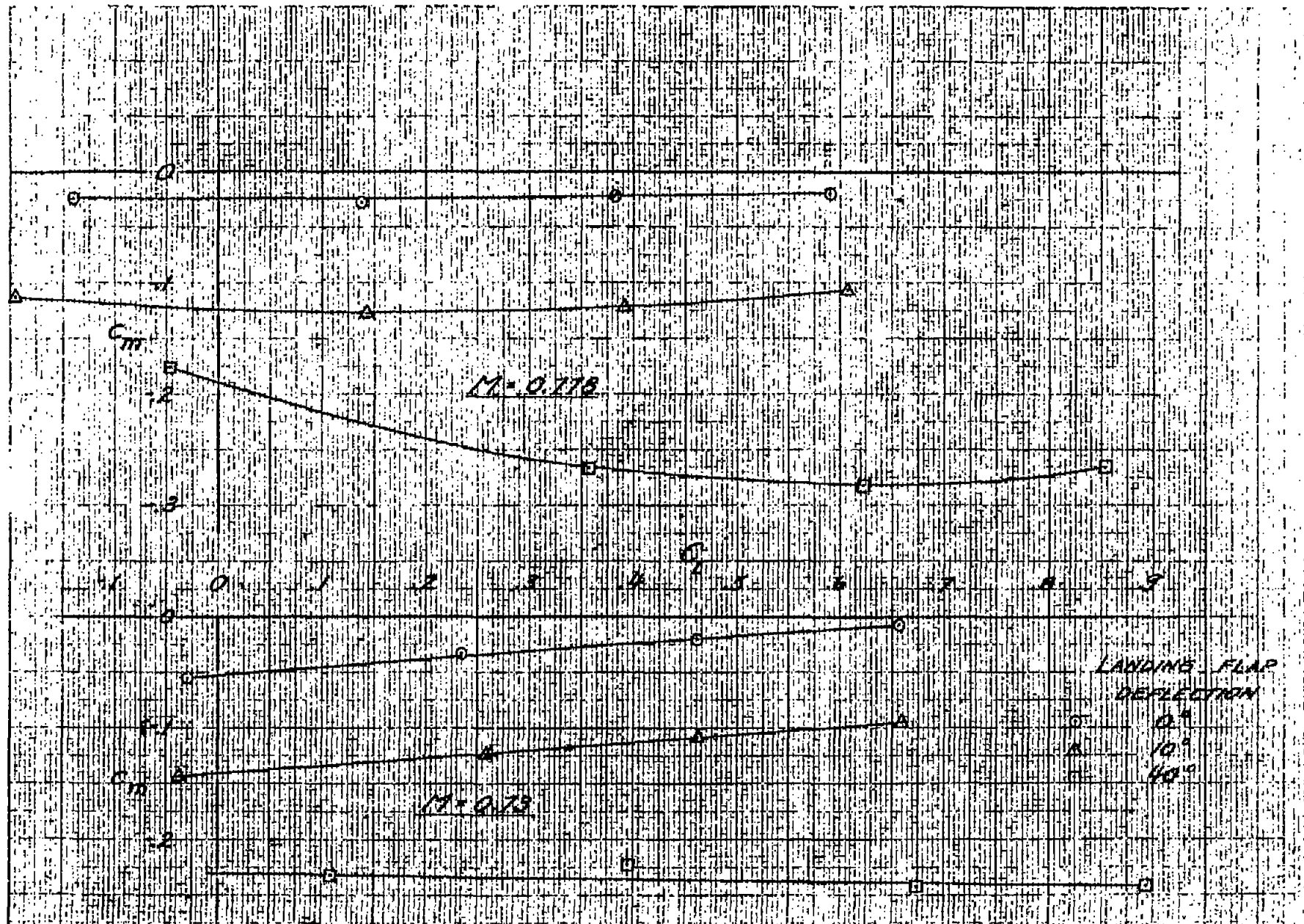


(b) *M* = 0.685, 0.730, AND 0.718
 FIGURE 15.- CONCLUDED



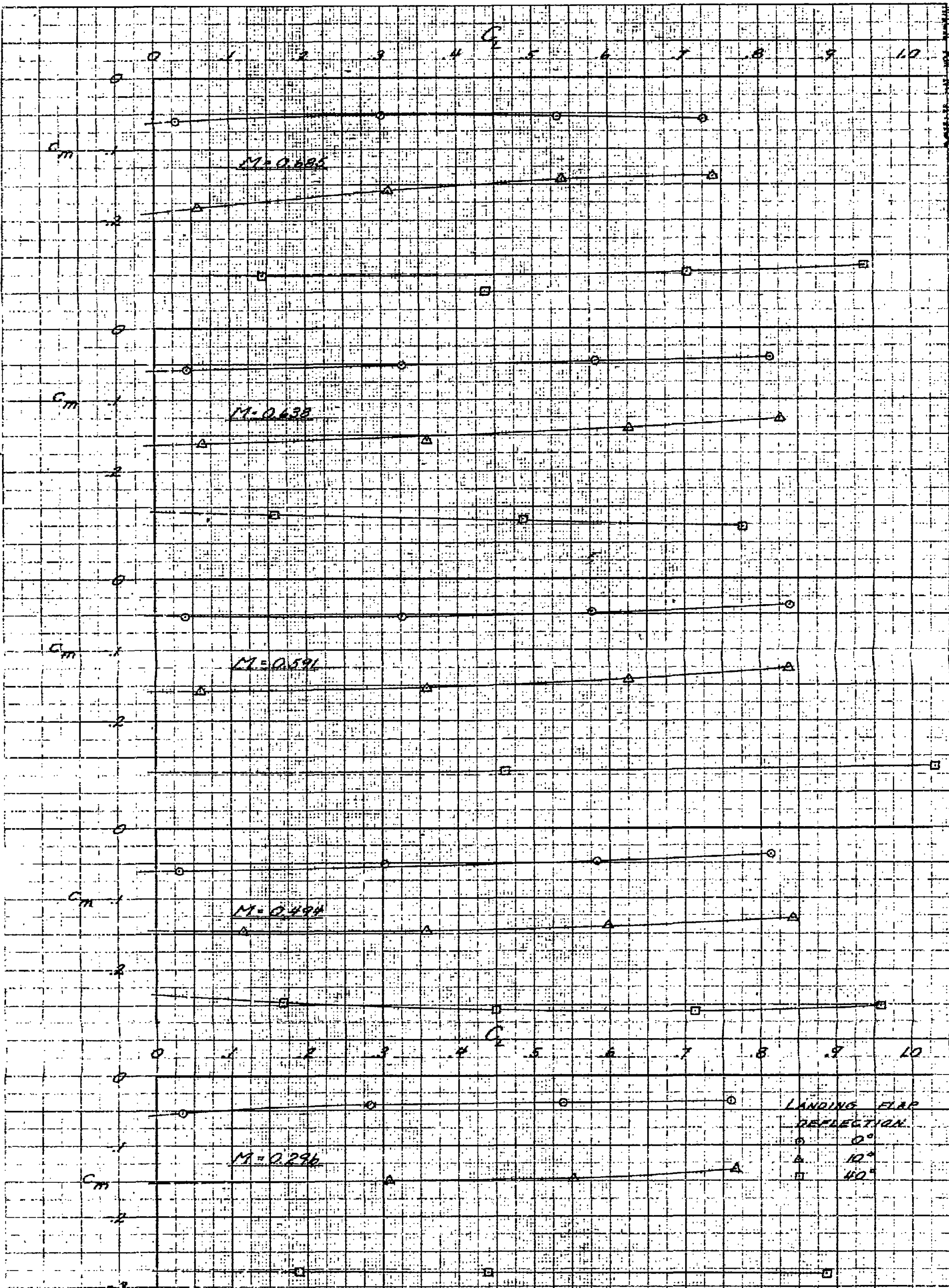
LANDING FLAP DEFLECTION
 ○ 0°
 △ 10°
 □ 40°

(G) M = 0.296, 0.494, 0.591, 0.638, AND 0.685
 FIGURE 16. - VARIATION OF SECTION PITCHING-MOMENT COEFFICIENT AT STATION 40.102 WITH TAIL-REEF LIFT COEFFICIENT, XSB20-L MODEL; MOMENT AXIS AT 25.75 PERCENT CHORD.



(b) $M = 0.75$ AND 0.775

FIGURE 16 - CONCLUDED.



LANDING FLAP DEFLECTION
 ○ 0°
 △ 10°
 □ 40°

(2) $M=0.296, 0.494, 0.591, 0.638, \text{ AND } 0.685$
 FIGURE 17.- VARIATION OF THE SECTION PITCHING-MOMENT COEFFICIENT AT STATION 77.500 WITH TAIL-OFF LIFT COEFFICIENT. XSRD-1 MODEL, MOMENT AXIS AT 25.4 PERCENT CHORD
 National Advisory Committee for Aeronautics

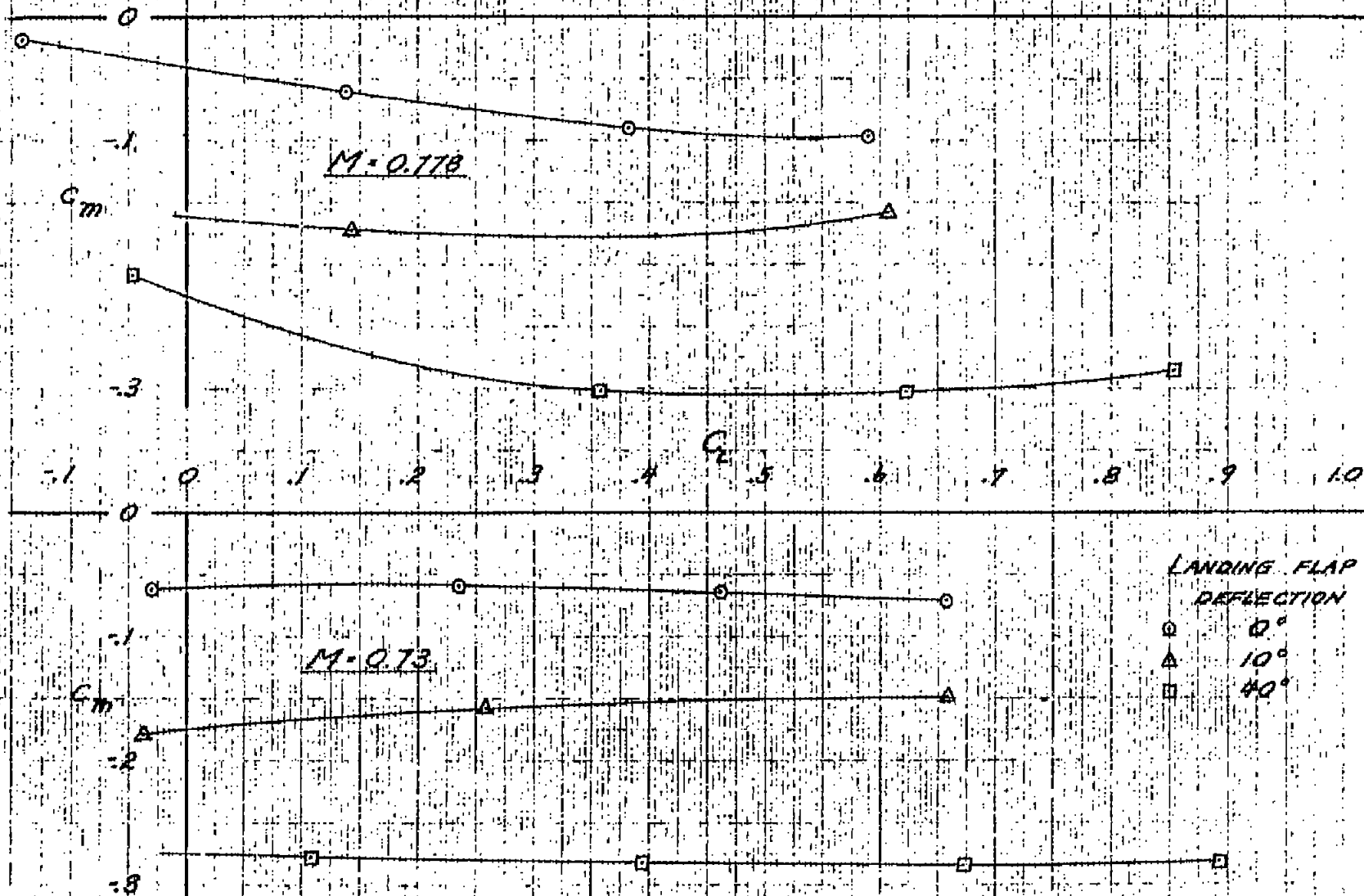
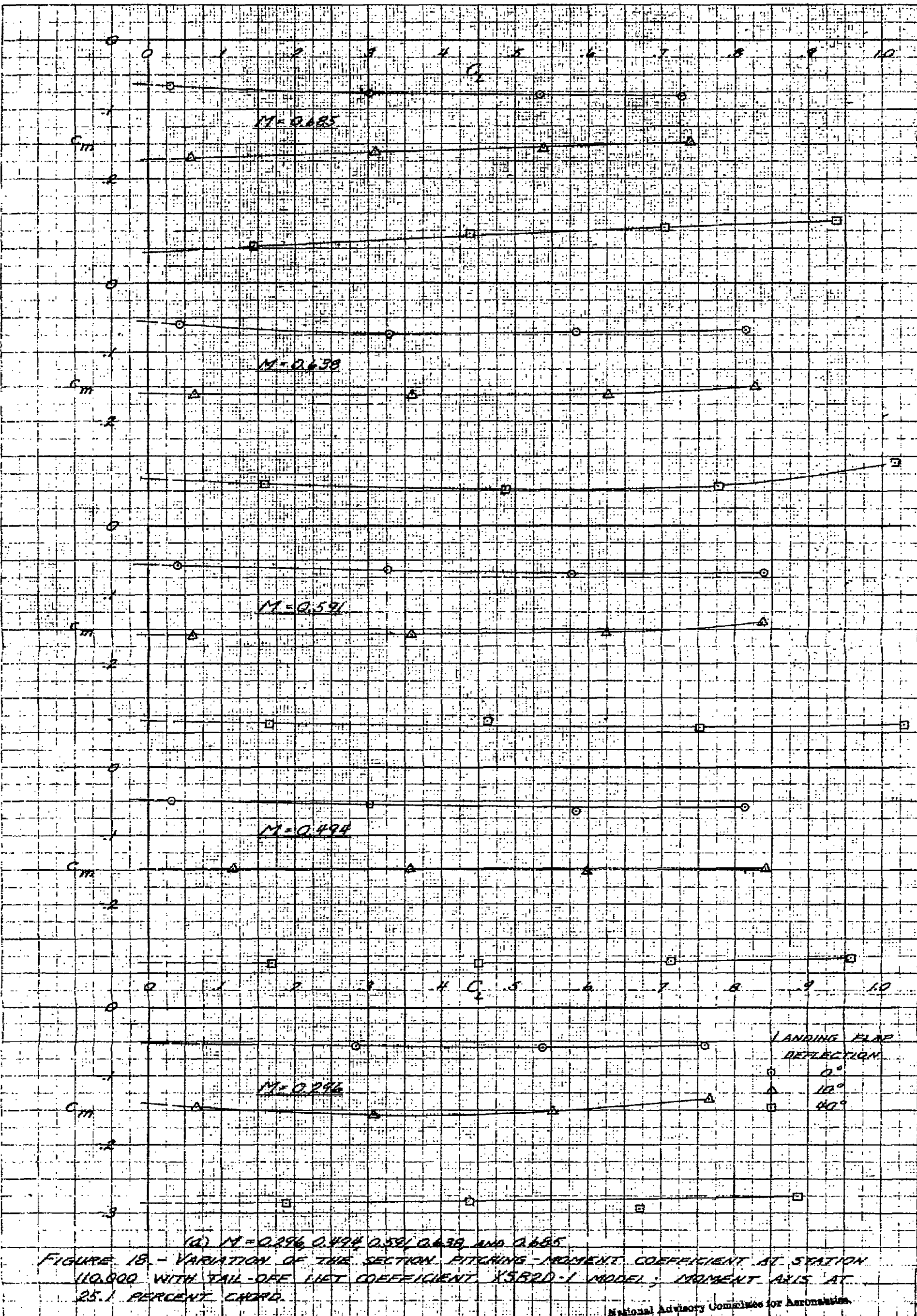
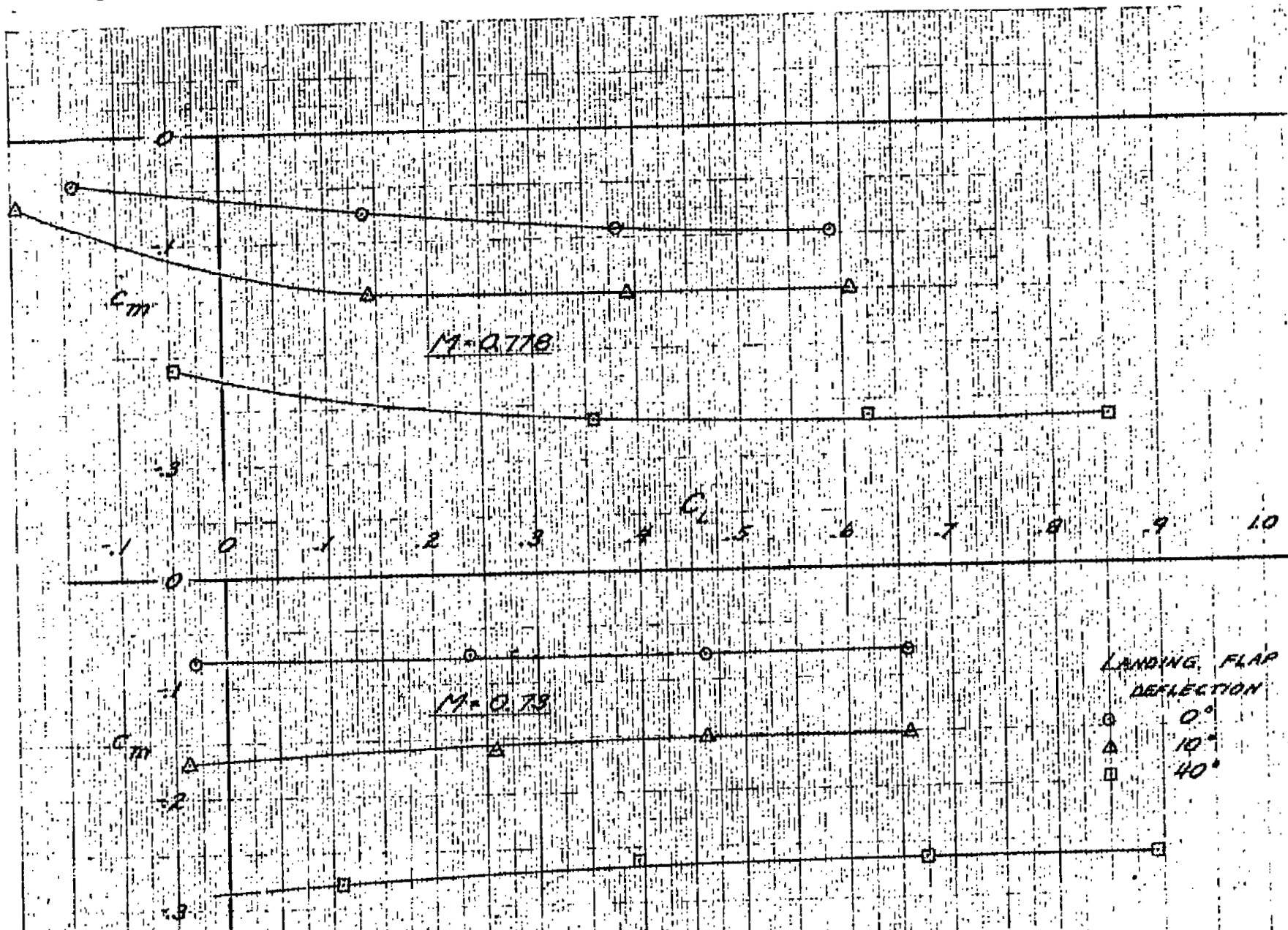
(b) $M = 0.73$ AND 0.778

FIGURE 17. CONCLUDED

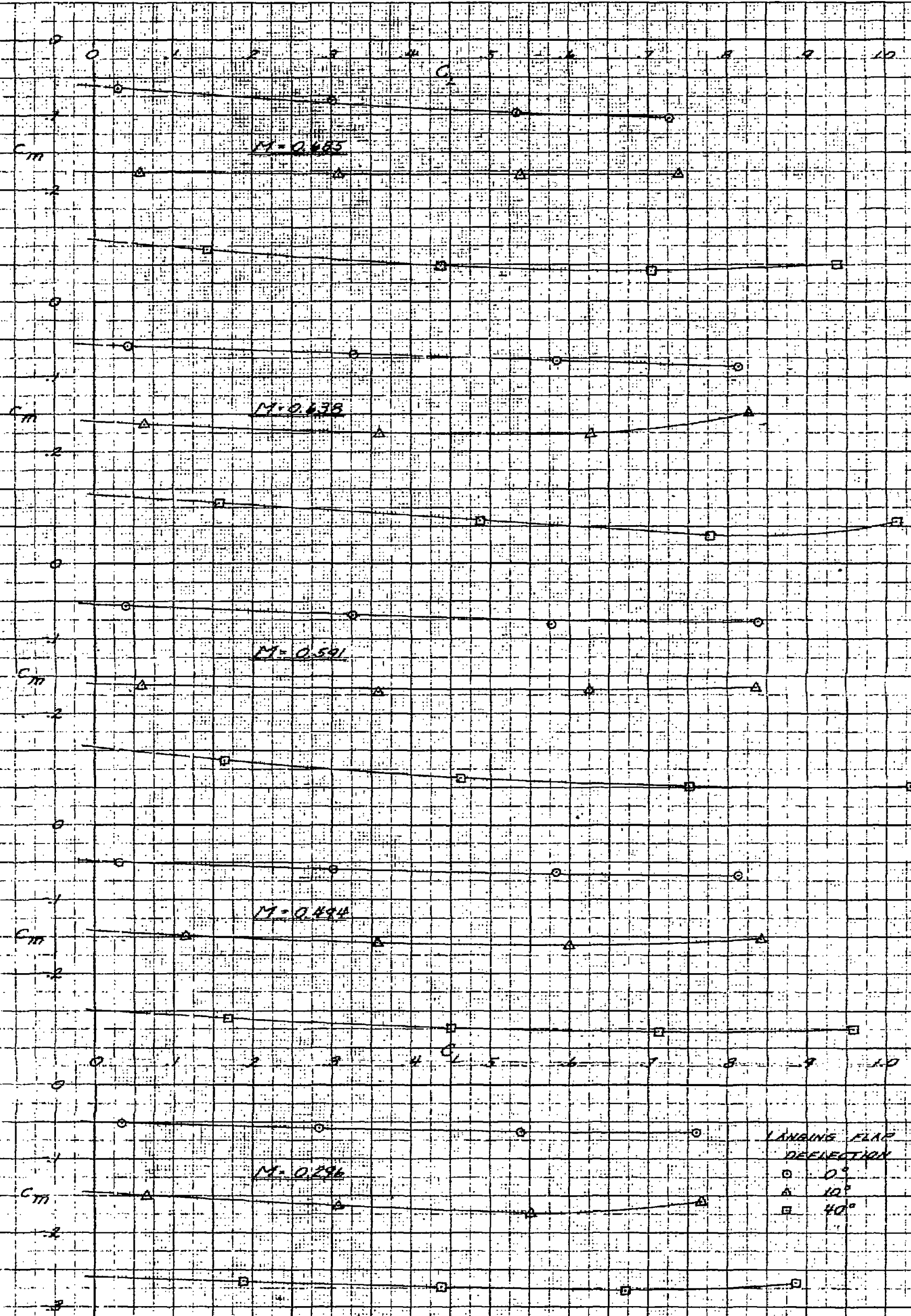




LANDING FLAP DEFLECTION
 ○ 0°
 △ 10°
 □ 40°

(b) $M = 0.73$ AND 0.778

FIGURE 18. CONCLUDED



(Q) $M = 0.296, 0.494, 0.591, 0.438$ AND 0.485
 FIGURE 18. - VARIATION OF THE SECTION PITCHING-MOMENT COEFFICIENT AT STATION 140.000 WITH TAIL-OFF LIFT COEFFICIENT, X5B20-1 MODEL, MOMENT AXIS AT 24.7 PERCENT CHORD.

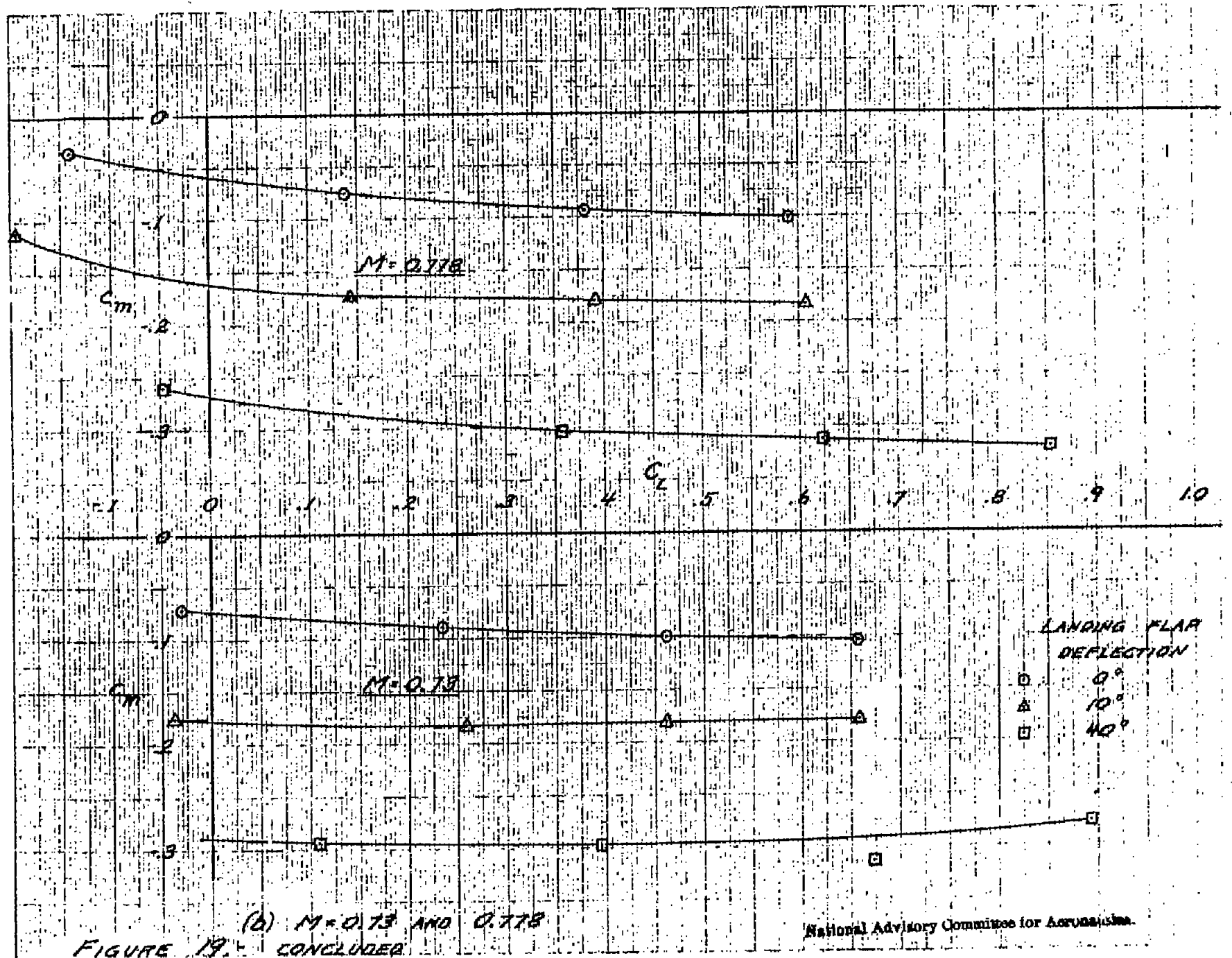
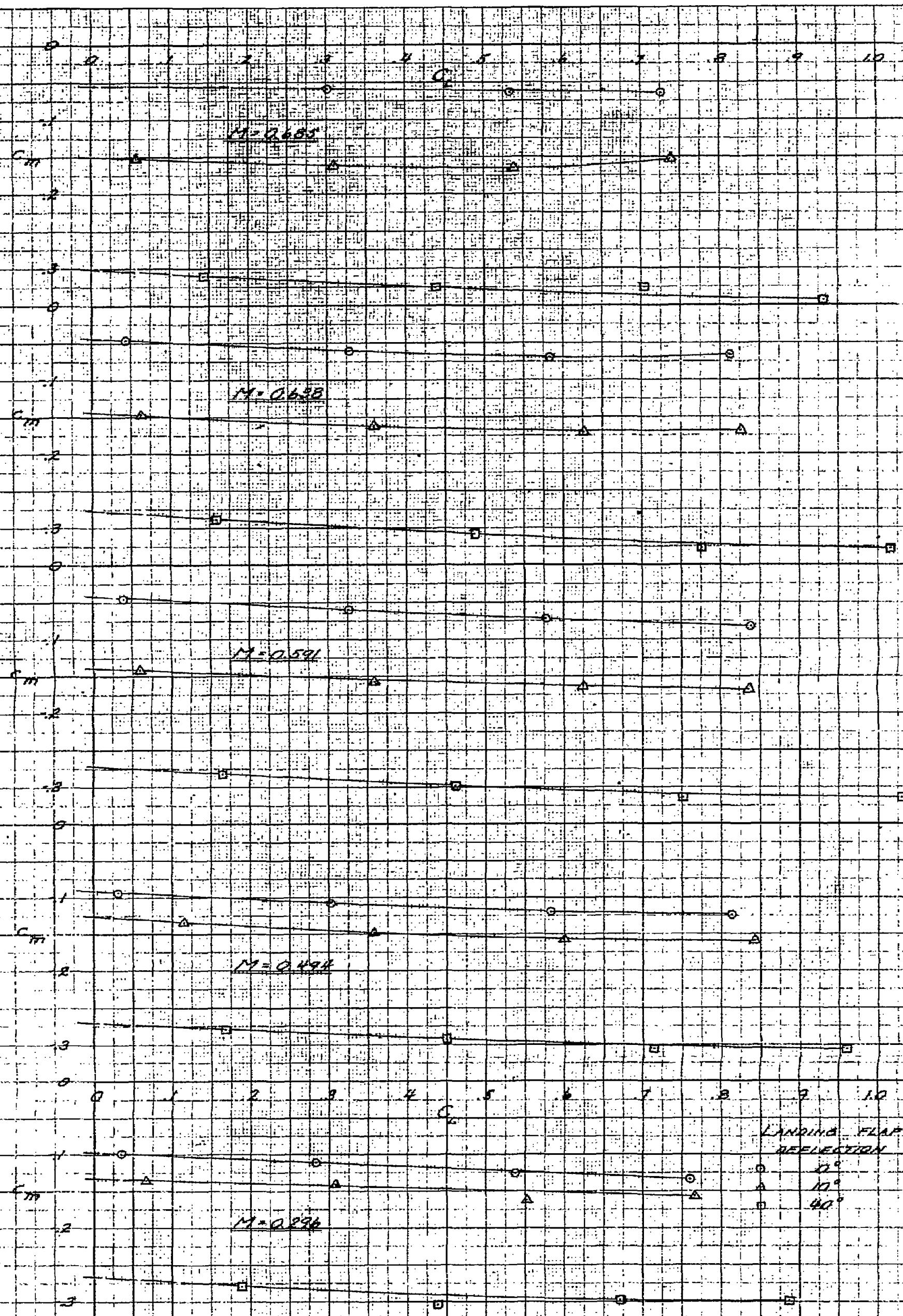


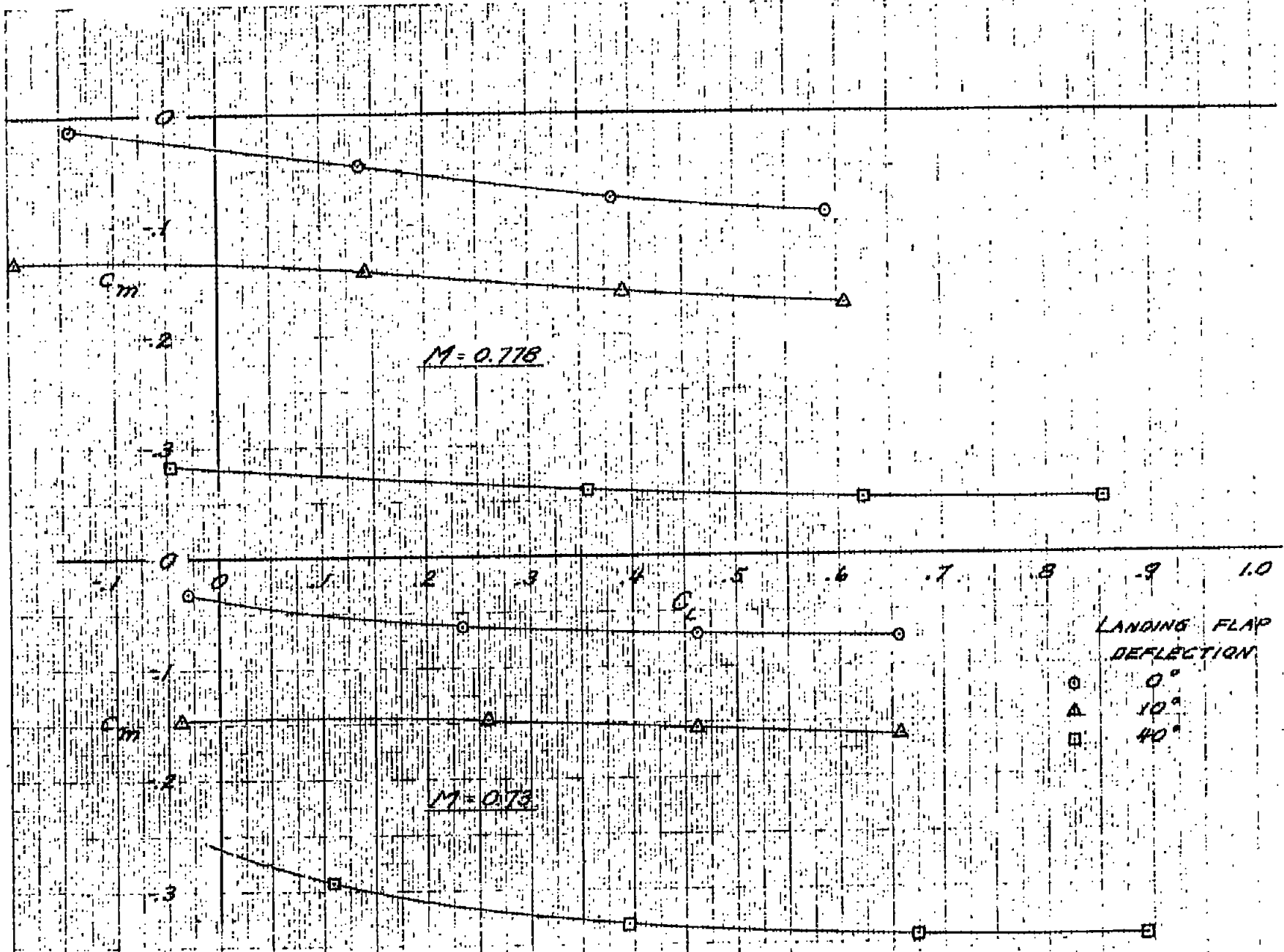
FIGURE 19. (b) $M = 0.13$ AND 0.778
CONCLUDED

National Advisory Committee for Aeronautics



LANDING FLAP
DEFLECTION
 \circ 0°
 \triangle 10°
 \square 40°

(2) $M = 0.296, 0.494, 0.591, 0.638$ AND 0.685
 FIGURE 20. - VARIATION OF THE SECTION PITCHING-MOMENT COEFFICIENT AT STATION 170.334 WITH TAIL-OFF LIFT COEFFICIENT XSRD-1 MODEL; MOMENT AXIS AT 24.3 PERCENT CHORD.



(b) $M = 0.73$ AND 0.778

FIGURE 20. CONCLUDED

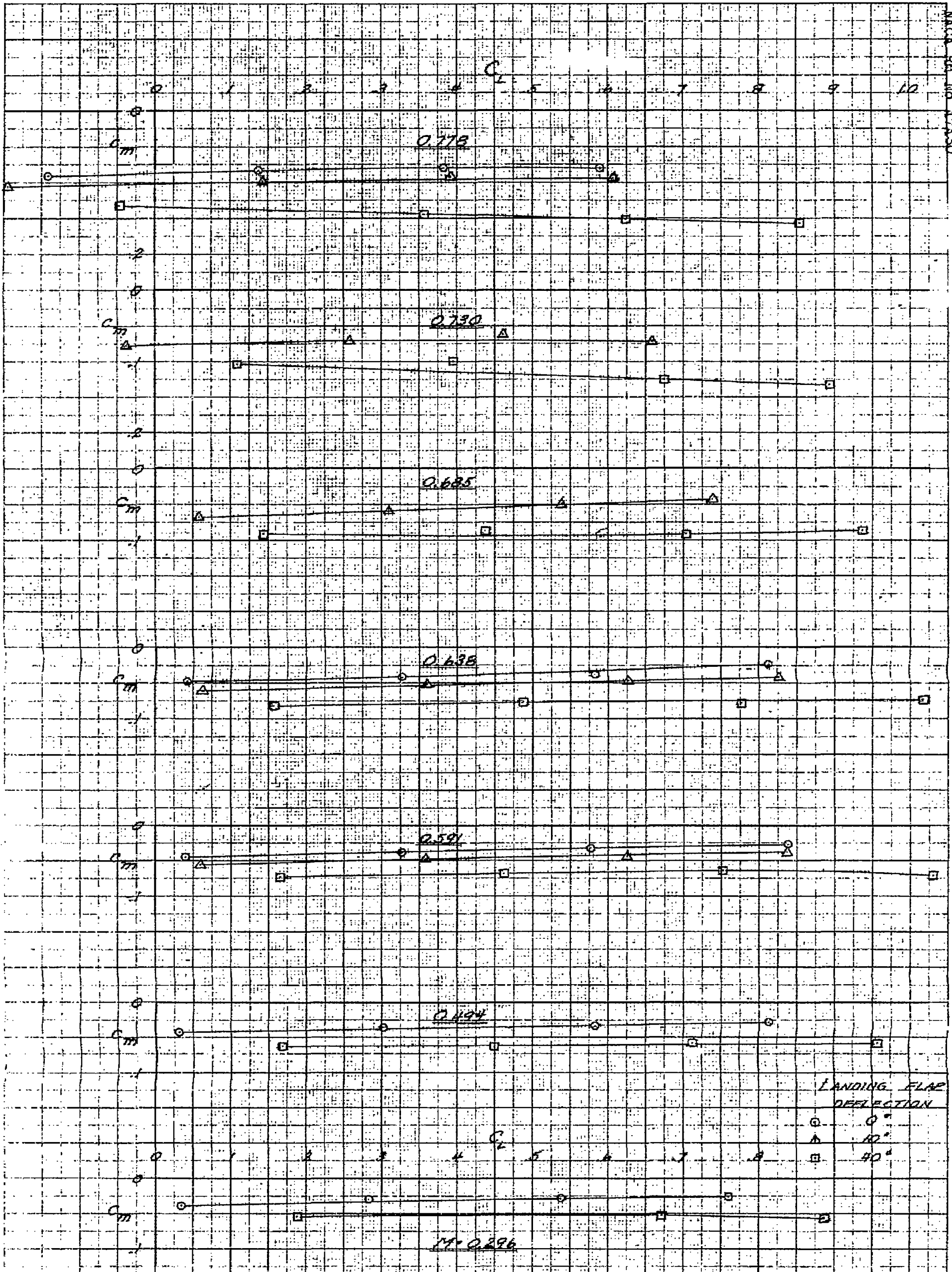


FIGURE 21 - VARIATION OF THE SECTION PITCHING-MOMENT COEFFICIENT AT STATION 218.029 WITH TAIL-OFF LIFT COEFFICIENT, X5B2D-1 MODEL; MOMENT AXIS AT 23.5 PERCENT CHORD.

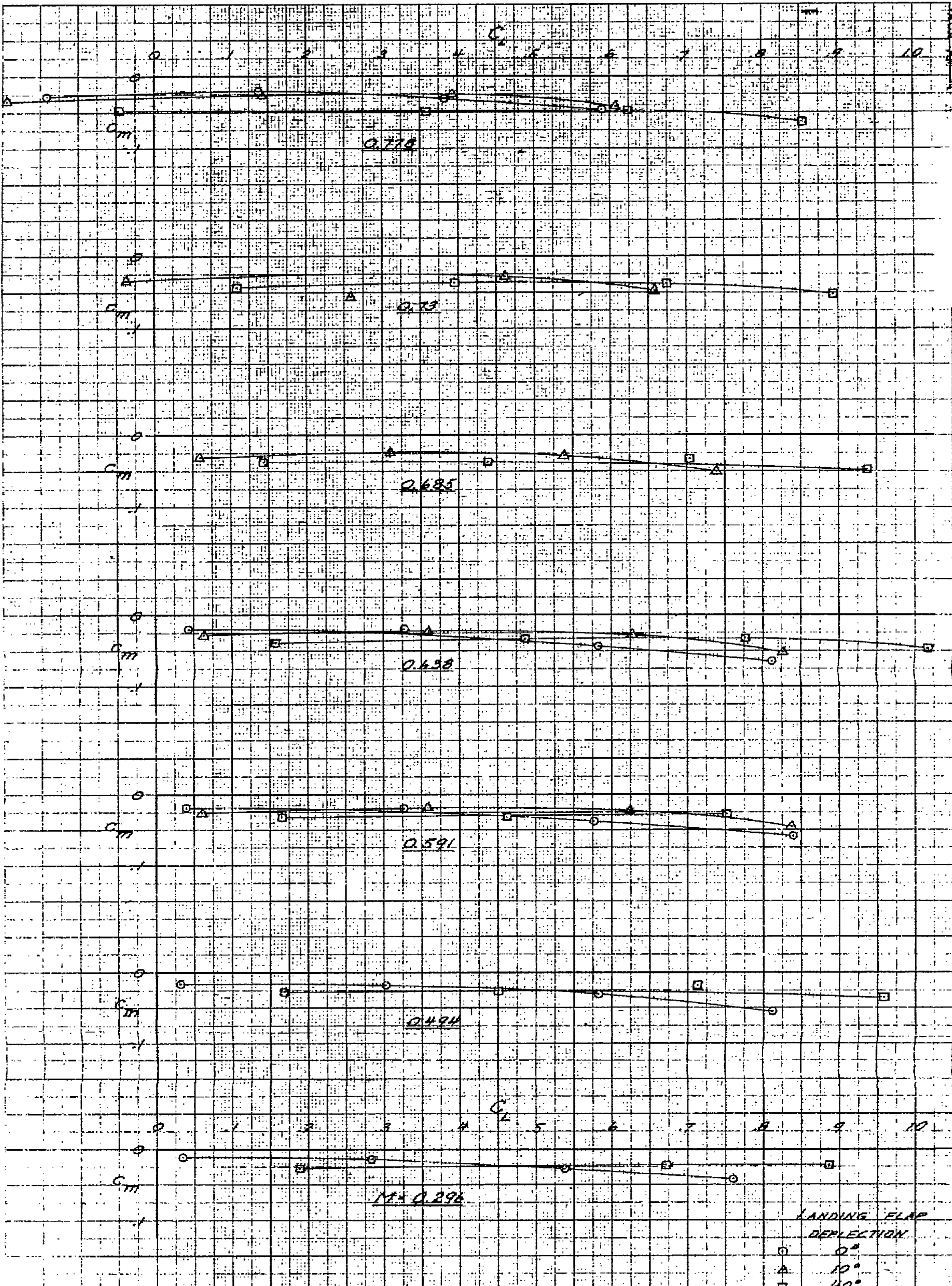
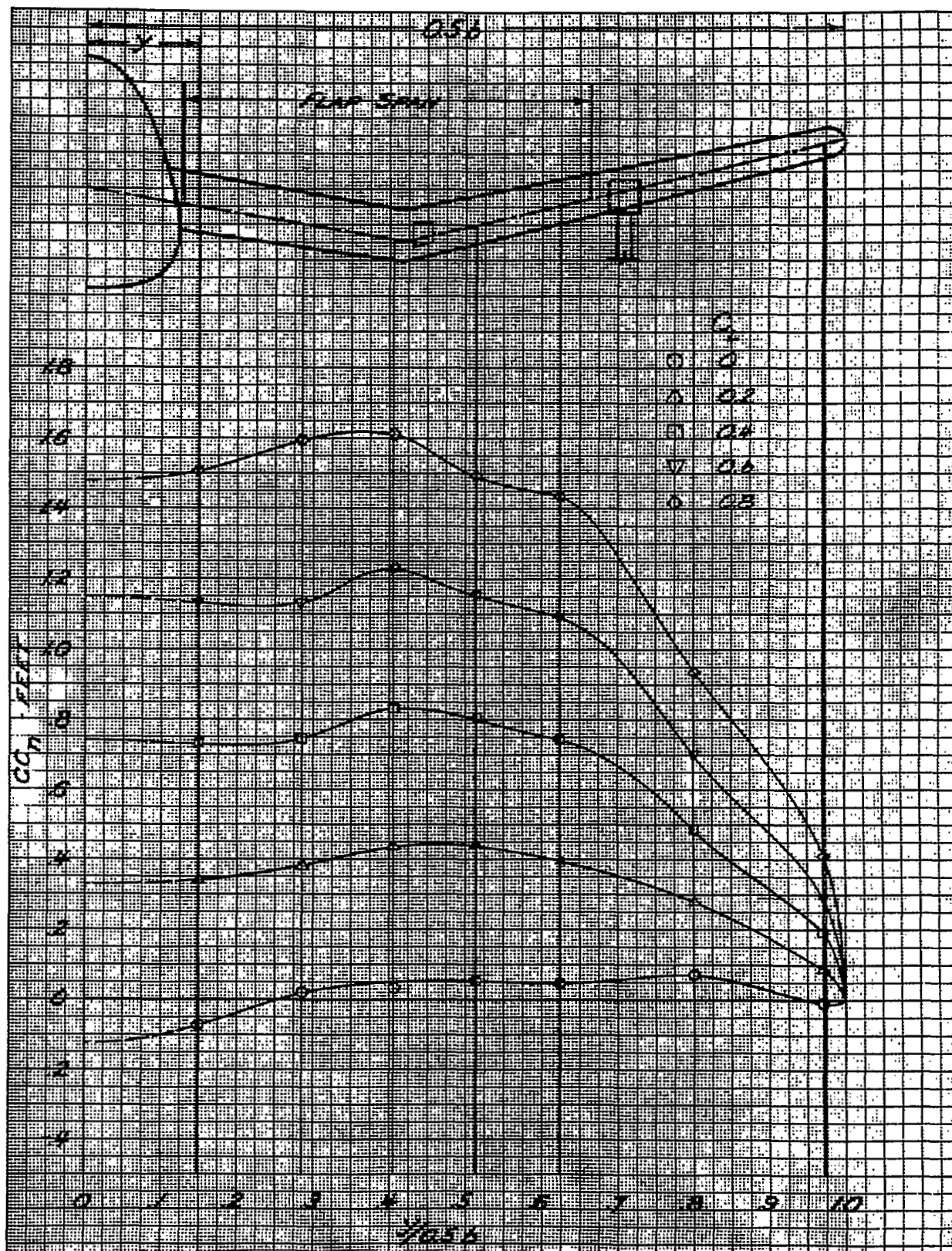
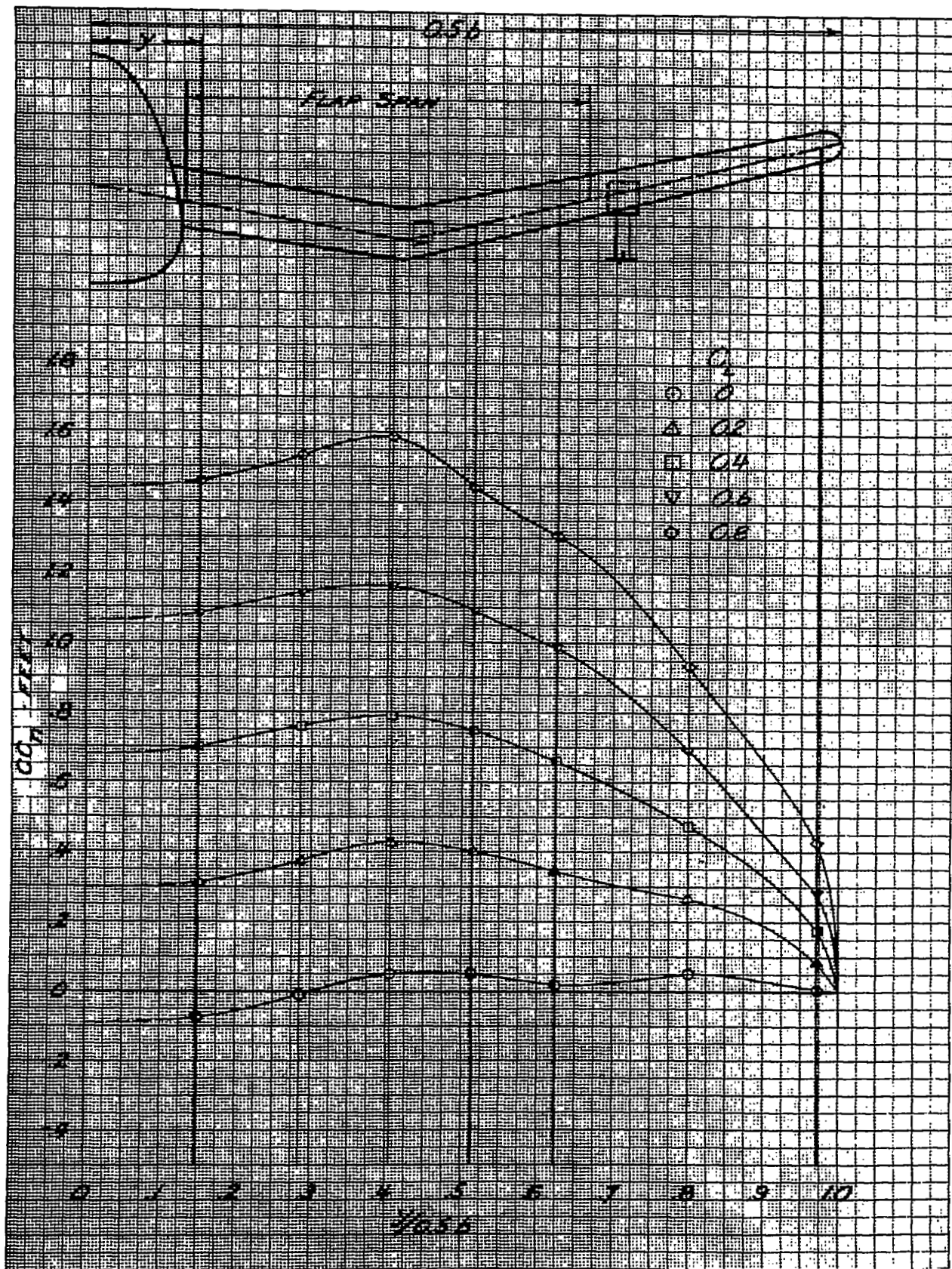


FIGURE 22. - VARIATION OF THE SECTION PITCHING-MOMENT COEFFICIENT AT STATION 266.334 WITH TAIL-OFF LIFT COEFFICIENT, X5B20-1 MODEL; MOMENT AXIS AT 22.5 PERCENT CHORD.

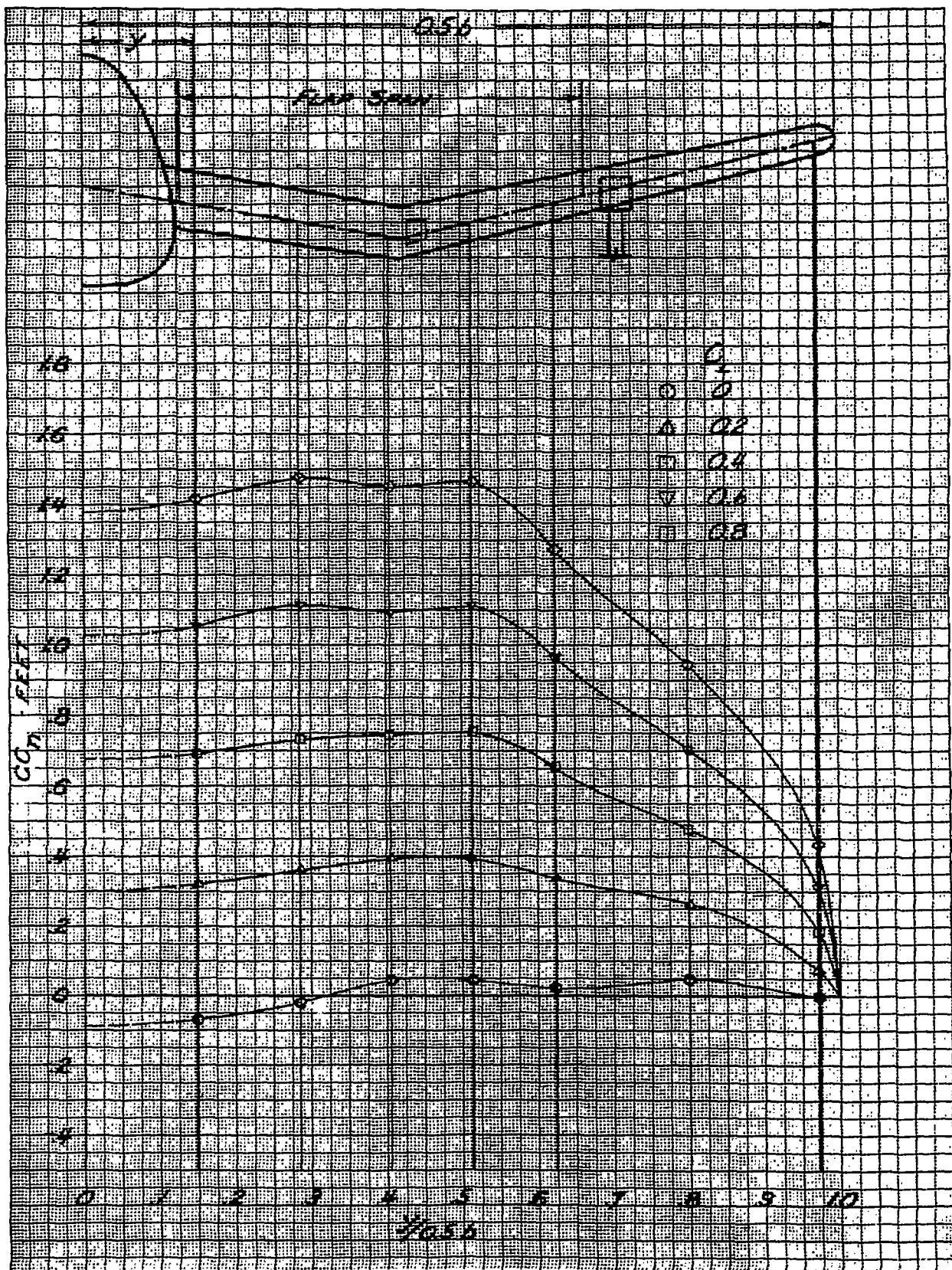


(a) $M = 0.296$
 FIGURE 23.- SPANWISE VARIATION OF THE NORMAL FORCE ON THE WING OF THE XSB2D-1 MODEL WITH LANDING FLAPS NEUTRAL.



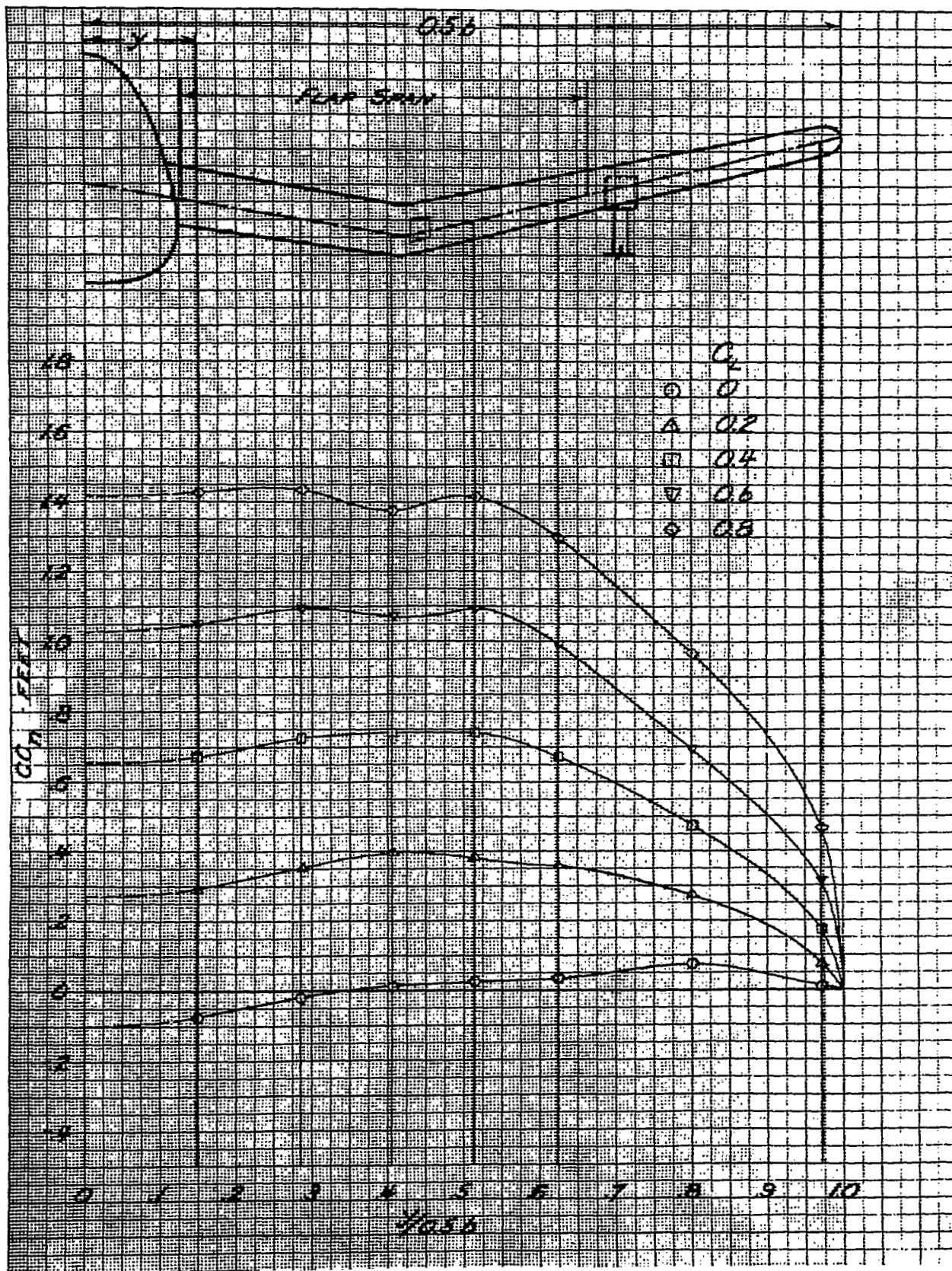
(b) $M=0.494$

FIGURE 23.- CONTINUED



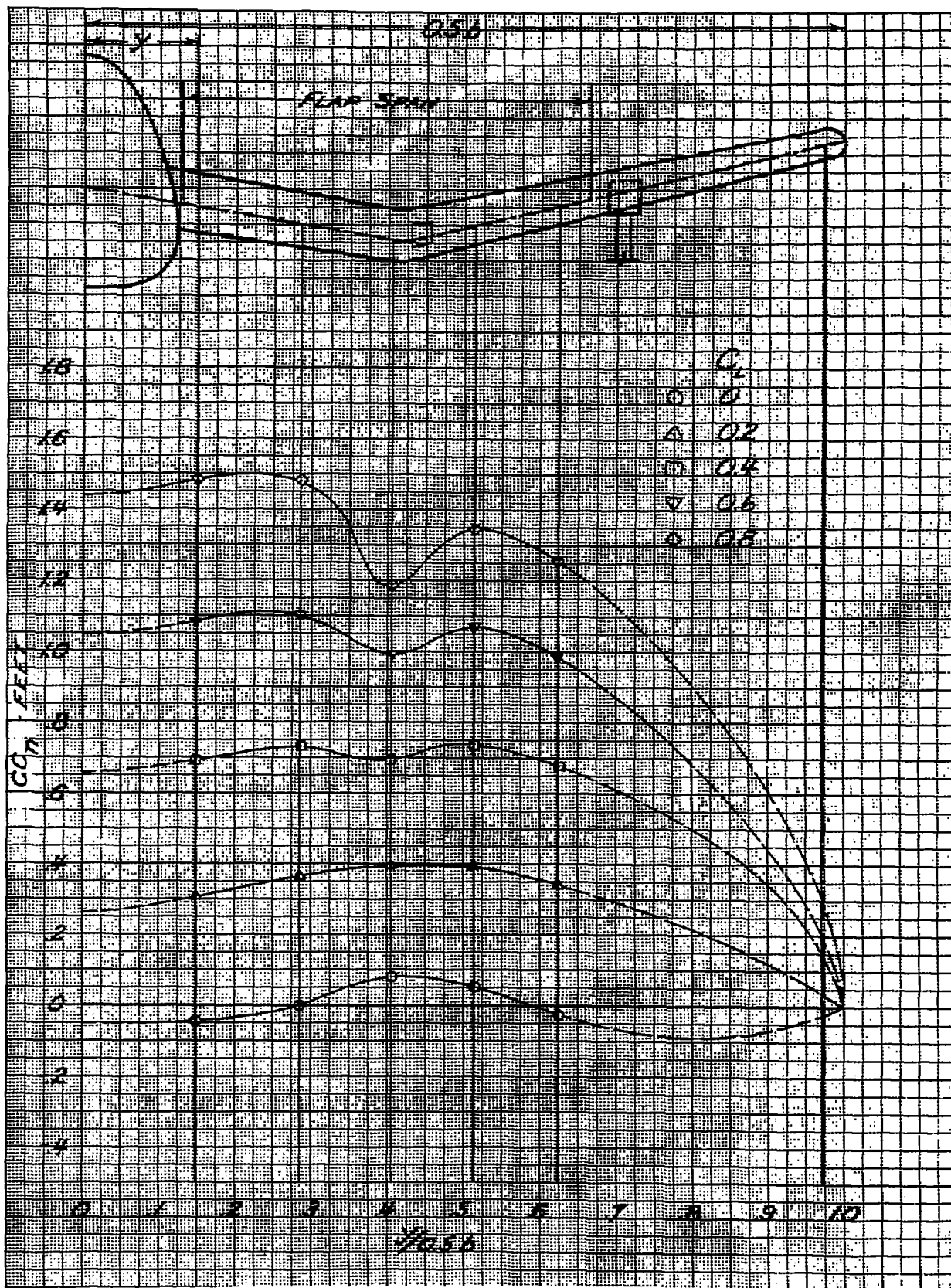
(c) $M=0.591$

FIGURE 23. - CONTINUED NATIONAL ADVISORY COMMITTEE FOR AERONAUTICS



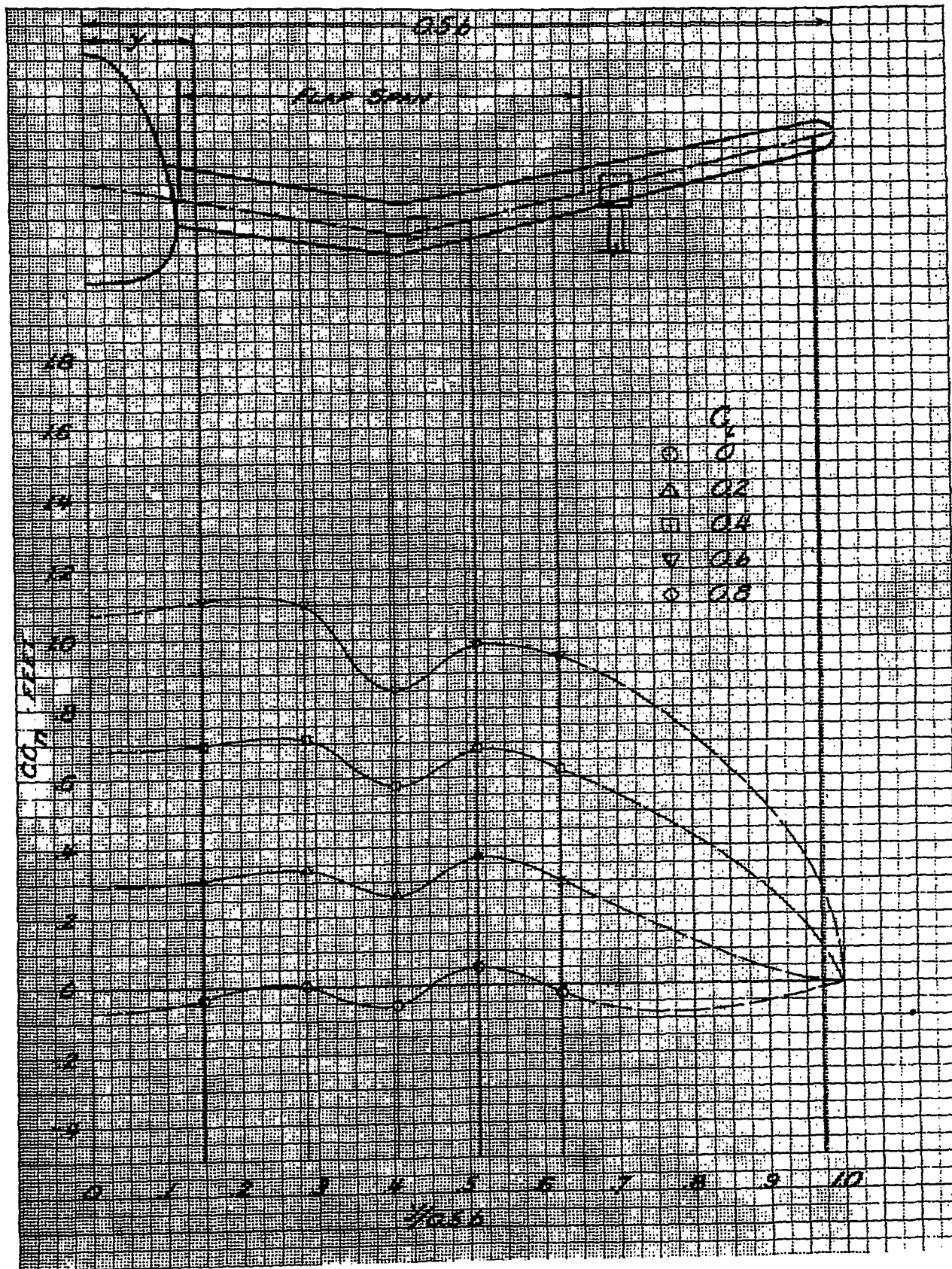
(d) $M=0.638$

FIGURE 23.- CONTINUED NATIONAL ADVISORY COMMITTEE FOR AERONAUTICS



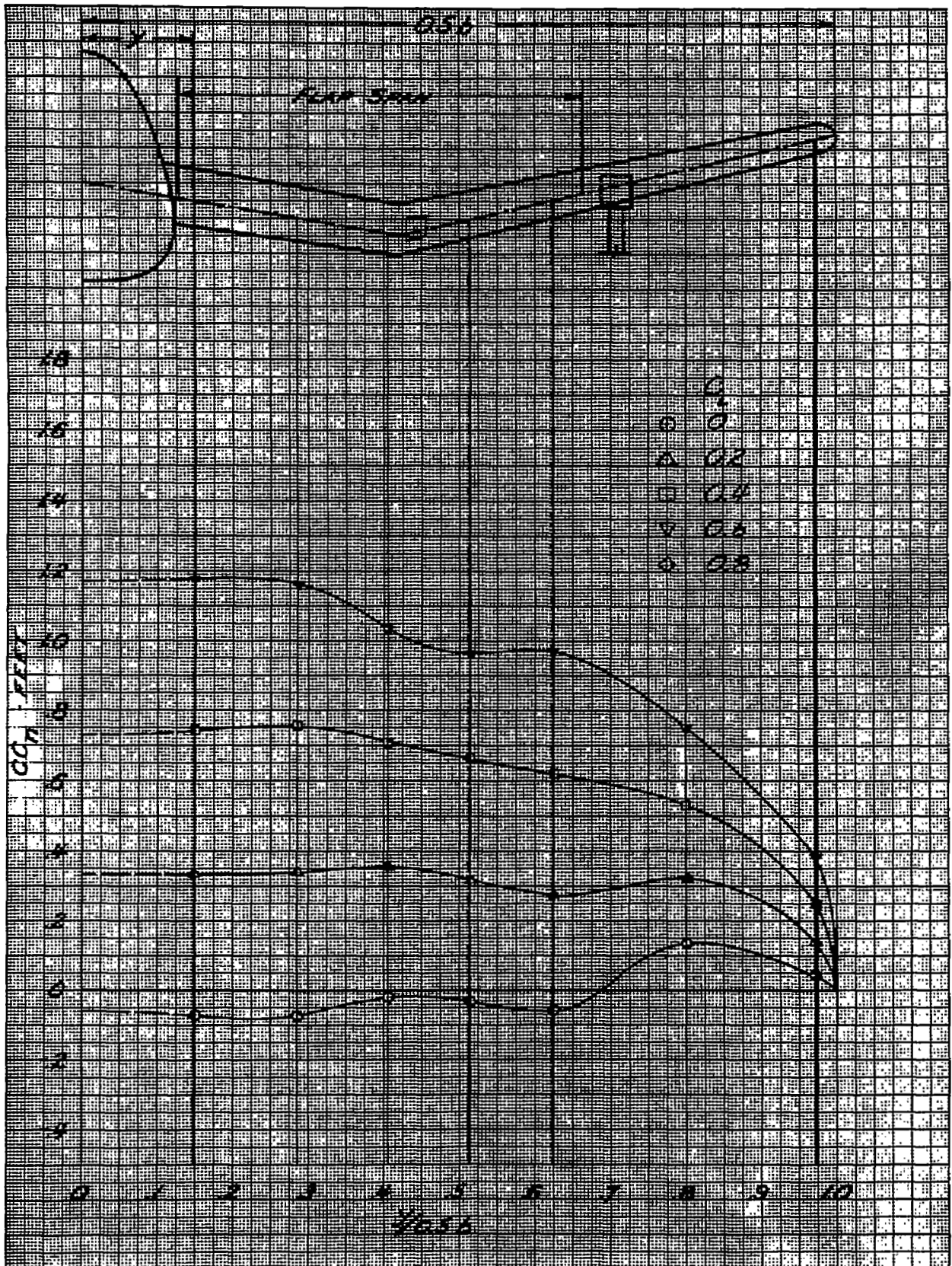
(e) $M=0.685$

FIGURE 23.- CONTINUED

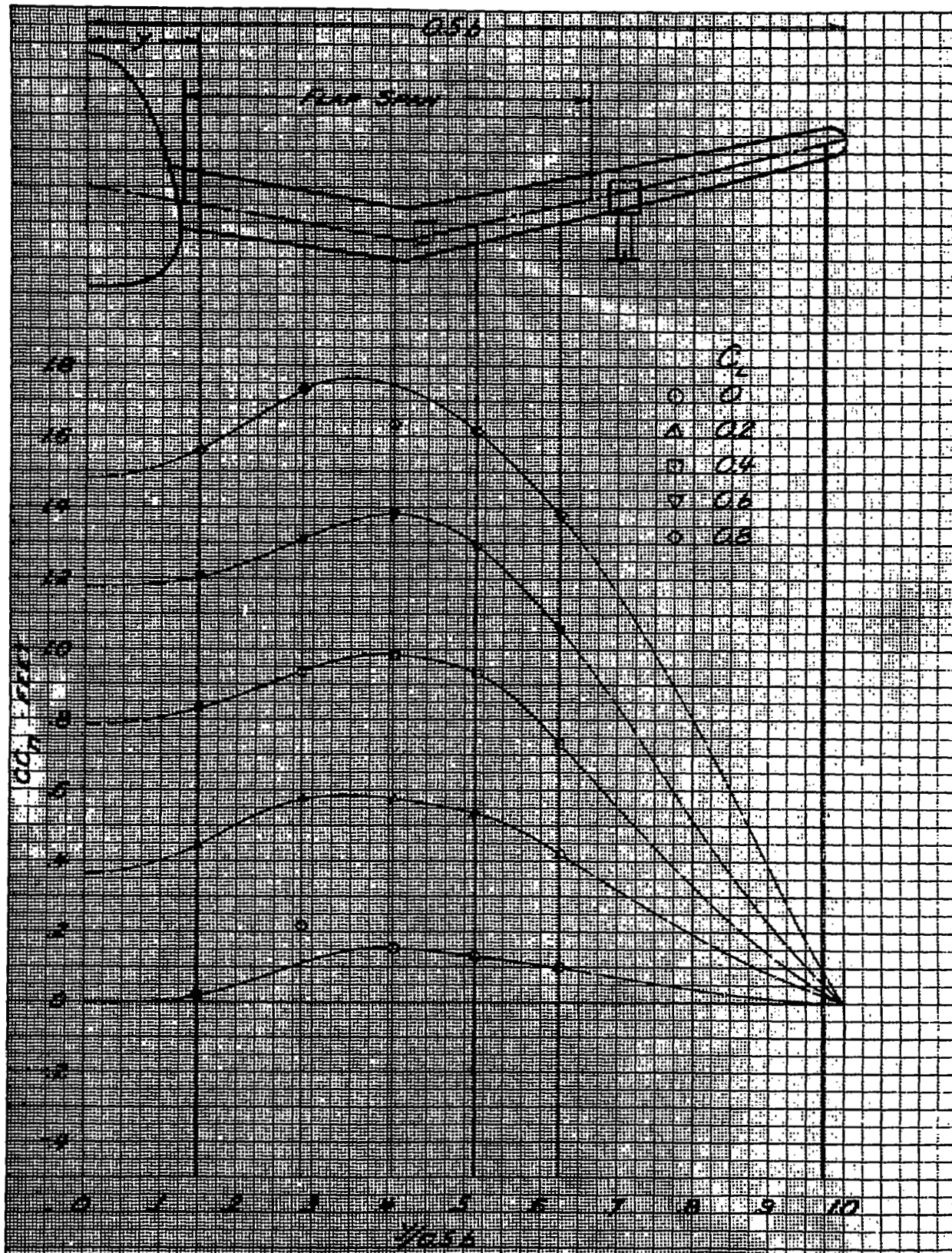


(f) $M=0.73$

FIGURE 23.- CONTINUED

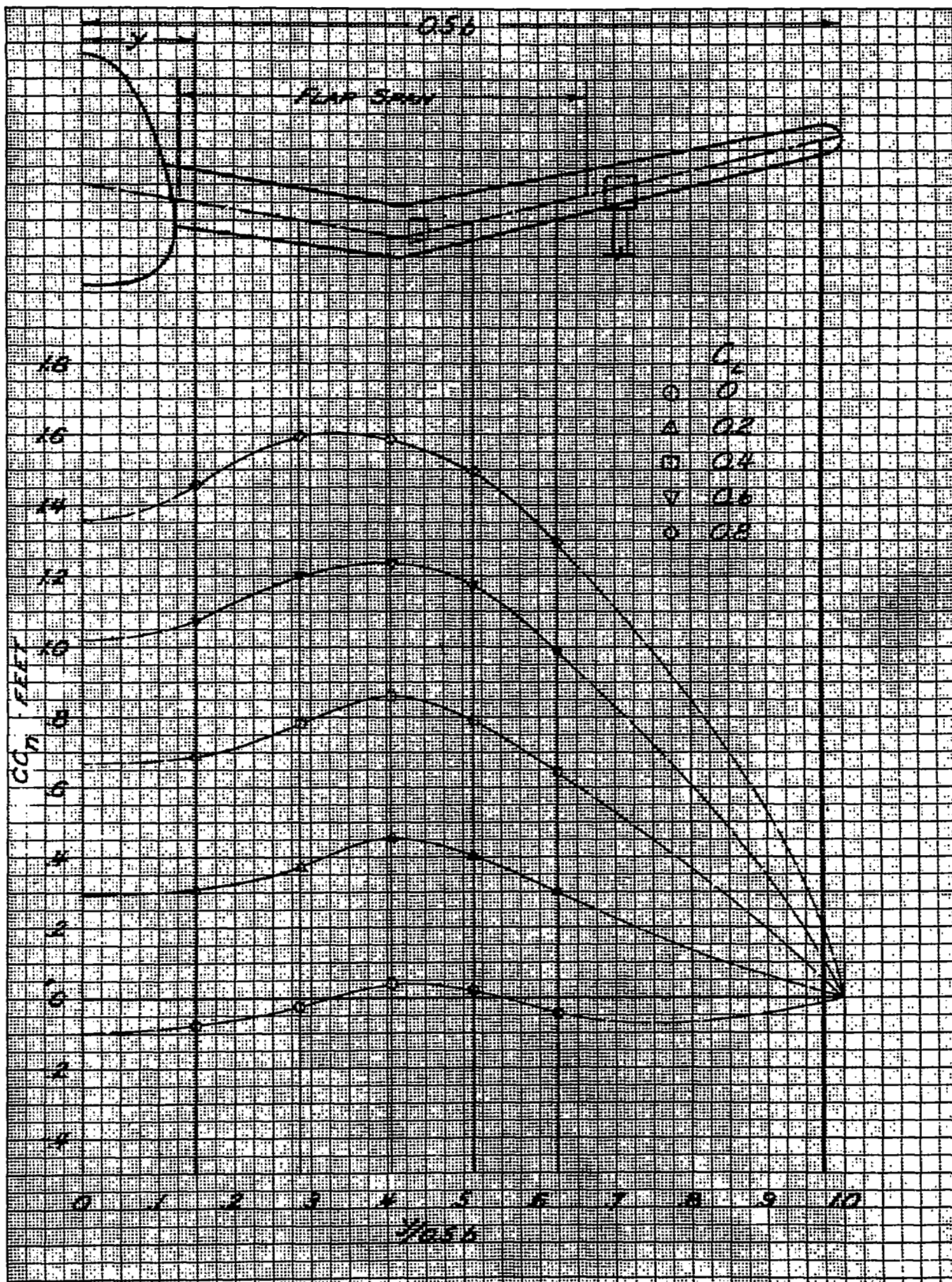


(g) M=0.778
 FIGURE 23. - CONCLUDED



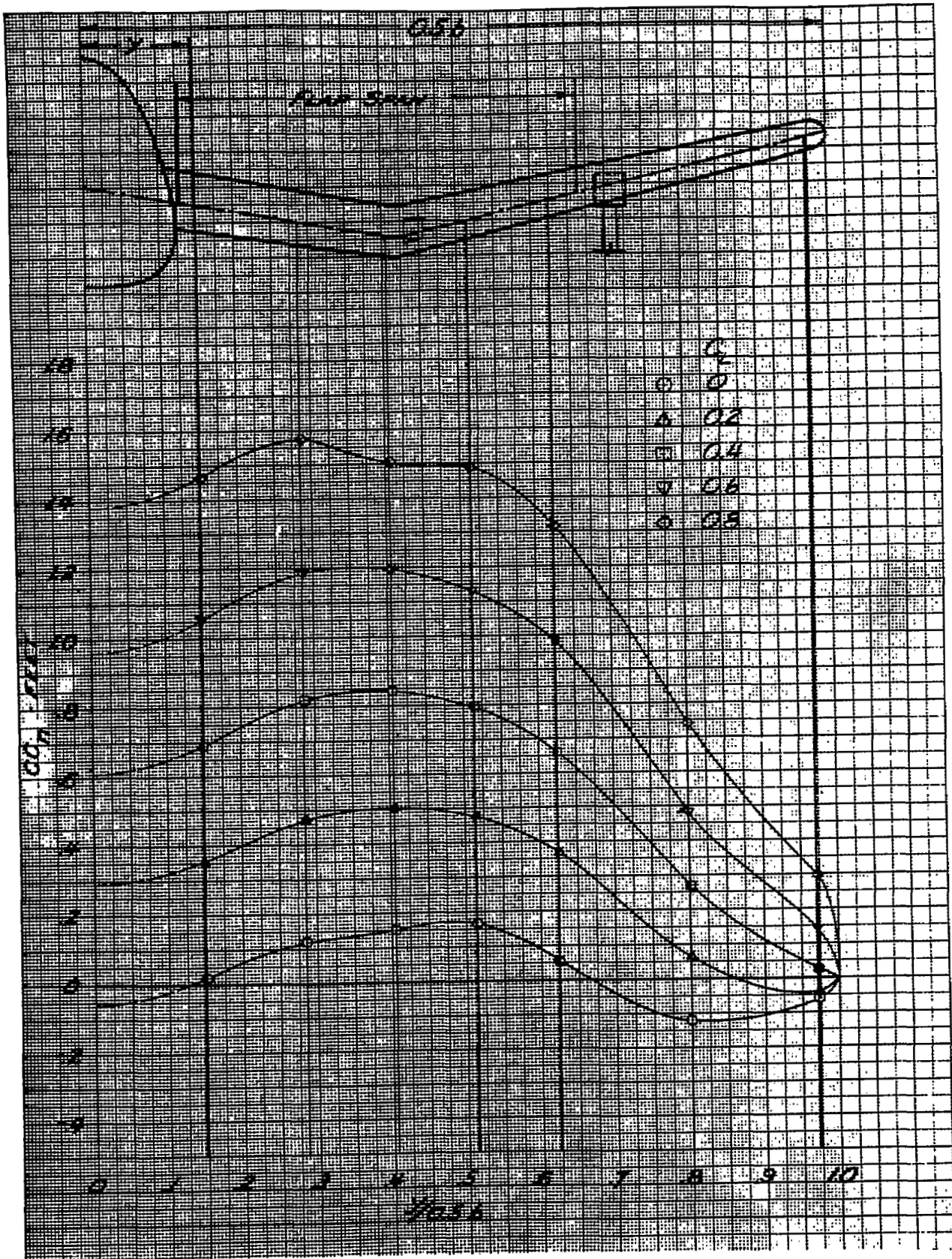
(a) $M=0.296$

FIGURE 24. - SPANWISE VARIATION OF THE NORMAL FORCE ON THE WING OF THE XSB2D-1 MODEL WITH LANDING FLAPS DEFLECTED 10°.



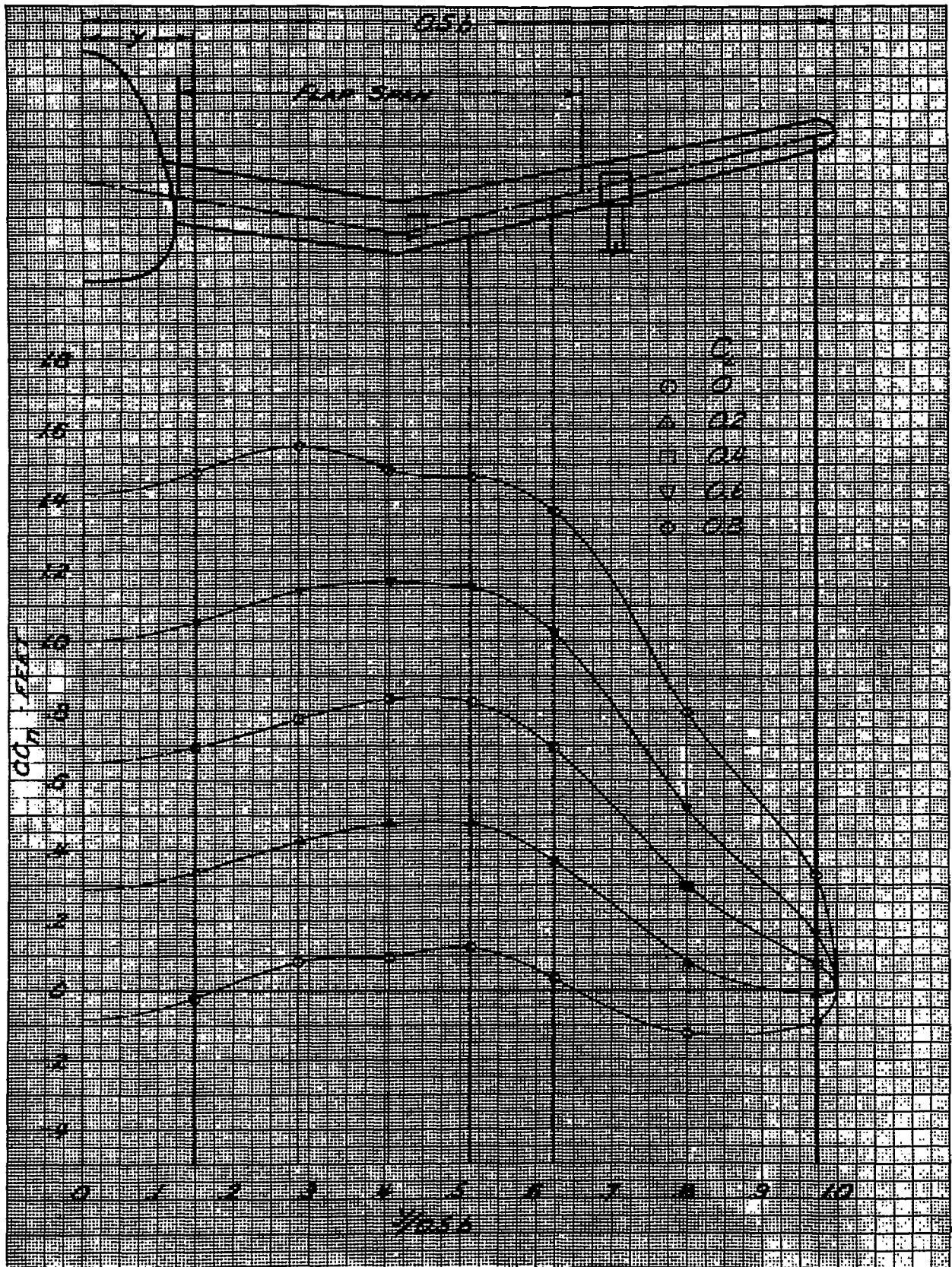
(b) M=0.494

FIGURE 24. - CONTINUED



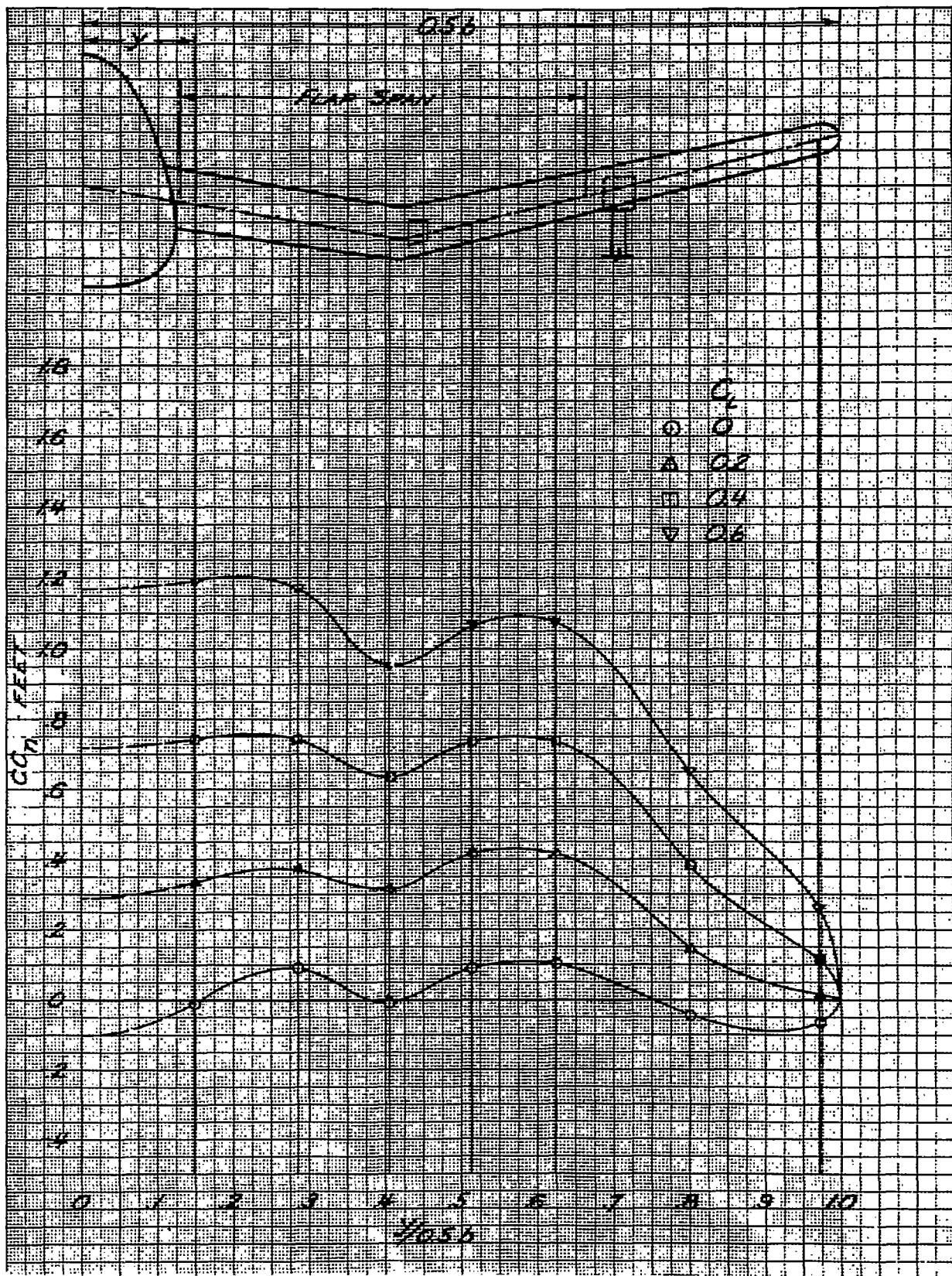
(c) $M=0.591$

FIGURE 24. - CONTINUED

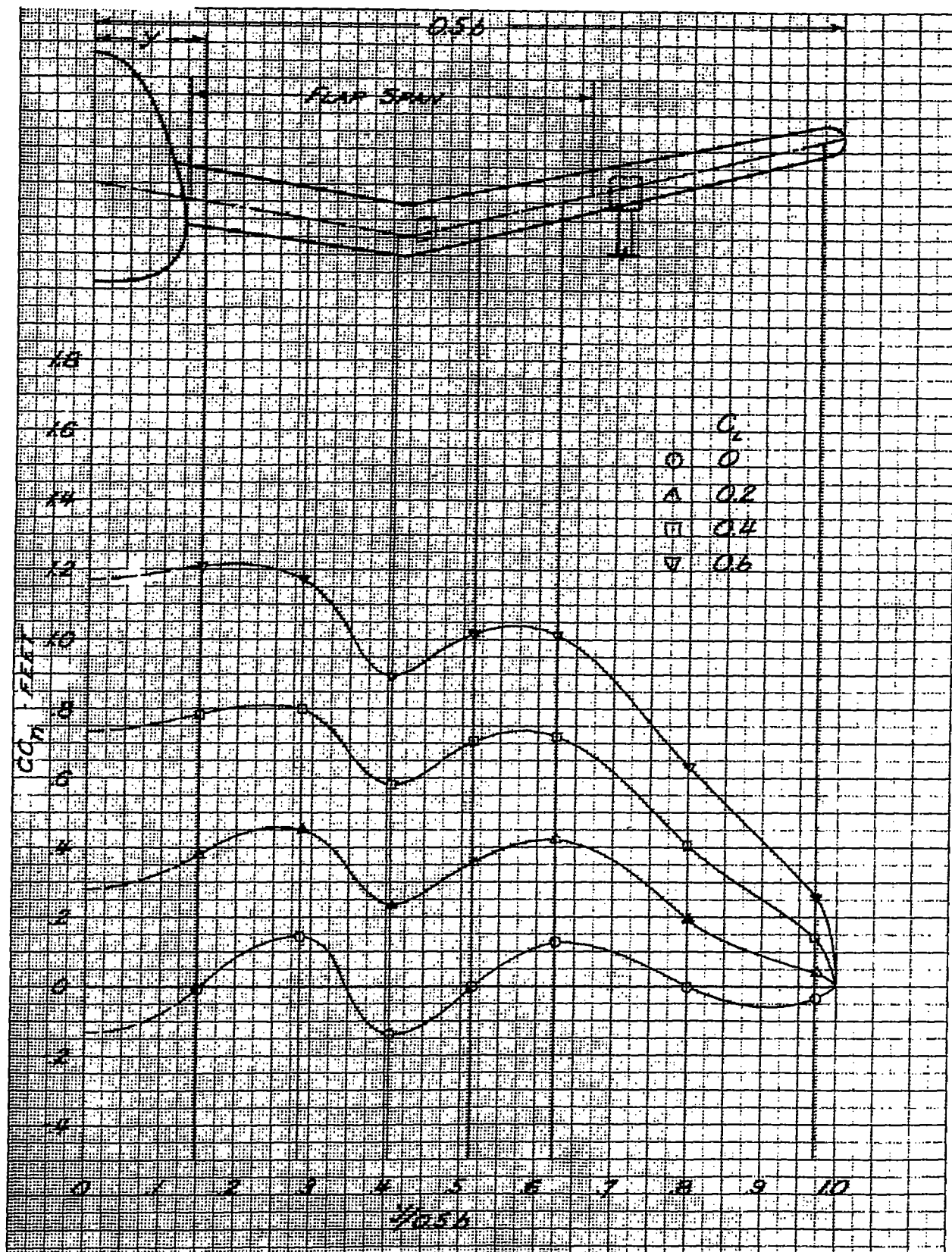


(d) M=0.638

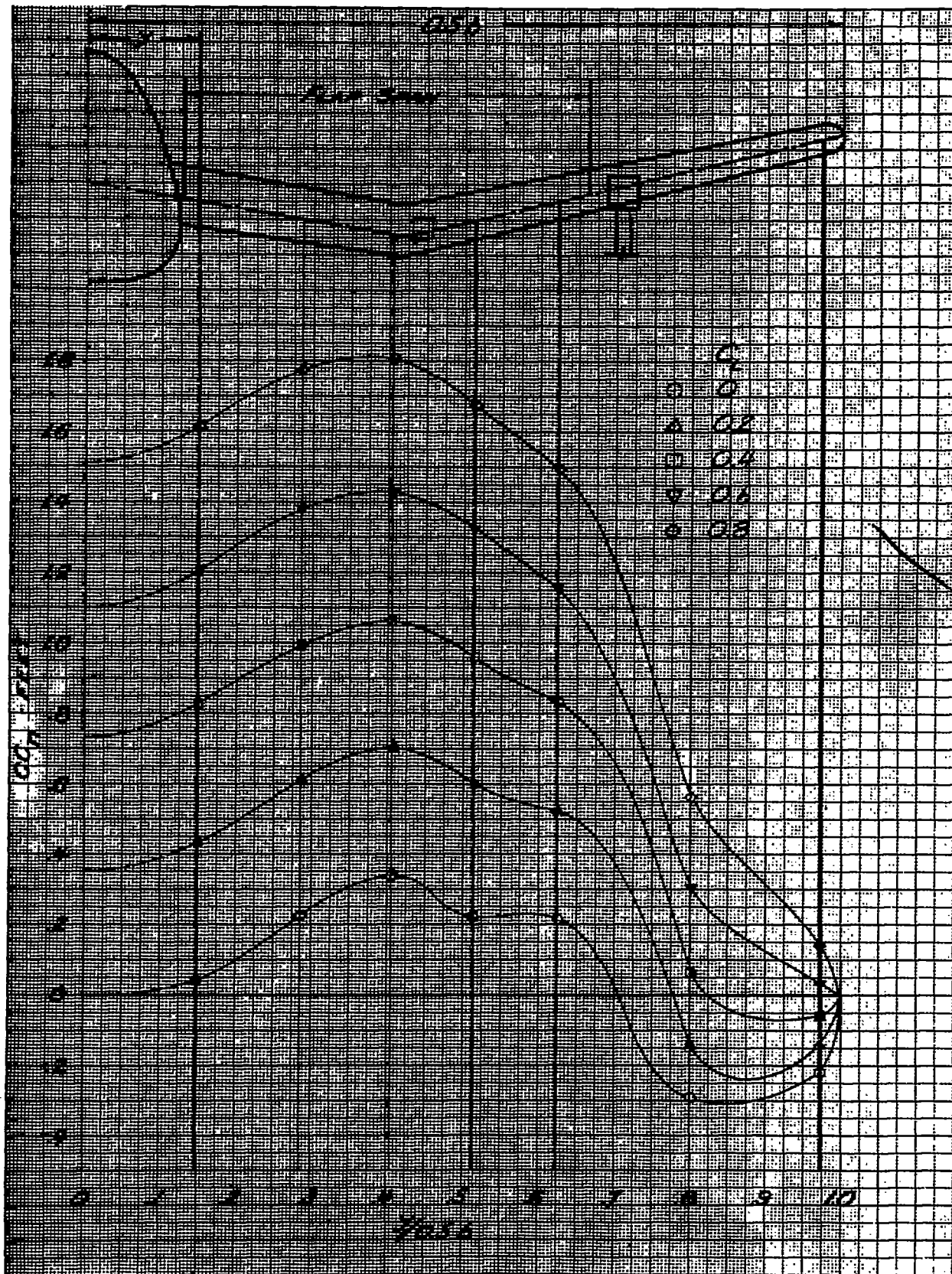
FIGURE 24.- CONTINUED NATIONAL ADVISORY COMMITTEE FOR AERONAUTICS



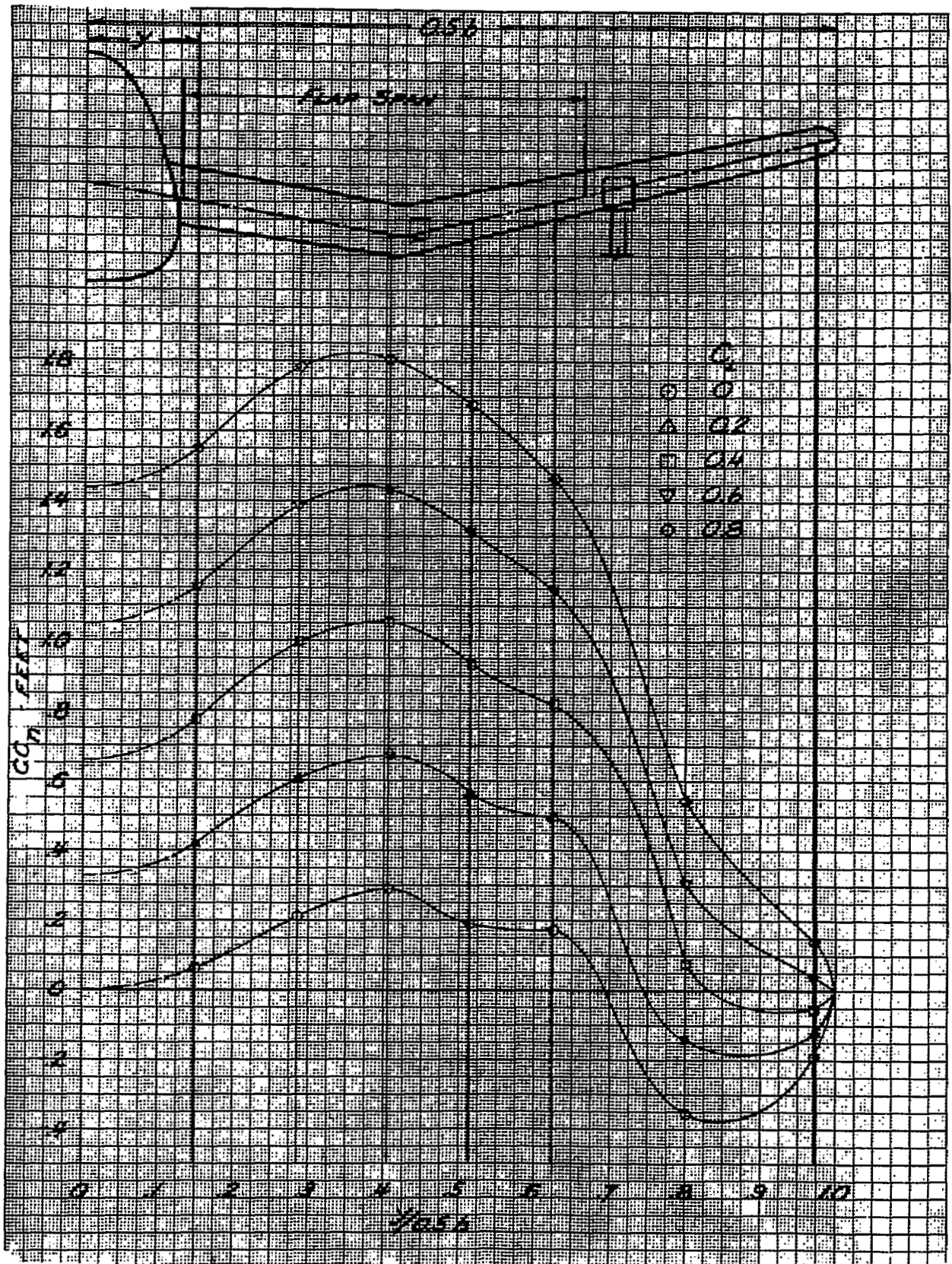
(f) $M=0.73$
 FIGURE 24.- CONTINUED



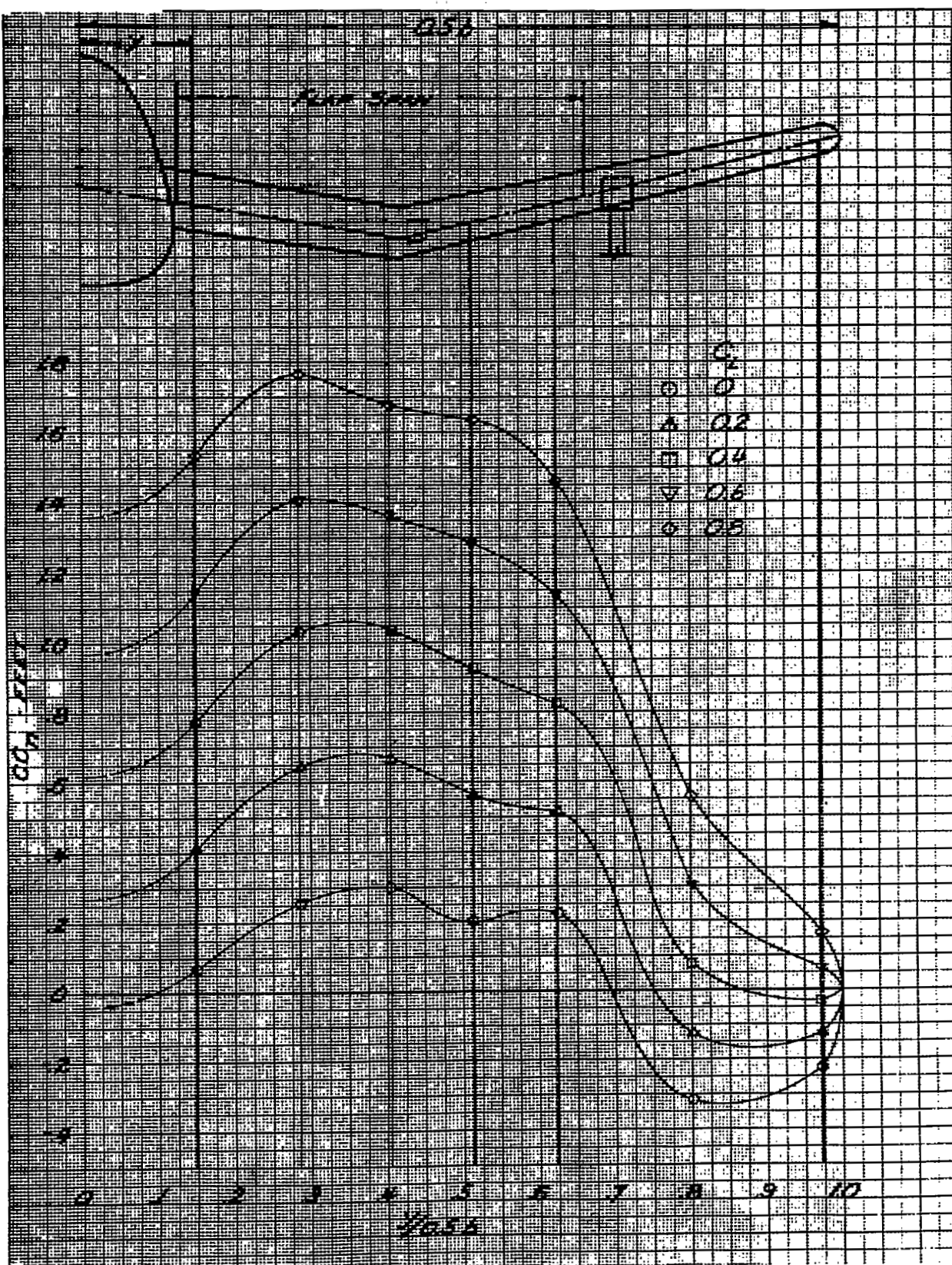
(g) $M=0.778$
 FIGURE 24.- CONCLUDED



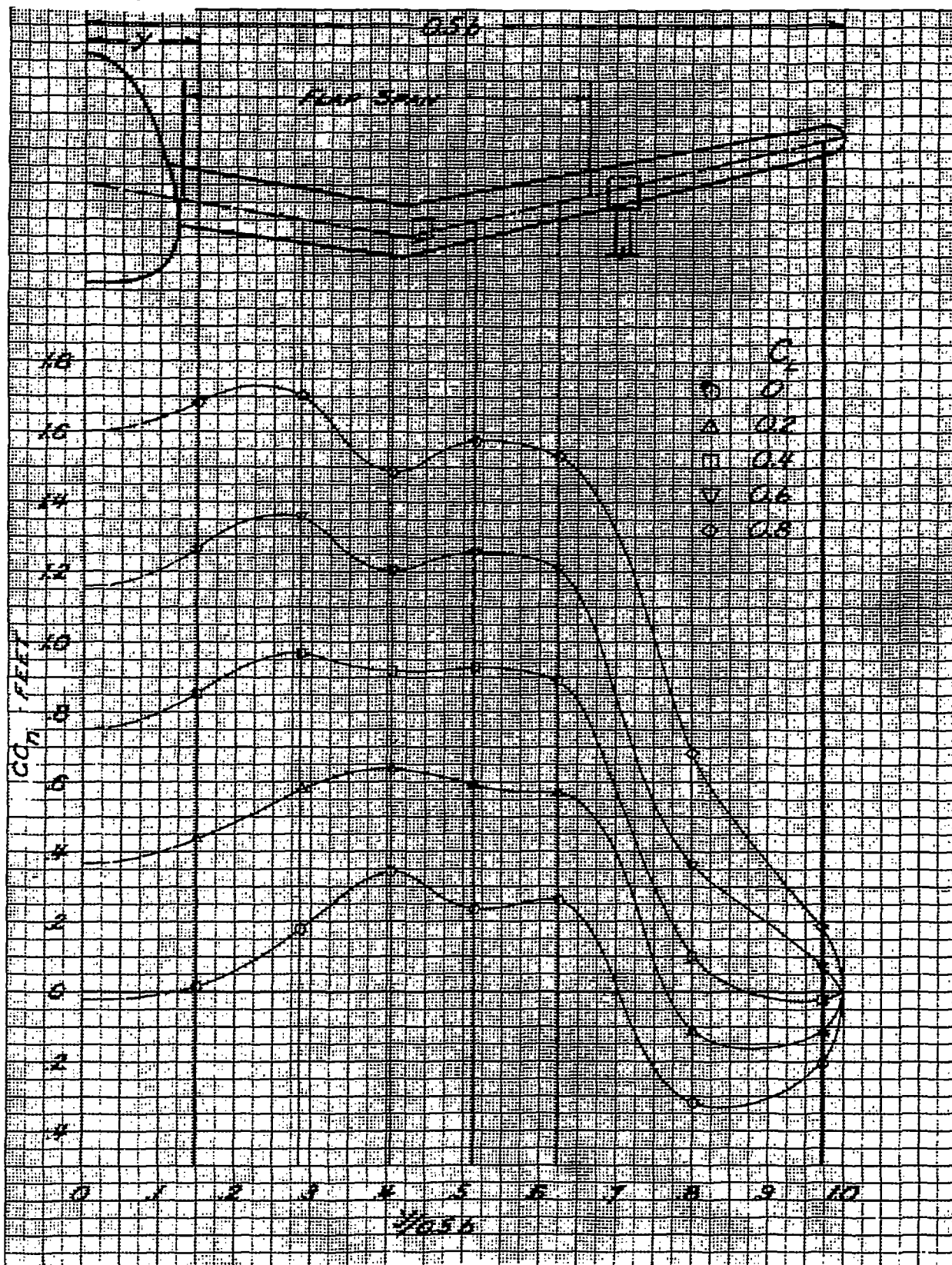
(b) $M=0.494$
 FIGURE 25.- CONTINUED



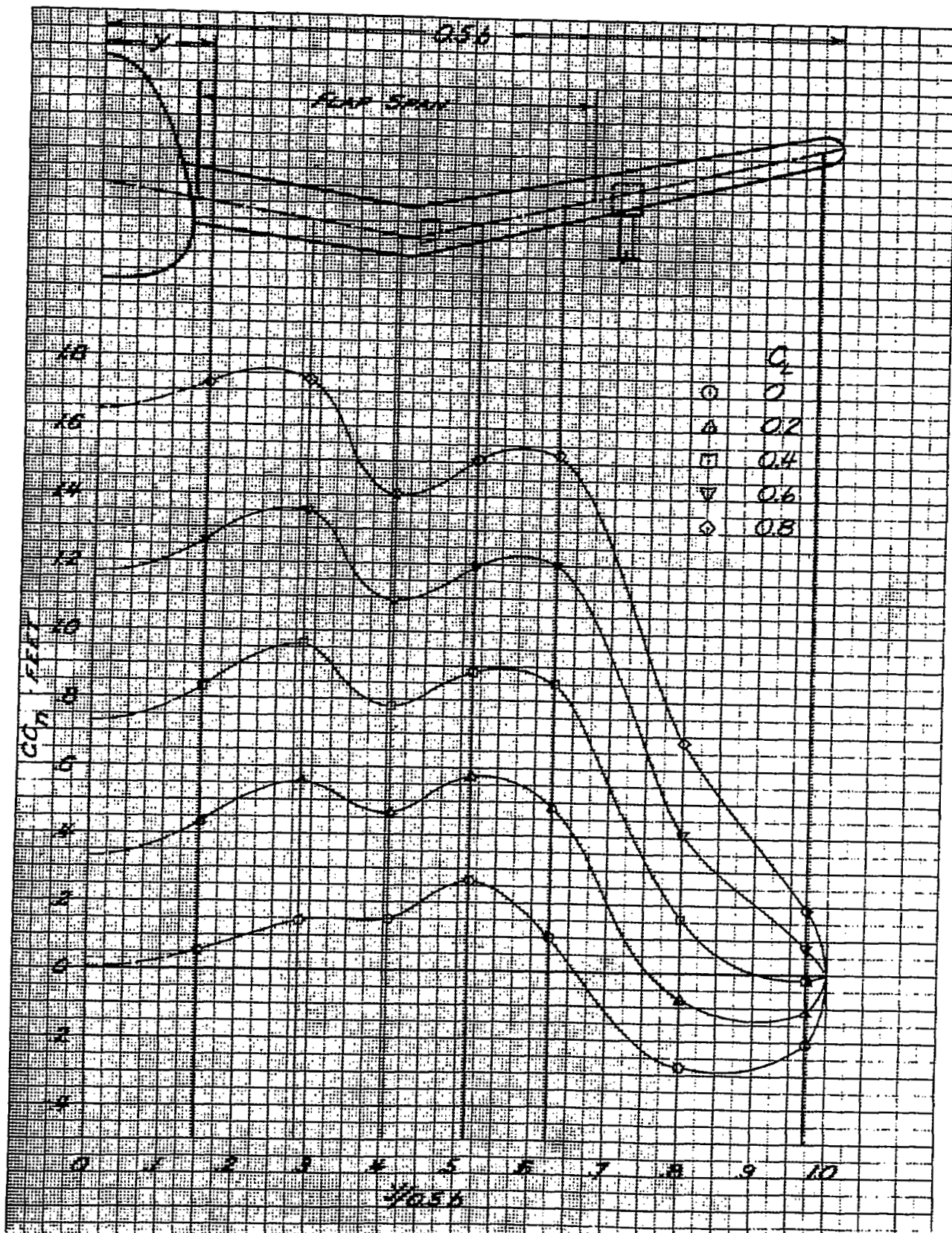
(c) $M=0.591$
 FIGURE 25.- CONTINUED



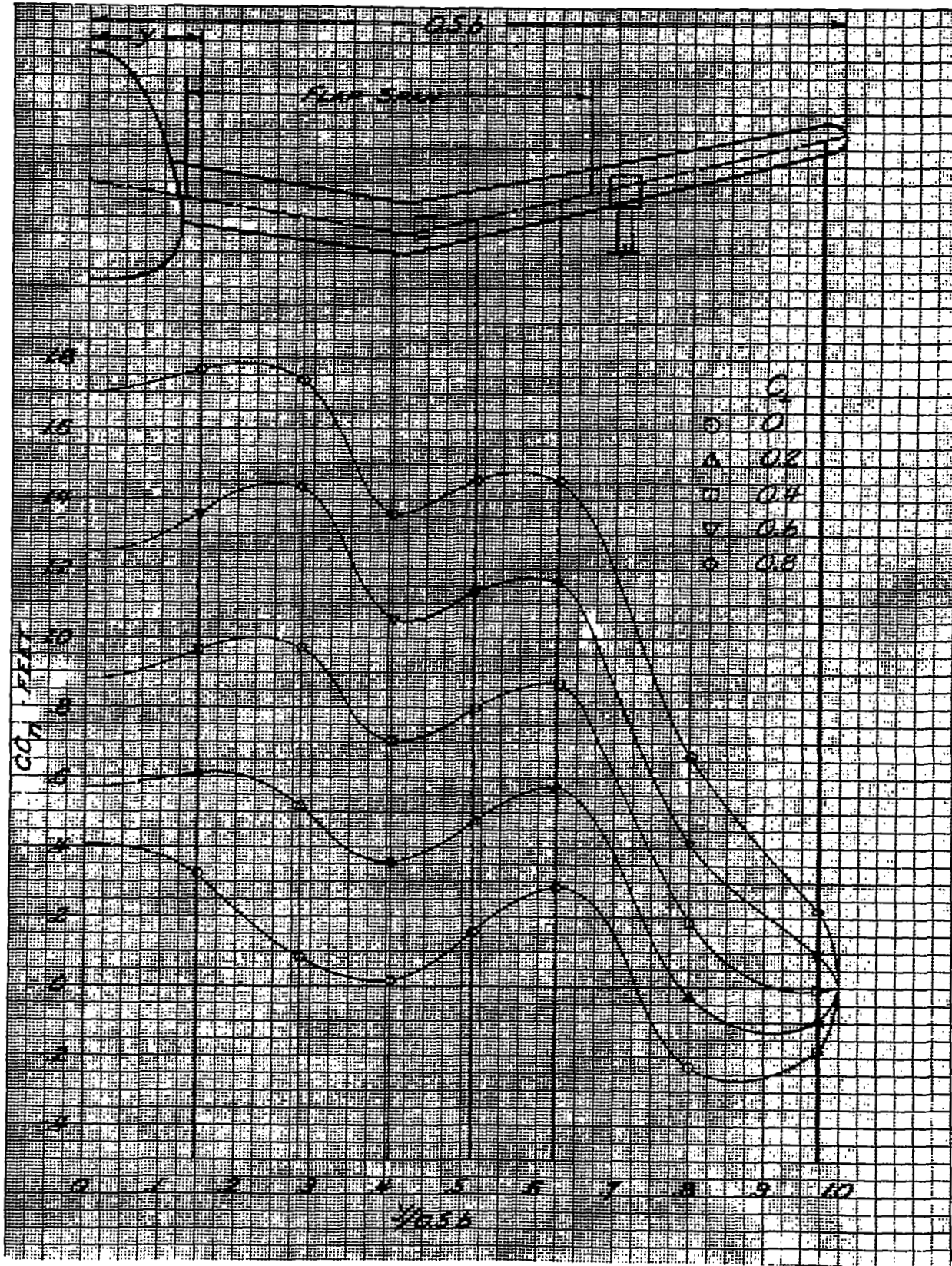
(d) $M=0.638$
 FIGURE 25.-CONTINUED



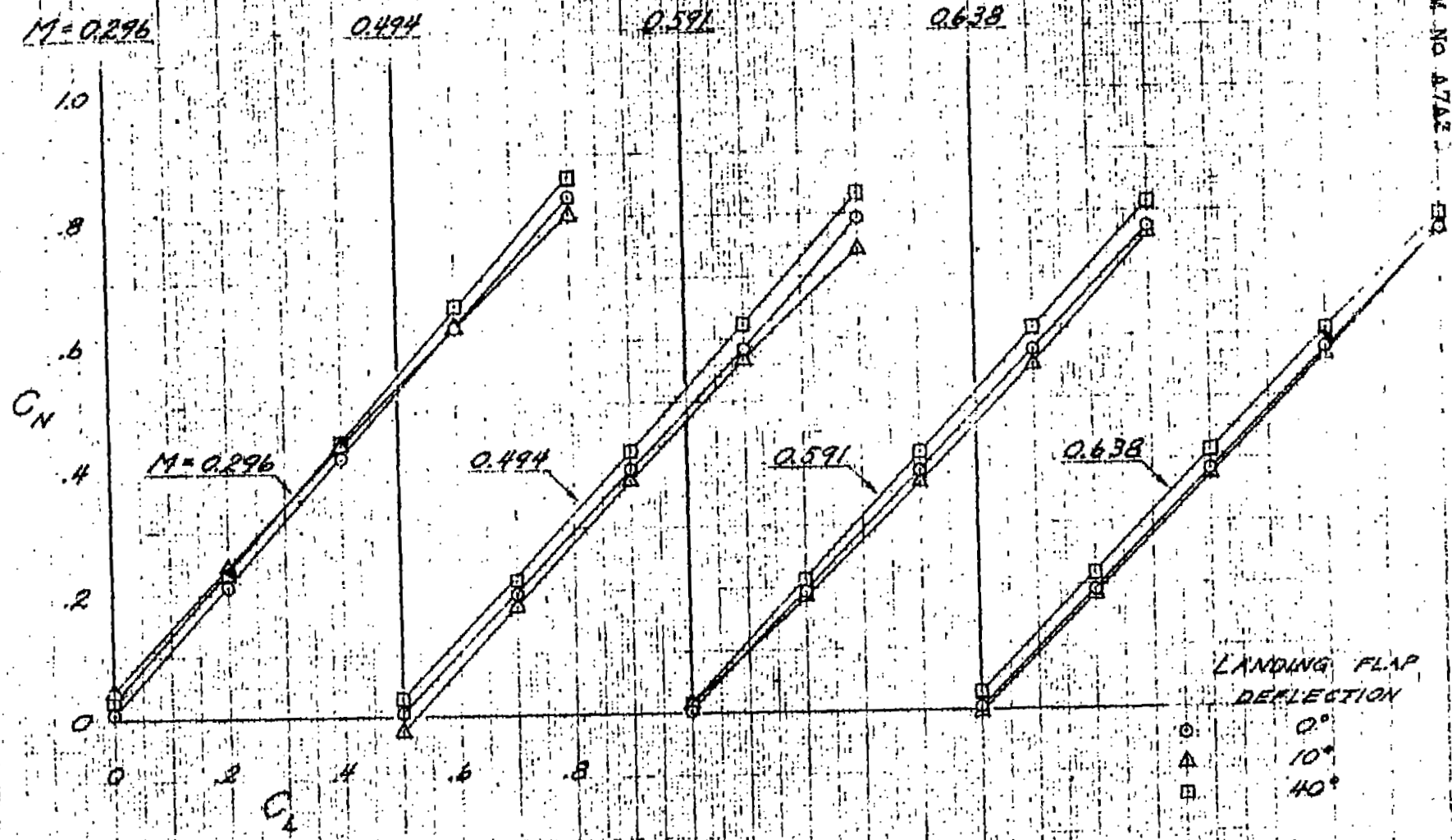
(e) $M=0.685$
 FIGURE 25. - CONTINUED



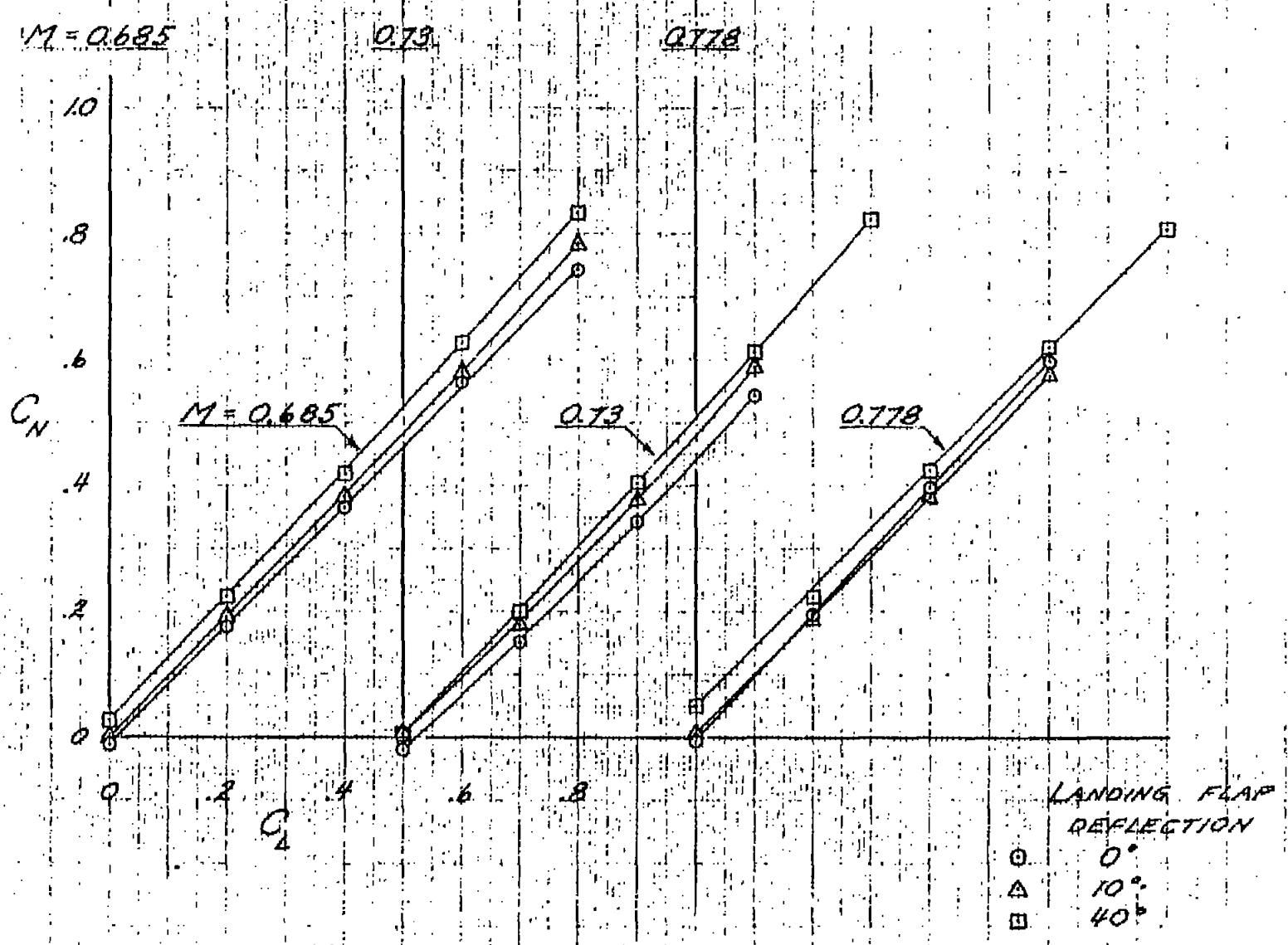
(f) $M = 0.73$
 FIGURE 25. - CONTINUED



(g) $M=0.778$
 FIGURE 25. - CONCLUDED

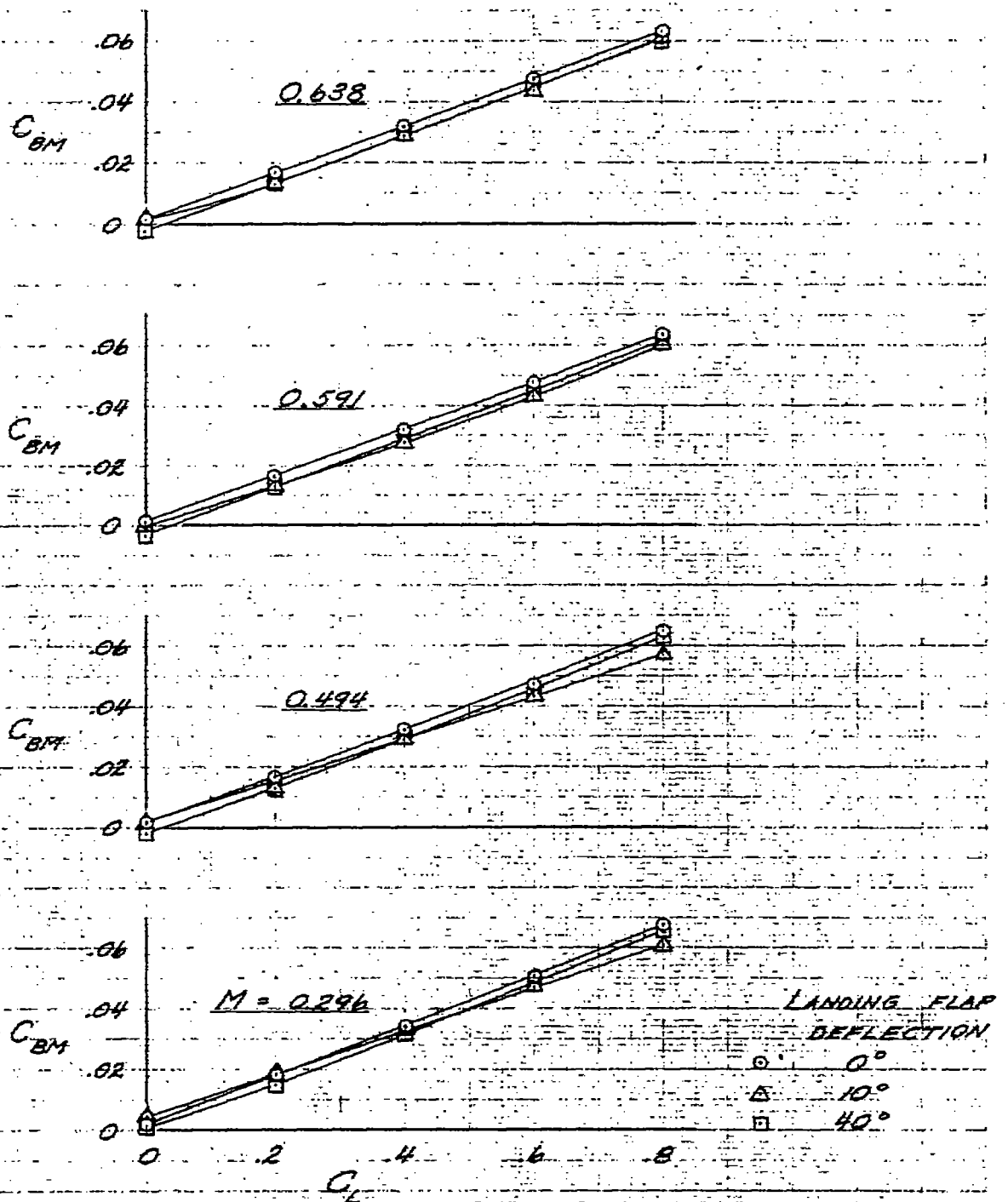


(a) $M = 0.296, 0.494, 0.591, \text{ and } 0.638$
 FIGURE 26. - VARIATION OF THE WING NORMAL-FORCE COEFFICIENT WITH THE TAIL-OFF LIFT COEFFICIENT FOR THE XSB2D-1 MODEL WITH THREE LANDING-FLAP DEFLECTIONS.

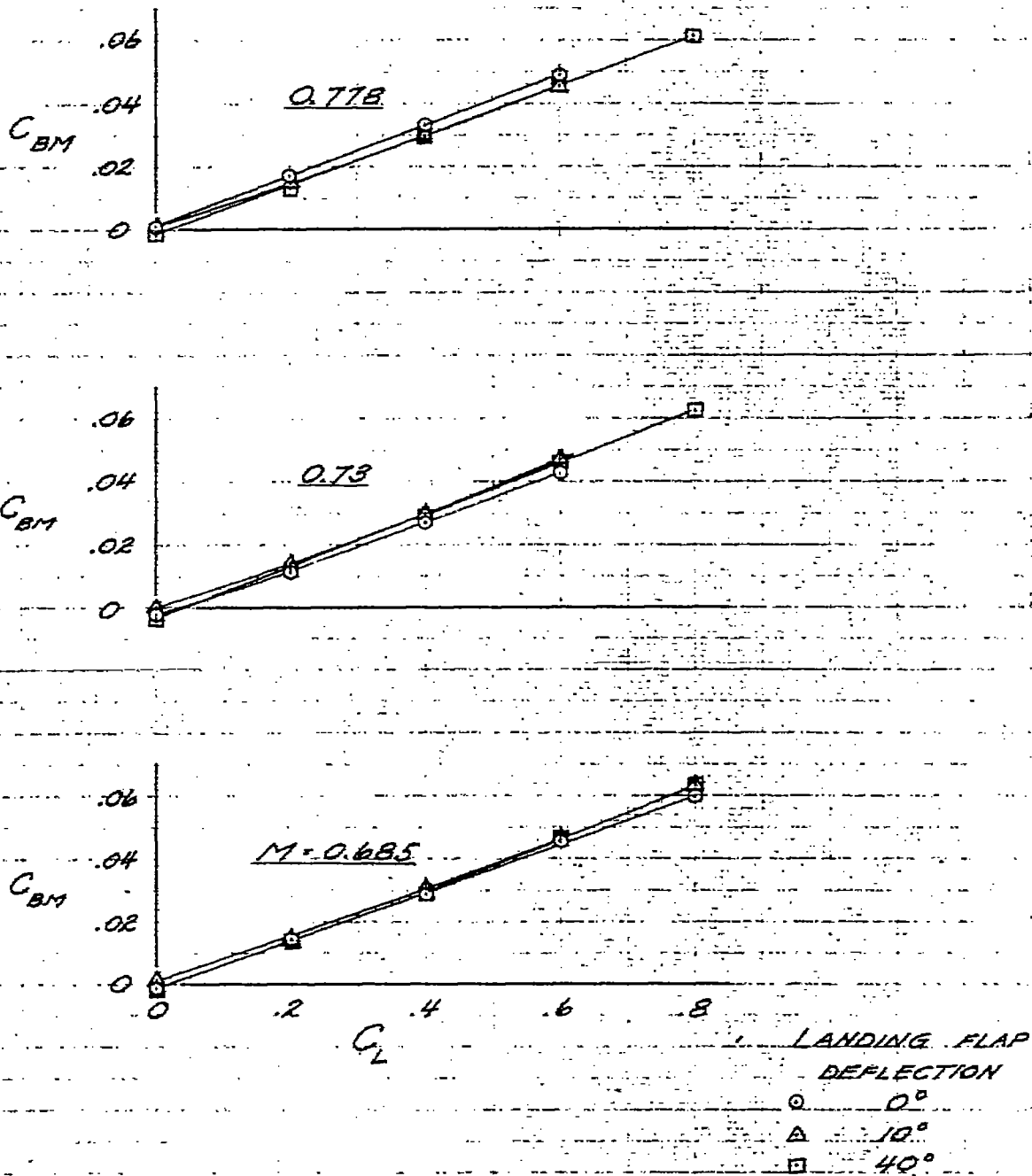


(b) $M = 0.685, 0.73, \text{ AND } 0.778$

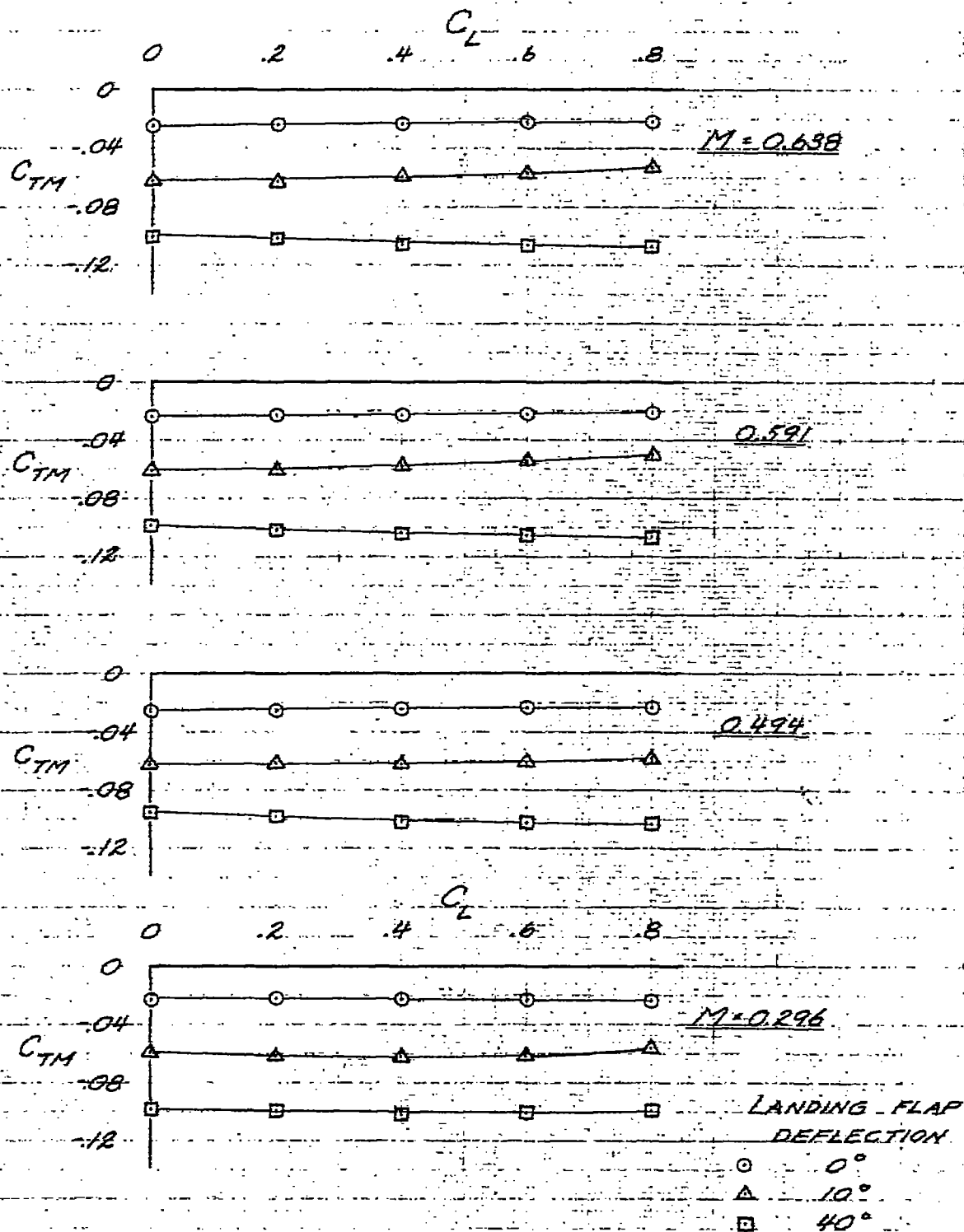
FIGURE 24 - CONCLUDED



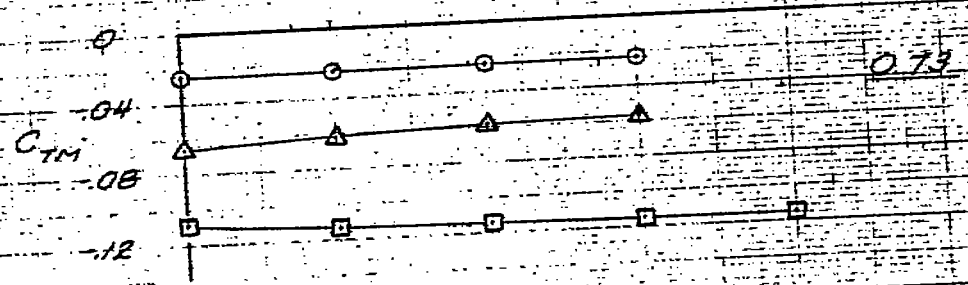
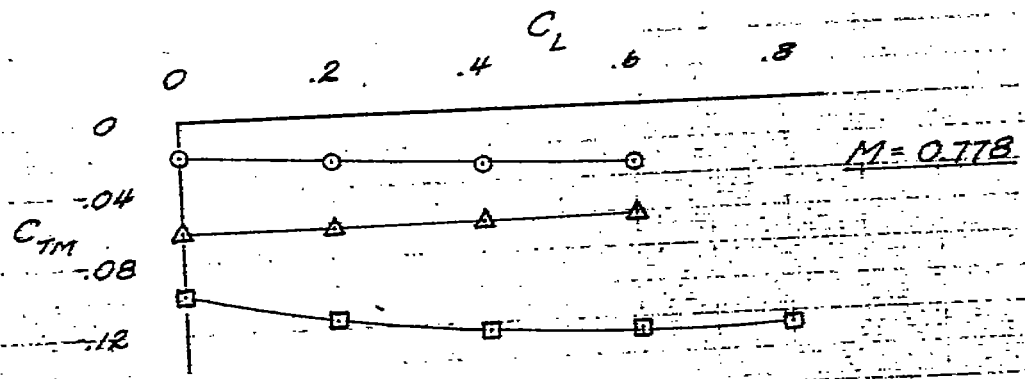
(2) $M = 0.296, 0.494, 0.591, \text{ AND } 0.638$
 FIGURE 27.- VARIATION OF THE ROOT BENDING-MOMENT COEFFICIENT WITH THE TAIL-OFF LIFT COEFFICIENT FOR THE XSB2D-1 MODEL WITH THREE LANDING-FLAP DEFLECTIONS.



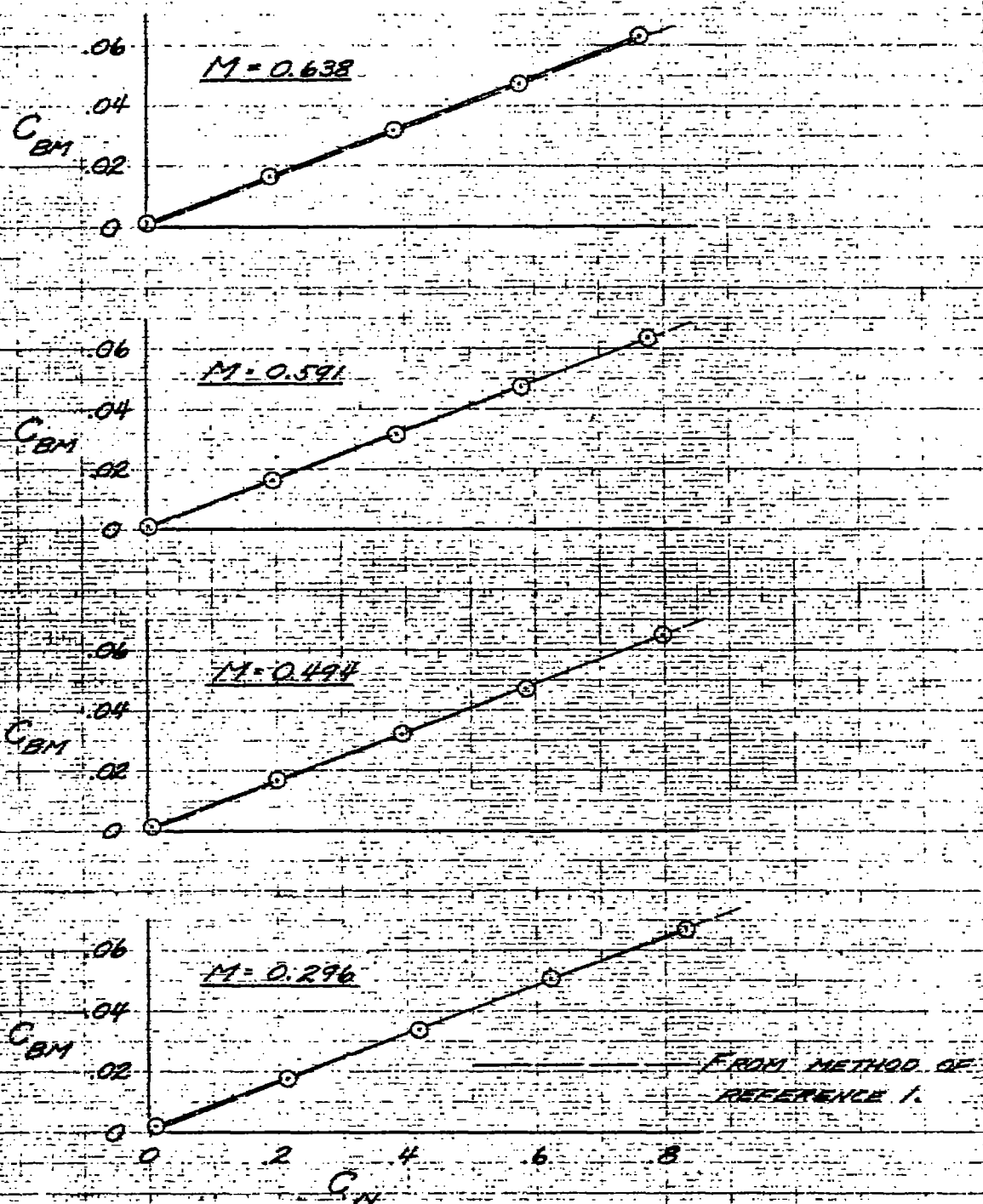
(b) $M = 0.685, 0.73, \text{ AND } 0.778$
 FIGURE 27. - CONCLUDED



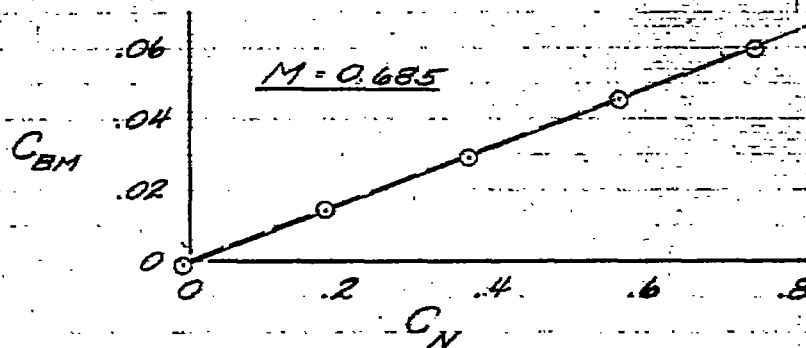
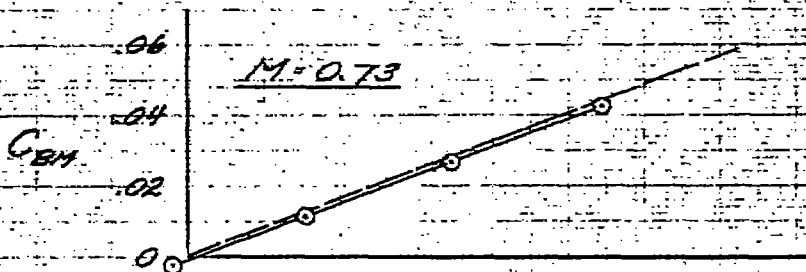
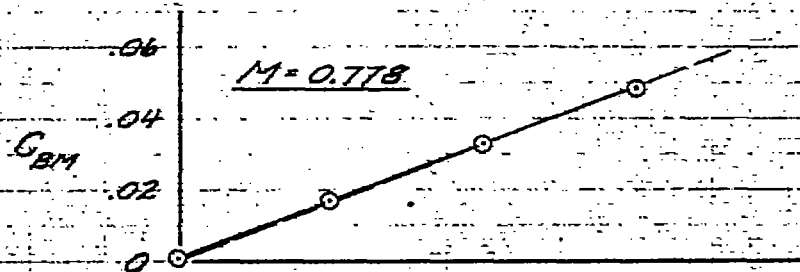
(a) $M = 0.296, 0.494, 0.591, \text{ AND } 0.638$
 FIGURE 28. - VARIATION OF THE ROOT TORSIONAL-MOMENT COEFFICIENT WITH THE TAIL-OFF LIFT COEFFICIENT FOR THE X5BRD-1 MODEL WITH THREE LANDING FLAP DEFLECTIONS.



(b) - $M = 0.685, 0.73, \text{ AND } 0.778$
 FIGURE 28 - (CONCLUDED)

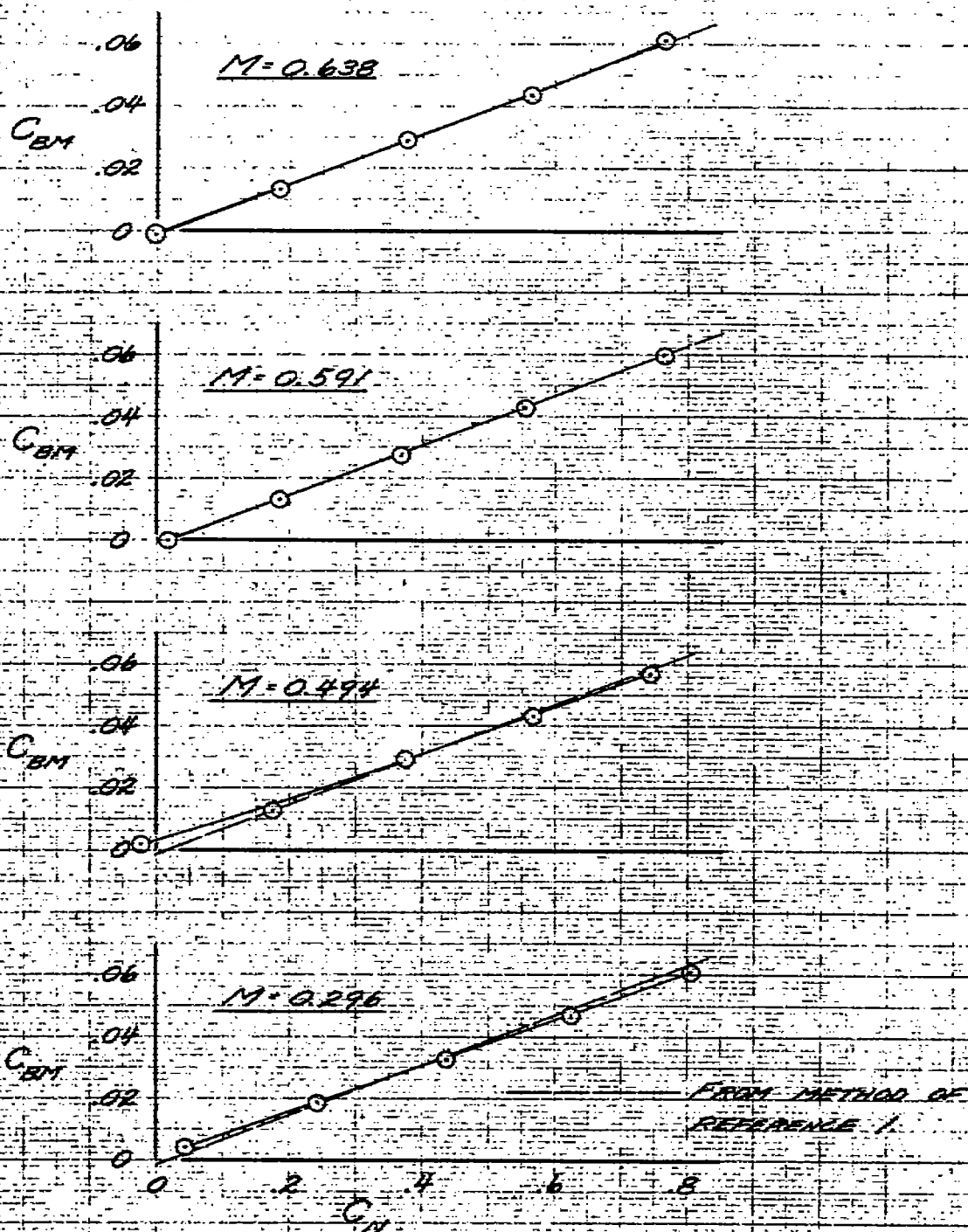


(a) $M=0.296, 0.494, 0.591, \text{ AND } 0.638$
 FIGURE 29.-COMPARISON OF THE VARIATION OF ROOT BENDING-MOMENT COEFFICIENT WITH NORMAL-FORCE COEFFICIENT AS DETERMINED EXPERIMENTALLY AND BY METHOD OF REFERENCE 1. XSB2D-1 MODEL; LANDING FLAPS NEUTRAL.



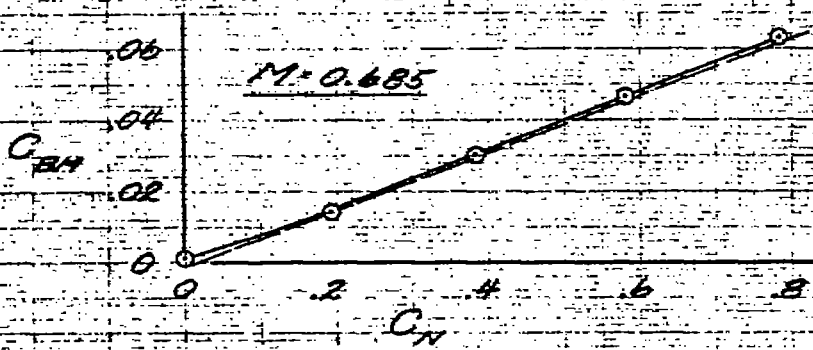
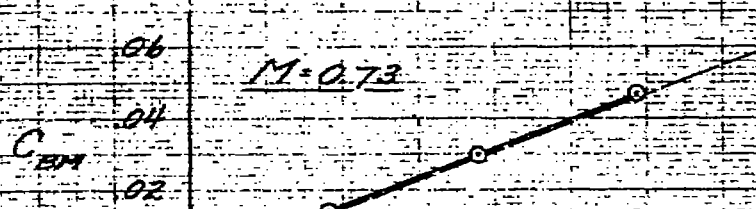
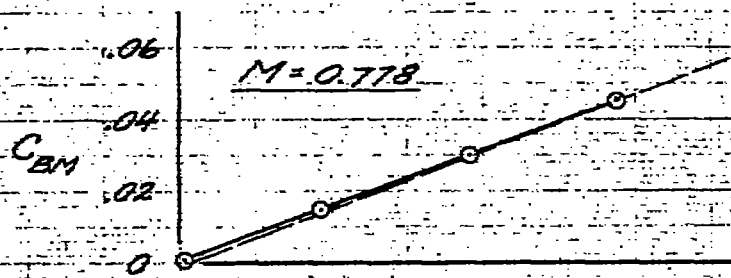
FROM METHOD OF REFERENCE 1.

(b) $M = 0.685, 0.73$ AND 0.778
 FIGURE 29.- CONCLUDED



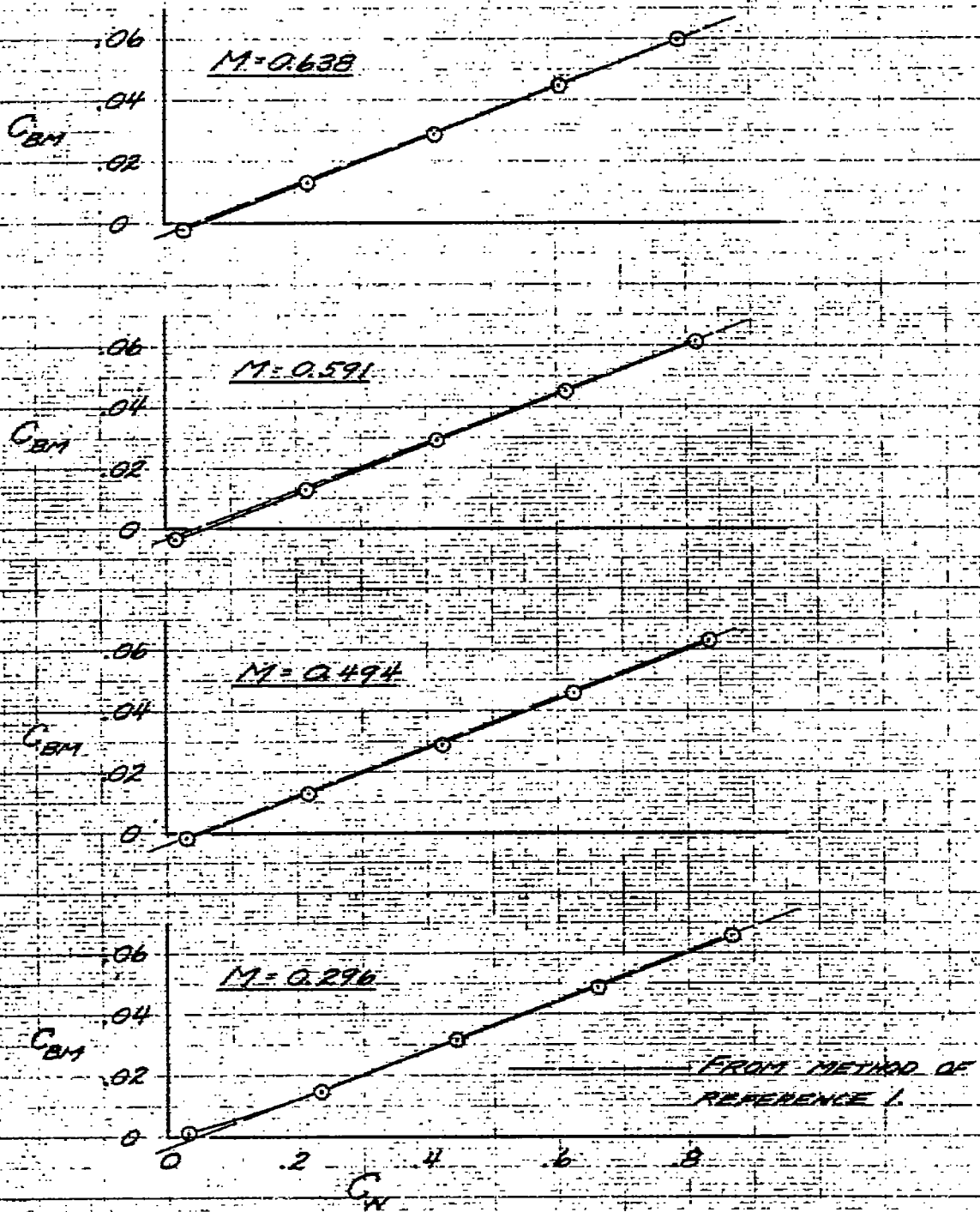
(a) $M = 0.296, 0.494, 0.591, \text{ AND } 0.638$

FIGURE 30.-COMPARISON OF THE VARIATION OF ROOT BENDING-MOMENT COEFFICIENT WITH NORMAL-FORCE COEFFICIENT AS DETERMINED EXPERIMENTALLY AND BY METHOD OF REFERENCE 1. XSB2D-1 MODEL; LANDING FLAPS DEFLECTED 70° .



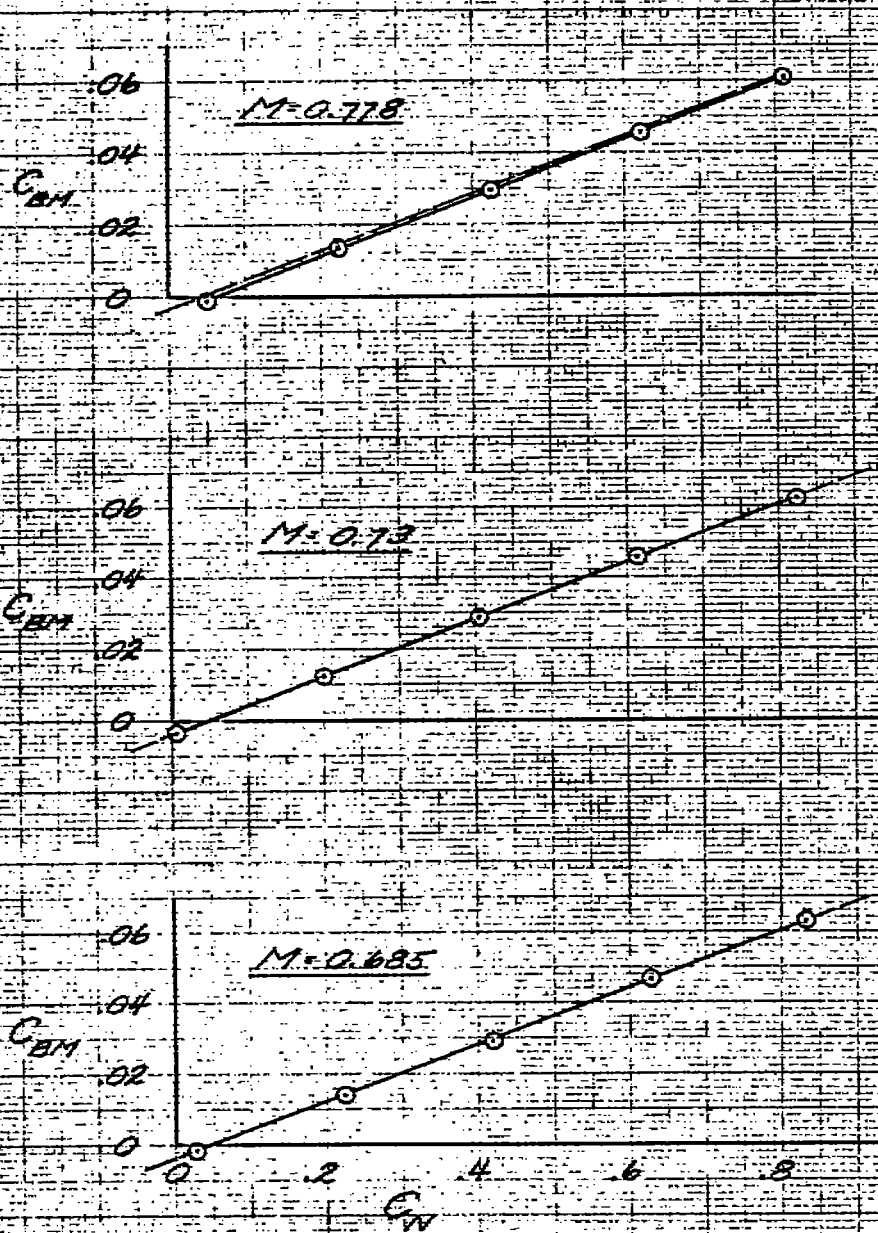
FROM METHOD OF REFERENCE 1.

(b) $M = 0.685, 0.73, \text{ AND } 0.778$
 FIGURE 30 - CONCLUDED



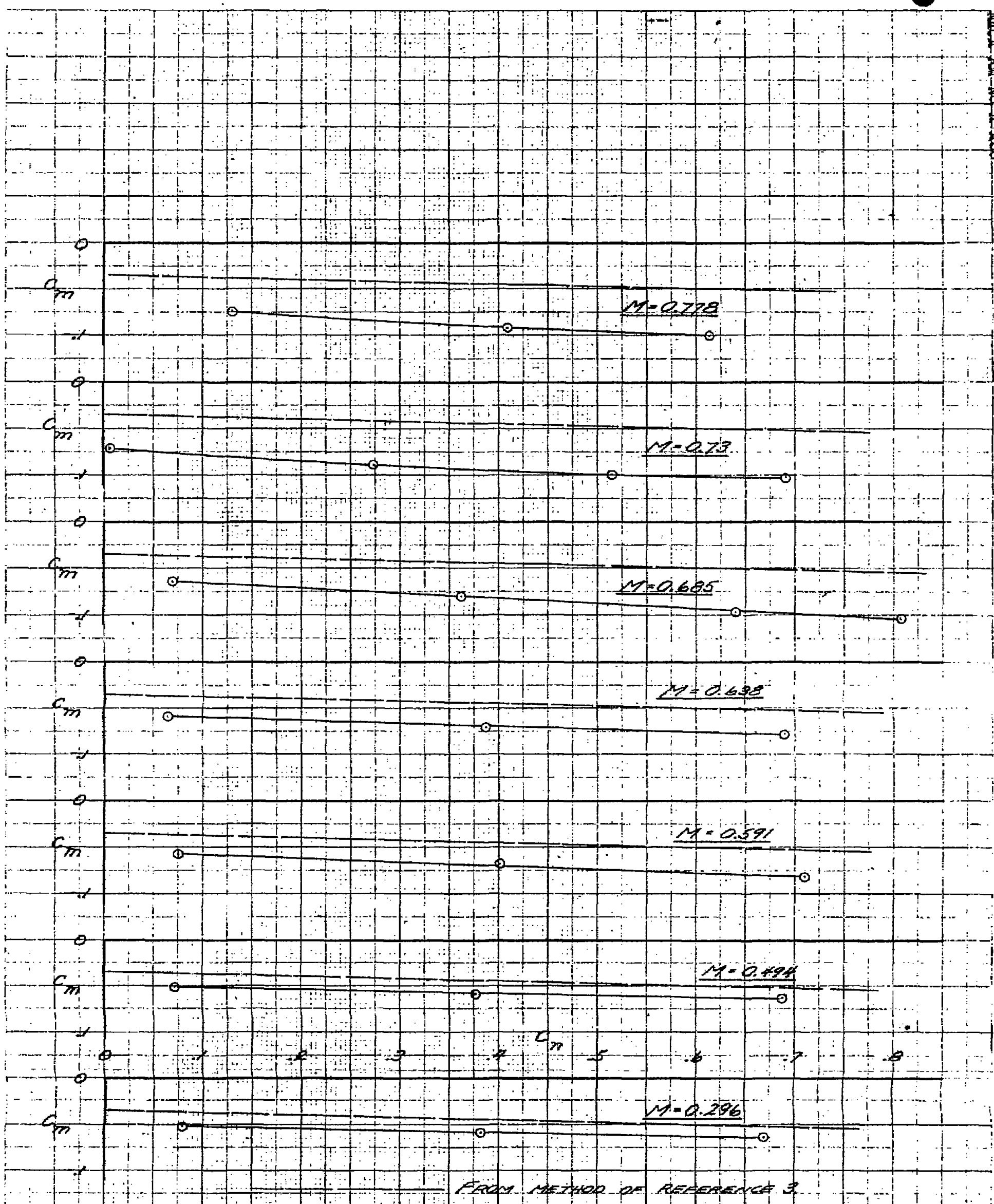
(a) $M = 0.296, 0.494, 0.591, \text{ and } 0.638$

FIGURE 31 - COMPARISON OF THE VARIATION OF ROOT BENDING-MOMENT COEFFICIENT WITH NORMAL FORCE COEFFICIENT AS DETERMINED EXPERIMENTALLY AND BY METHOD OF REFERENCE 1. (X5BRD-1) MODEL; LANDING FLAPS DEFLECTED 40°



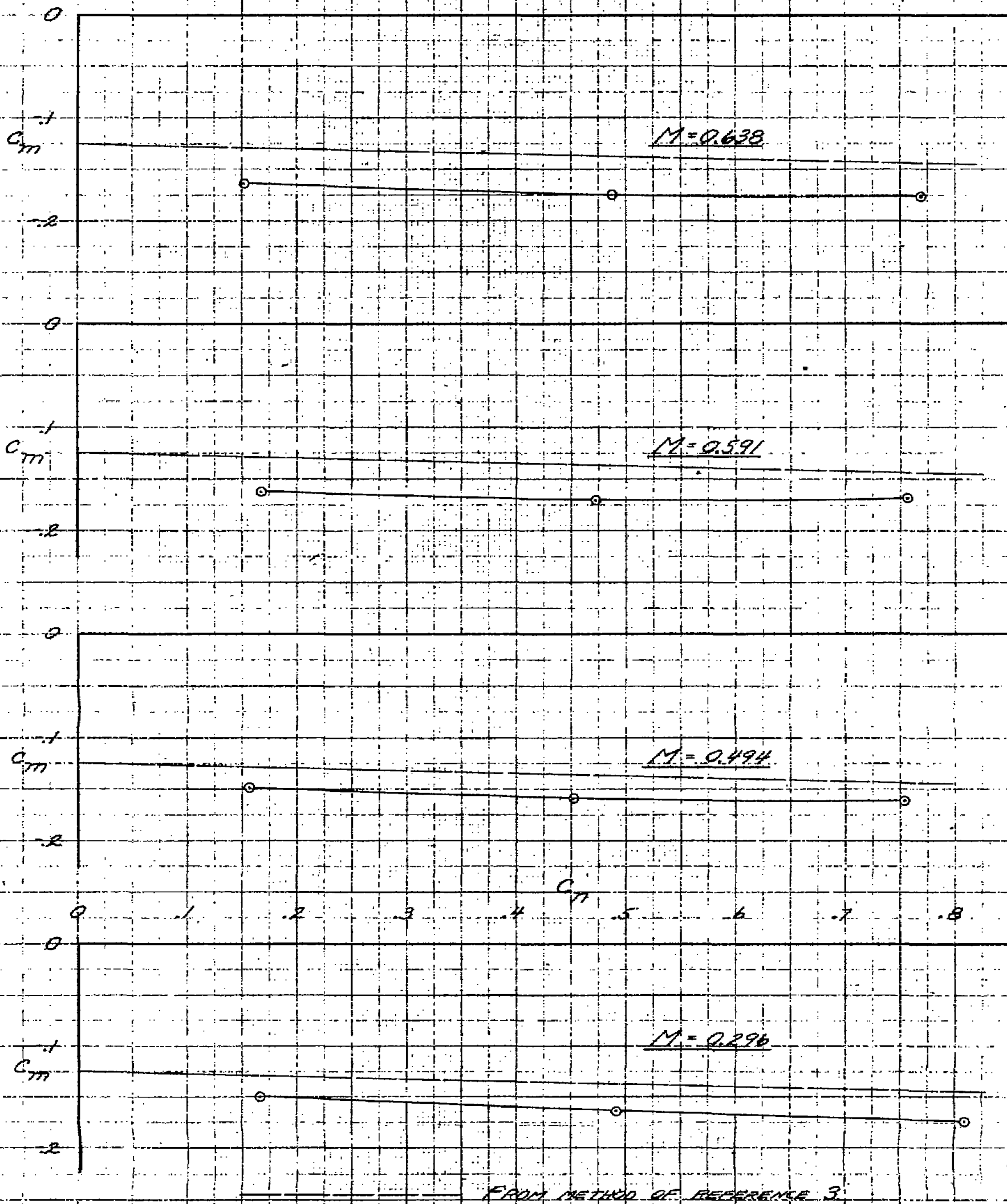
FROM METHOD OF REFERENCE 1

(b) $M=0.685, 0.73, \text{ AND } 0.778$
 FIGURE 31 -- CONCLUDED



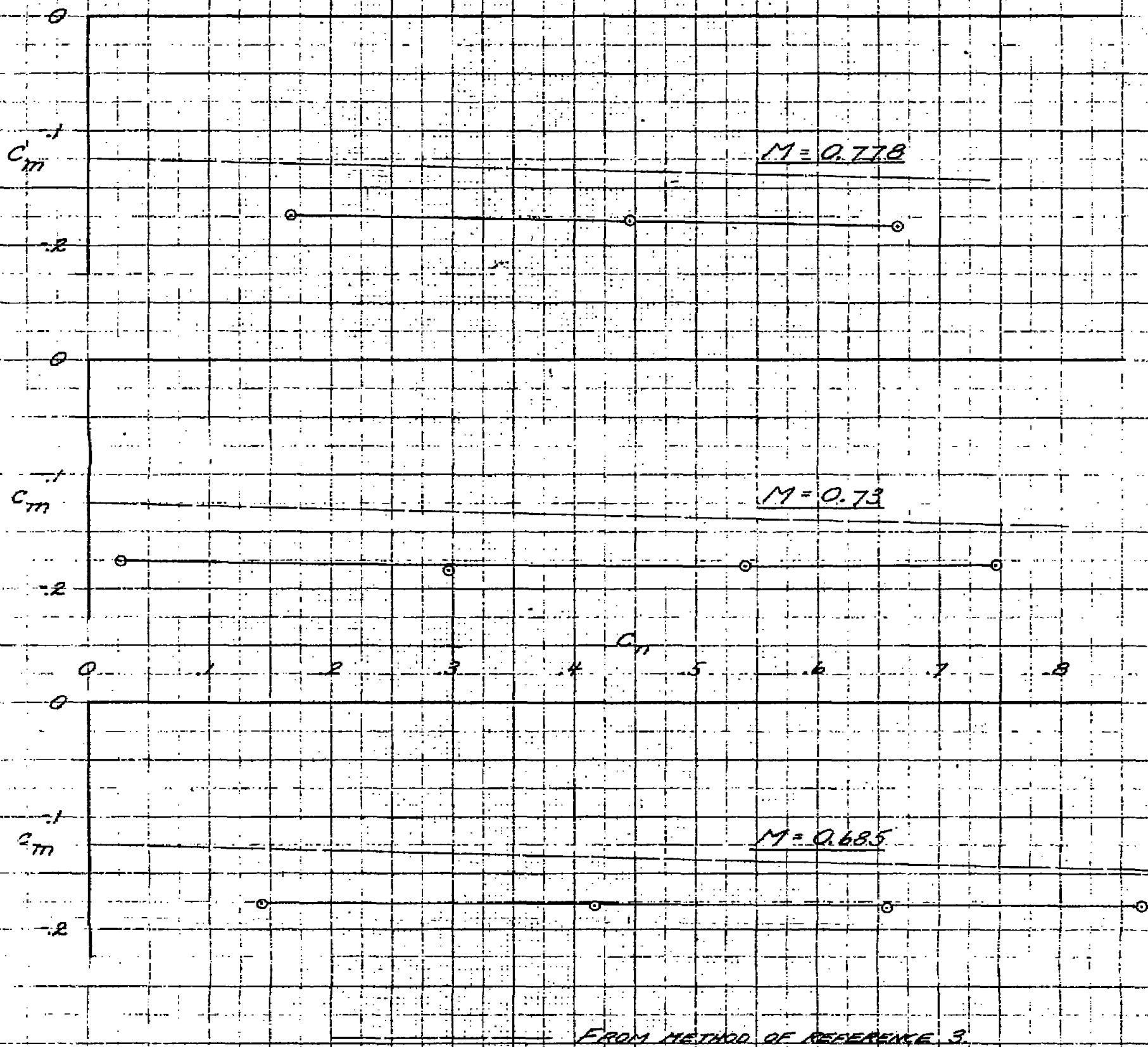
FROM METHOD OF REFERENCE 3.

FIGURE 32. - COMPARISON OF THE VARIATION OF SECTION PITCHING-MOMENT COEFFICIENT WITH SECTION NORMAL-FORCE COEFFICIENT WITH LANDING FLAPS NEUTRAL AS DETERMINED EXPERIMENTALLY AND BY THE METHOD OF REFERENCE 3. XSB27-1 MODEL; STATION 140; MOMENT AXIS 24.7 PERCENT CHORD.



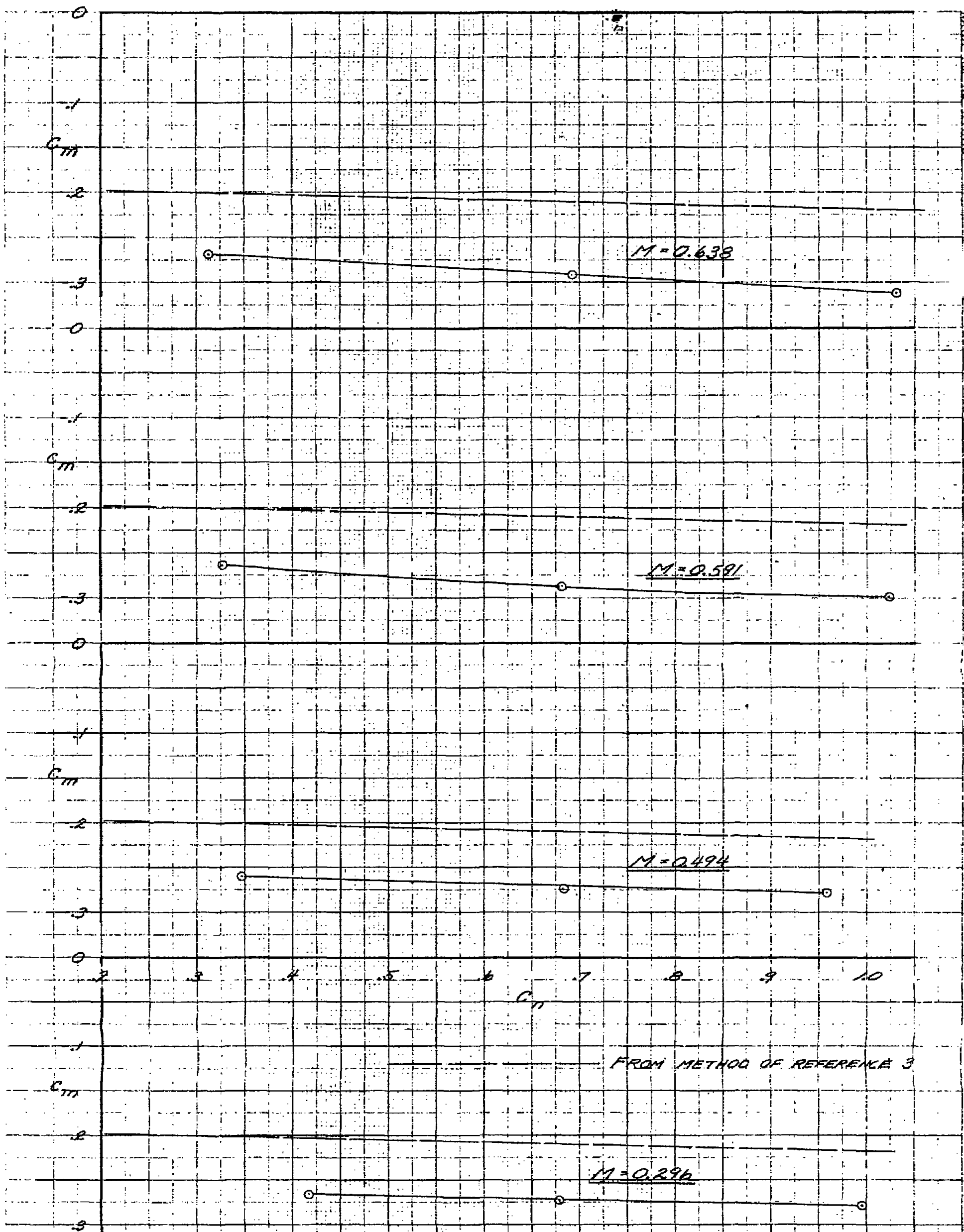
(a) $M = 0.296, 0.494, 0.591, \text{ and } 0.638$

FIGURE 39. - COMPARISON OF THE VARIATION OF SECTION PITCHING-MOMENT COEFFICIENT WITH SECTION NORMAL-FORCE COEFFICIENT FOR A LANDING FLAP DEFLECTION OF 10° AS DETERMINED EXPERIMENTALLY AND BY THE METHOD OF REFERENCE 3. XSB2D-1 MODEL; STATION 140; MOMENT AXIS 24.7 PERCENT CHORD.



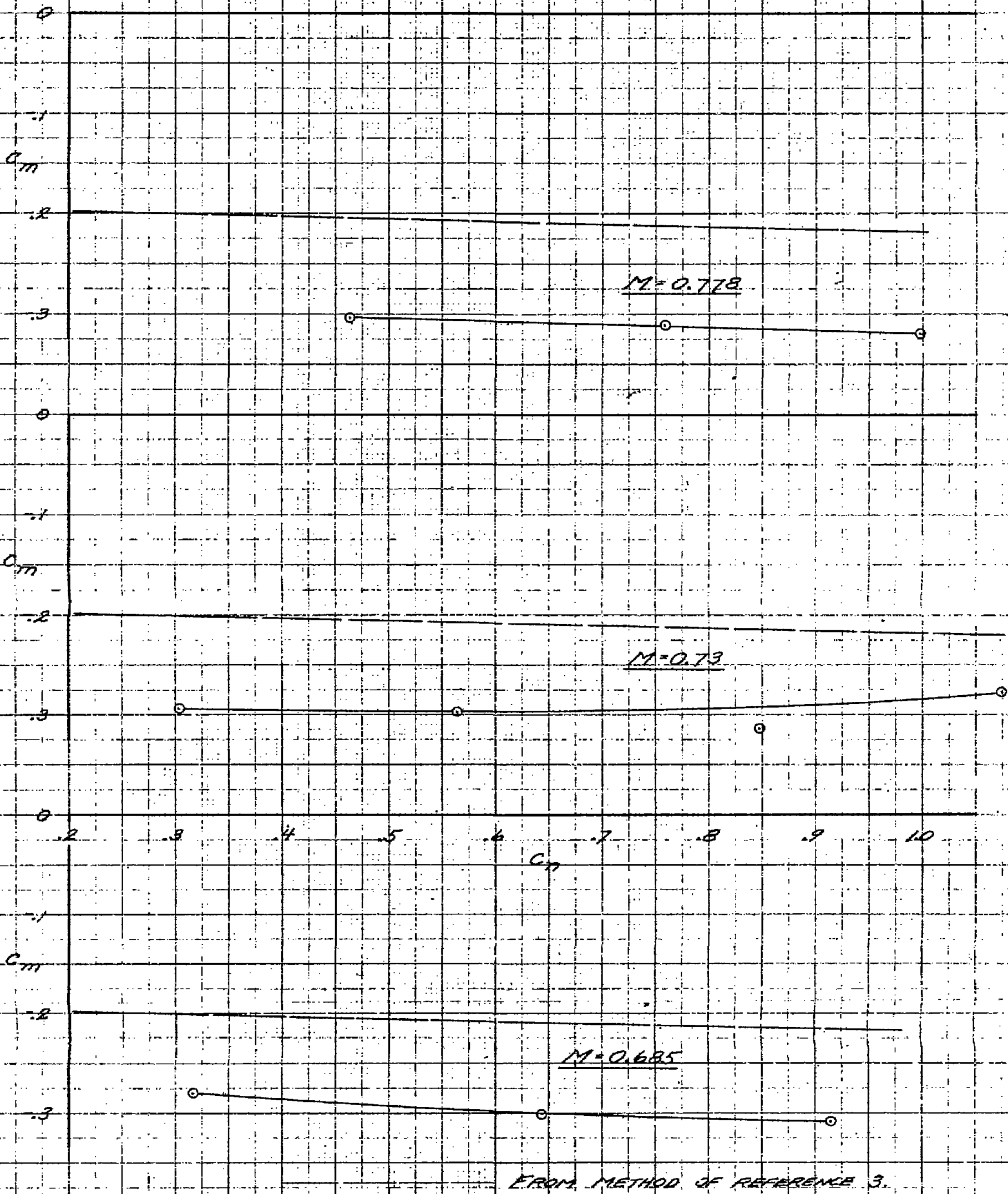
(b) $M = 0.685, 0.73, \text{ AND } 0.778$

FIGURE 33 - CONCLUDED



(a) $M = 0.296, 0.494, 0.591, \text{ AND } 0.638$

FIGURE 34 - COMPARISON OF THE VARIATION OF SECTION PITCHING-MOMENT COEFFICIENT WITH SECTION NORMAL-FORCE COEFFICIENT FOR A LANDING FLAP DEFLECTION OF 40° AS DETERMINED EXPERIMENTALLY AND BY THE METHOD OF REFERENCE 3. X5B2D-1; STATION 140; MOMENT AXIS 24.7 PERCENT CHORD.



FROM METHOD OF REFERENCE 3.

(b) $M = 0.685, 0.73, \text{ AND } 0.778$

FIGURE 34 - CONCLUDED

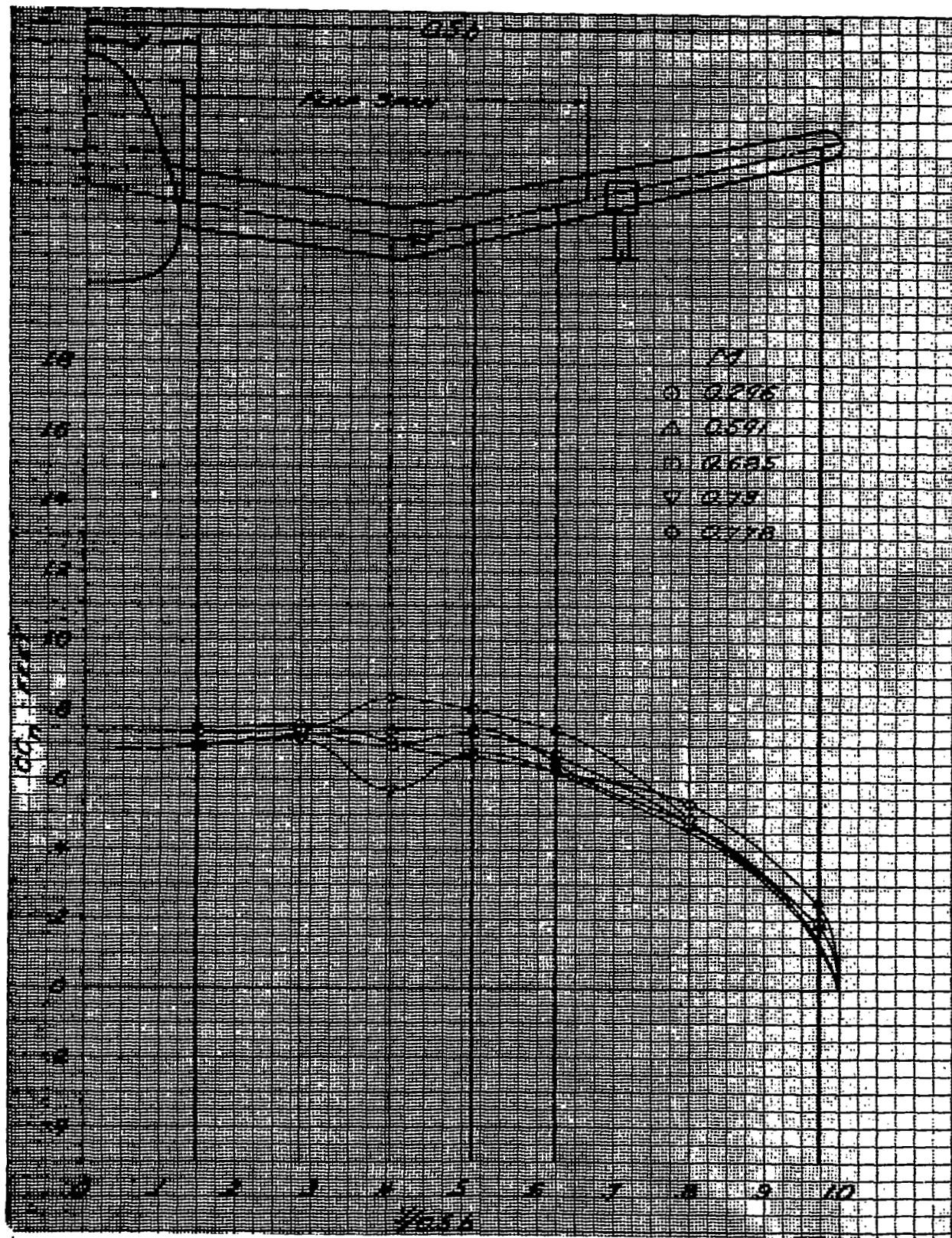
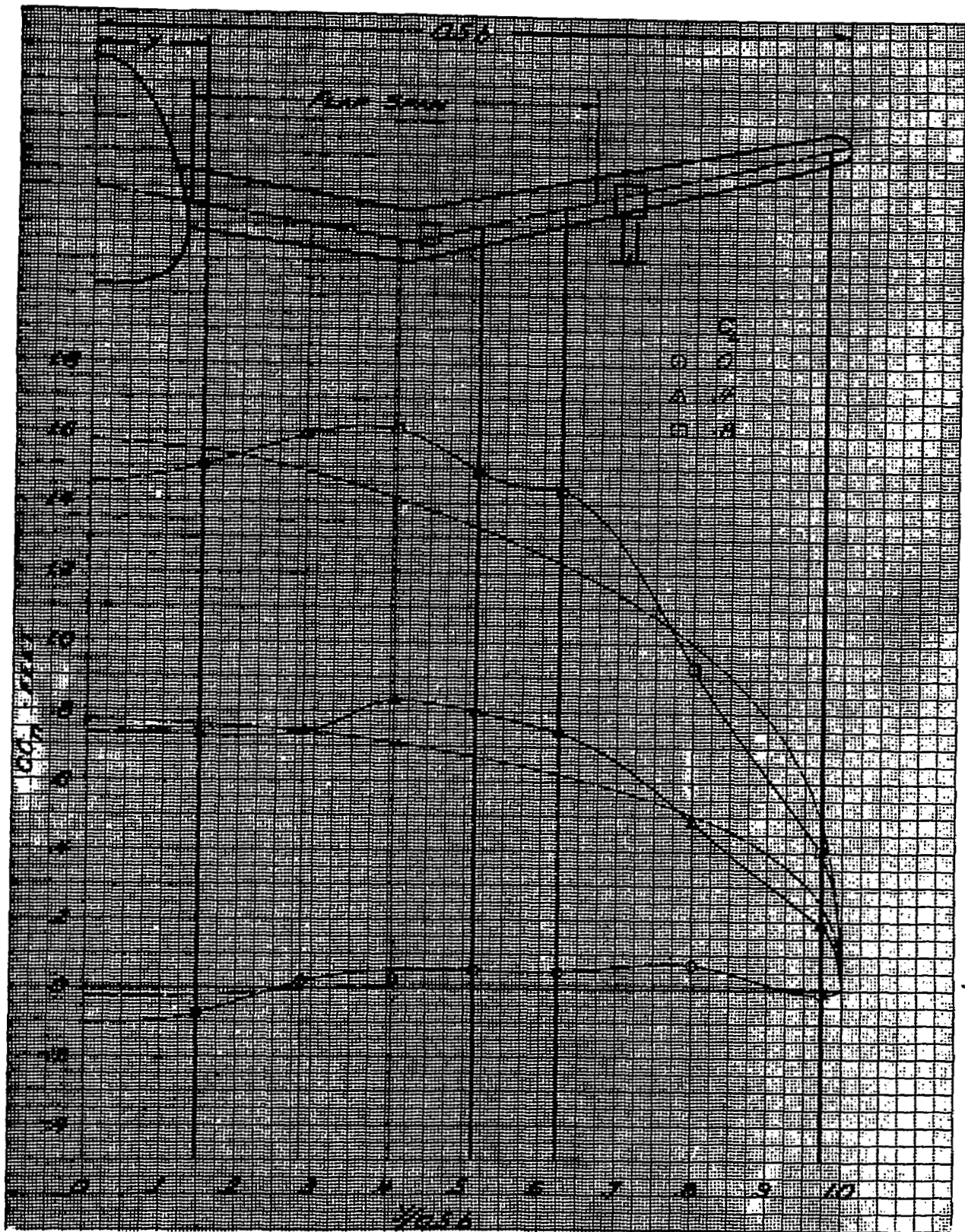
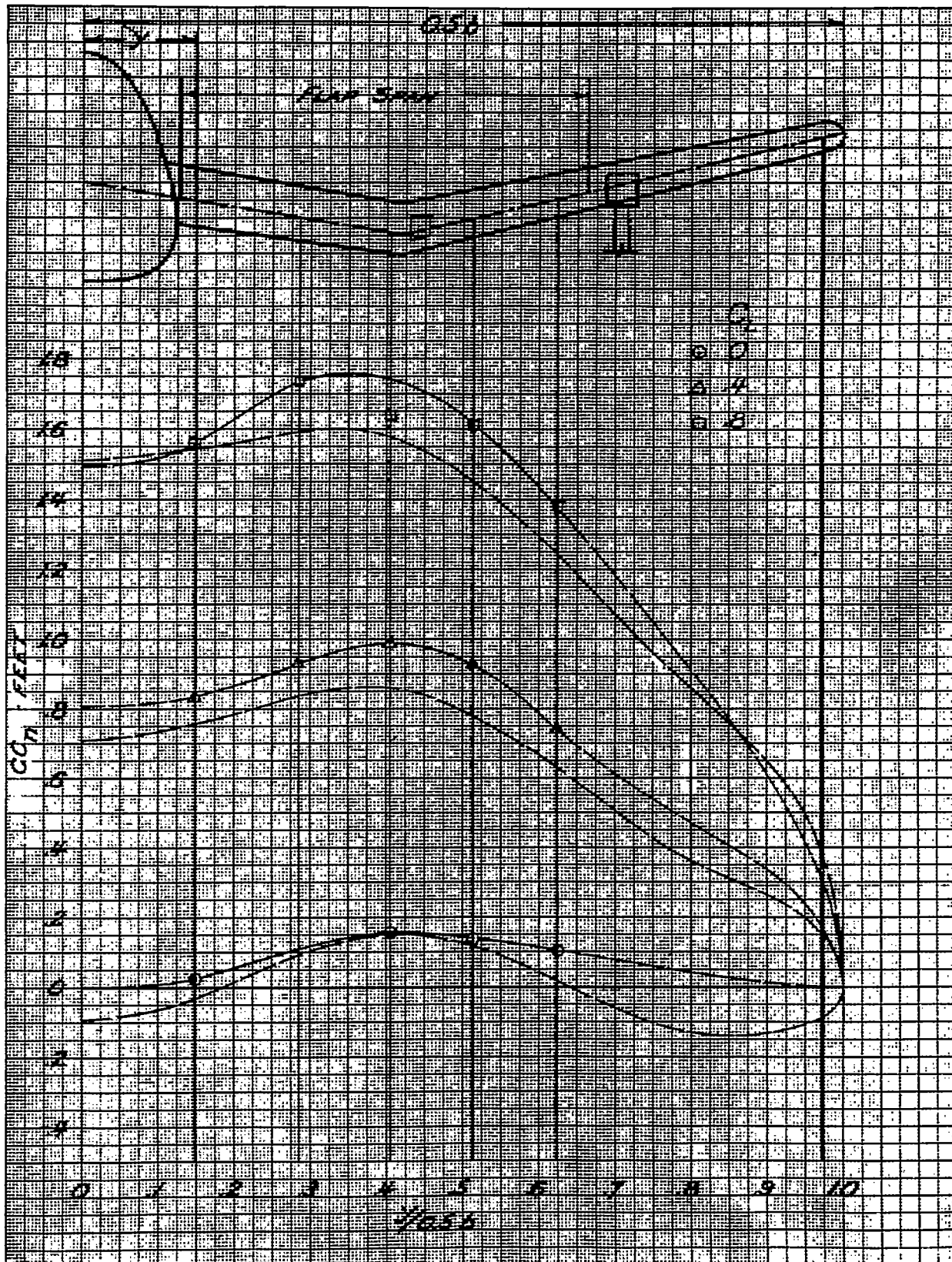


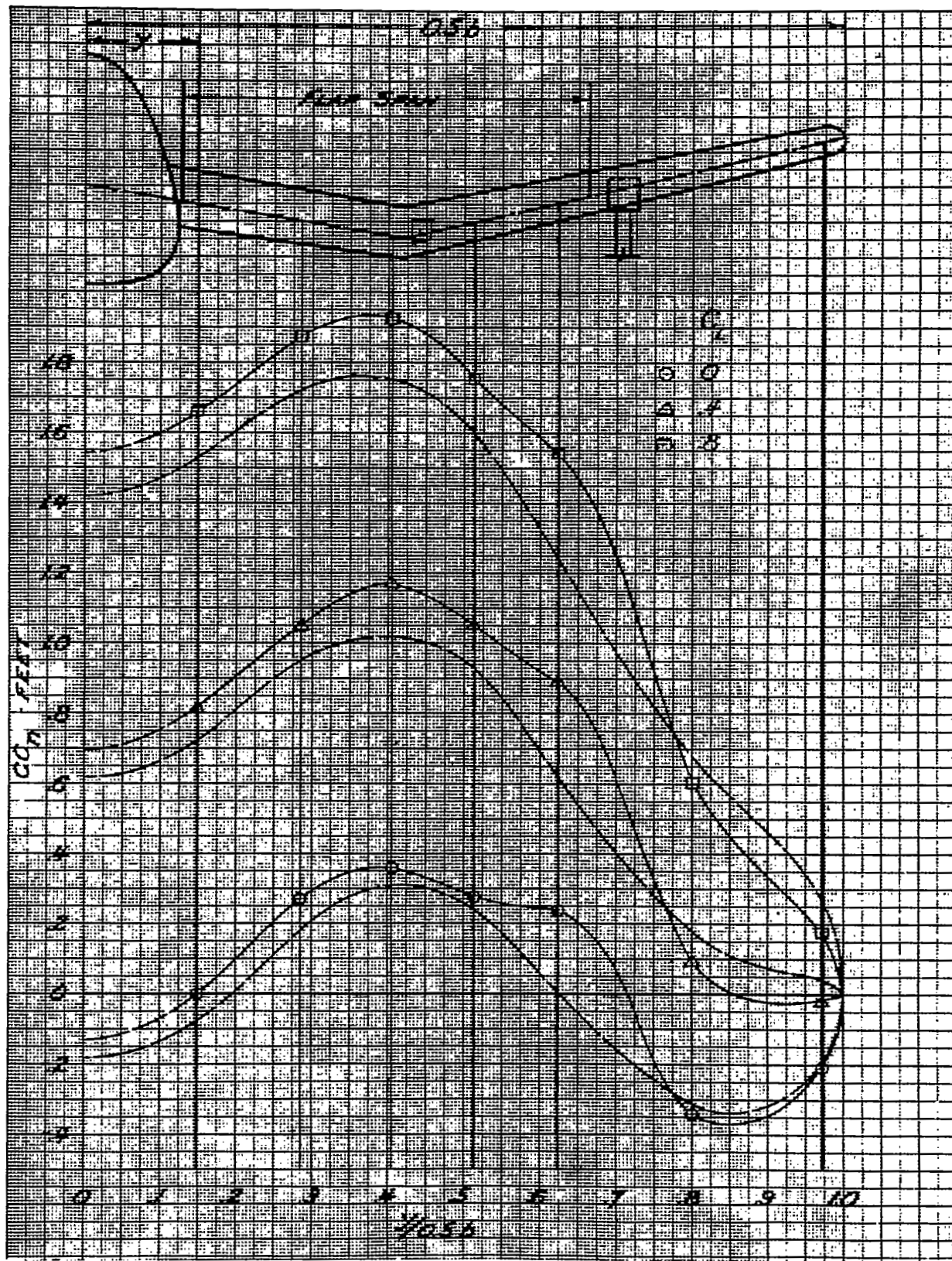
FIGURE 35.-EFFECTS OF MACH NUMBER ON THE SPANWISE NORMAL-FORCE DISTRIBUTION ON THE XSB2D-1 MODEL. FLAPS NEUTRAL;
 $C_L=0.4$



(a) LANDING FLAPS NEUTRAL
 FIGURE 36.- COMPARISON OF SPANWISE NORMAL-FORCE DISTRIBUTION AS DETERMINED EXPERIMENTALLY AND BY METHOD OF REFERENCE 1 FOR THE XSB2D-1 MODEL. $M=0.296$



(b) LANDING FLAPS DEFLECTED 10°
 FIGURE 36. - CONTINUED NATIONAL ADVISORY COMMITTEE FOR AERONAUTICS



(c) LANDING FLAPS DEFLECTED 40°
 FIGURE 36. - CONCLUDED

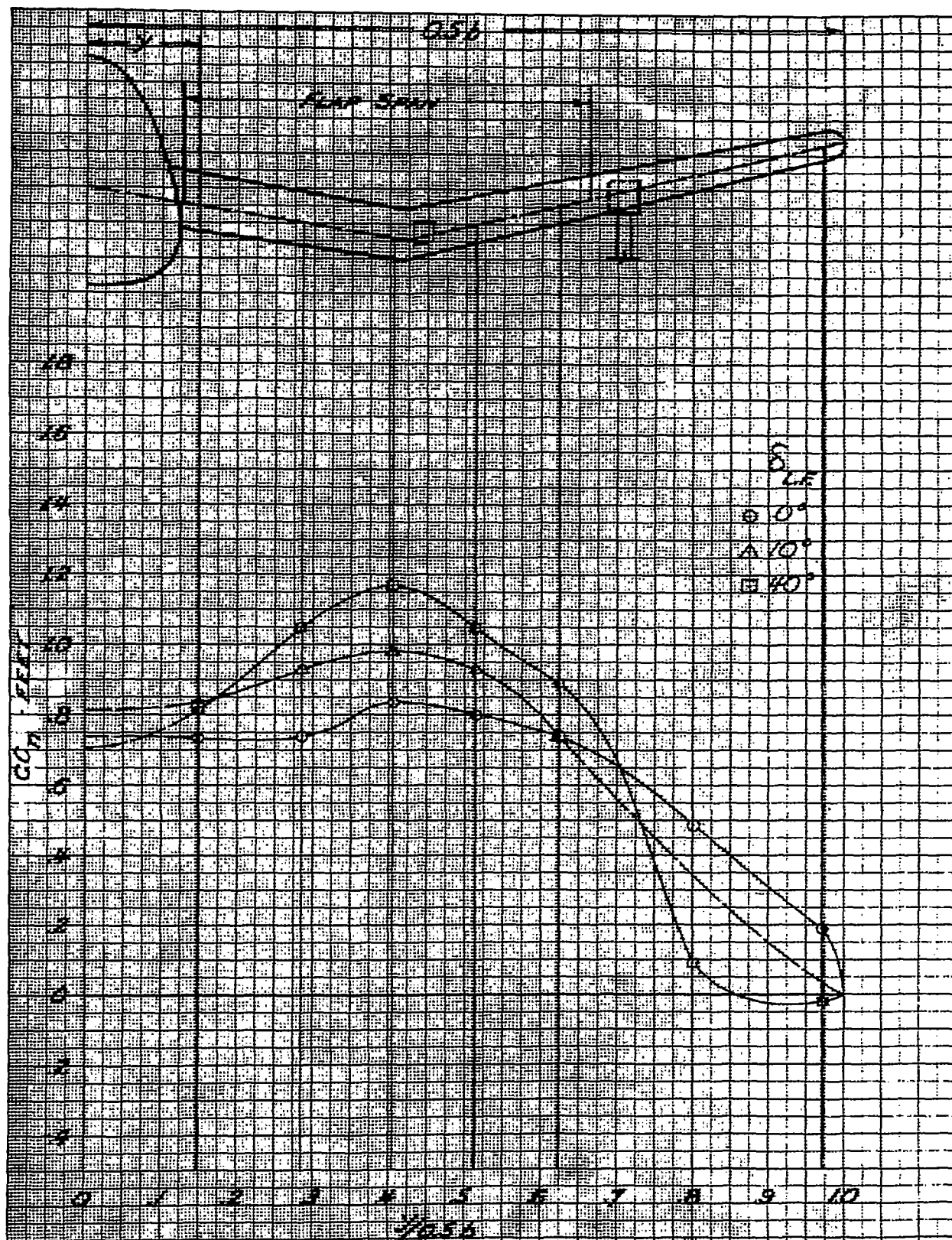


FIGURE 37.- TYPICAL EFFECTS OF LANDING-FLAP DEFLECTION ON THE SPANWISE NORMAL-FORCE DISTRIBUTION ON THE XSB2D-1 MODEL. $M=0.296$; $C_L=0.4$



3 1176 01434 4114

9

Buckley

Regions - Bureau of Aeronautics

and the Army Air Corps. 1924-1

and the Army Air Corps

and the Army Air Corps